Universidade de Aveiro
2014
Departamento de Electrónica, Telecomunicações e Informática

Luis Pedro Marques Brás

Antenas Setoriais para Sistemas de Localização em Redes de Sensores sem Fios

Sectorial Antennas for WSN Localization Systems

Universidade de Aveiro
2014

Departamento de Electrónica, Telecomunicações e Informática

Luis Pedro Marques Brás

Antenas Setoriais para Sistemas de Localização em Redes de Sensores sem Fios

Tese apresentada à Universidade de Aveiro para cumprimento dos requisitos necessários à obtenção do grau de Doutor em Engenharia Electrotécnica, realizada sob a orientação científica do Professor Doutor Nuno Miguel Gonçalves Borges de Carvalho, Professor Catedrático do Departamento de Electrónica, Telecomunicações e Informática da Universidade de Aveiro e do Professor Pedro Renato Tavares Pinho, Professor Adjunto no Departamento de Engenharia de Electrónica e Telecomunicações e de Computadores do Instituto Superior de Engenharia de Lisboa.

Apoio financeiro da Fundação da Ciência e Tecnologia (FCT), referência SFRH/BD/61834/2009,Lisboa,Portugal.

Dedico este trabalho aos meus pais Manuel e Natália, irmão Nuno, e aos meus orientadores Prof. Nuno Borges Carvalho e Prof. Pedro Pinho, pelo incansável apoio, motivação e compreensão em todas as etapas referentes à realização desta tese.

"We build too many walls and not enough bridges"

"Truth is ever to be found in simplicity, and not in the multiplicity of things"

by Isaac Newton

o júri / the jury

presidente / president

Prof. Dr. Manuel João Senos Matias
Professor Catedrático do Departamento de Geociências de Aveiro

vogais / examiners committee

Prof. Dr. Nuno Miguel Gonçalves Borges de Carvalho
Professor Catedrático da Universidade de Aveiro (orientador)

Prof. Dr. Jorge Manuel Lopes Leal Rodrigues da Costa
Professor Associado com Agregação do Intituto Superior de Ciências do Trabalho e da Empresa, Instituto Universitário de Lisboa

Prof. Dr. Henrique Manuel de Castro Faria Salgado
Professor Associado da Faculdade de Engenharia da Universidade do Porto

Prof. Dr. João Nuno Pimentel da Silva Matos
Professor Associado da Univerdidade de Aveiro

Prof. Dr. Rafael Ferreira da Silva Caldeirinha
Professor Coordenador da Escola Superior de Tecnologia e Gestão de Leiria

agradecimentos / acknowledgements

Gostaria de agradecer aos meus orientadores Prof. Nuno Borges Carvalho e Prof. Pedro Pinho por todo o apoio, disponibilidade e motivação. Sem a sua ajuda e colaboração todo este trabalho não seria exequível.

Gostaria também de deixar uma palavra especial de agradecimento a todos os amigos e colegas de trabalho por toda a amizade, apoio, disponibilidade e motivação.

Agradeço ainda à Universidade de Aveiro, mais concretamente ao Instituto de Telecomunicações e ao Departamento de Electrónica, Telecomunicações e Informática por me terem proporcionado os meios de trabalho necessários. Da mesma forma agradeço também a todos os colaboradores do Instituto de Telecomunicações pelo maravilhoso ambiente de trabalho e respectivas condições.

Sou também grato à Fundação para a Ciência e a Tecnologia pelo inestimável apoio monetário. O meu agradecimento ainda a todos os participantes da COST action IC0803 pelo financiamento de uma missão de curta duração à Gdansk Faculty of Electronics, Telecommunications and Informatics, na qual aproveito para agradecer a hospitalidade e colaboração do Prof, Lukasz Kulas e Krzystof Nyka.

Finalmente gostaria de agradecer a todos os meus familiares, com especial destaque à minha namorada Raluca, irmão Nuno, aos meus pais Manuel e Natália pela imensa presença, apoio e compreensão nos momentos que mais necessitei.

A todos o meu Muito Obrigado!

palavras-chave

Ângulo de chegada, antena sectorial, antena impressa, *Hive5*, intensidade do sinal, protocolo, sistema de localização.

Resumo

O presente trabalho investiga sistemas de localização (SL) de baixo custo baseados na intensidade do sinal (RSS) e integrados com diferentes tipos de antenas com principal destaque para antenas sectoriais. Os últimos anos testemunharam um crescimento surpreendente de redes de sensores sem fios (RSSF), onde entre diversas aplicações possíveis, a localização tornou-se uma das principais áreas de pesquisa. Técnicas baseadas na intensidade do sinal caracterizam-se pela simplicidade e baixo custo de integração. A integração de SL baseados na intensidade do sinal recebido e antenas sectoriais (AS) oferecem uma solução eficaz para reduzir o número de nós necessários e para combinar diversas técnicas de localização.

Esta tese de doutoramento foca-se no estudado de técnicas, antenas e protocolos de acordo com os requisitos de cada sistema localização com especial atenção para sistemas de baixo custo baseados na intensidade do sinal e no ângulo de chegada.

Inicialmente são estudadas técnicas e SL de acordo com as necessidades do utilizador e as antenas que melhor se enquadram de acordo com a natureza do sinal. Esta etapa tem como objectivo proporcionar a compreensão fundamental do trabalho desenvolvido.

Em seguida são apresentadas as antenas desenvolvidas divididas em: antenas sectorias e antenas impressas de baixo custo. Duas antenas sectoriais são apresentadas: uma de banda estreita a operar a 2,4-2,5GHz e outro de banda larga 800MHz-2.4GHz. As antenas impressas foram desenvolvidas para operar a 5 GHz, pelo que podem ser utilizadas para comunicação veicular.

Após apresentação das diversas antenas vários protótipos de SL interiores/exteriores são implementados e analisados.

Protocolos de localização são também propostos, um baseado na simplicidade e baixo consumo, outro na interoperabilidade com diferentes tipos de antenas e requisitos do sistema.

keywords

Angle of arrival, Hive5, localization system, microstrip antenna, protocol, received signal strength, sectorial antenna.

abstract

This work investigates low cost localization systems (LS) based on received signal strength (RSS) and integrated with different types of antennas with main emphasis on sectorial antennas. The last few years have witnessed an outstanding growth in wireless sensor networks (WSN). Among its various possible applications, the localization field became a major area of research. The localization techniques based on RSS are characterized by simplicity and low cost of integration. The integration of LS based on RSS and sectorial antennas (SA) was proven to provide an effective solution for reducing the number of required nodes of the networks and allows the combination of several techniques, such as RSS and angle of arrival (AoA).

This PhD thesis focuses on studying techniques, antennas and protocols that best meet the needs of each LS with main focus on low cost systems based on RSS and AoA.

Firstly there are studied localization techniques and system that best suit the requirements of the user and the antennas that are most appropriate according to the nature of the signal. In this step it is intended to provide a fundamental understanding of the undertaken work.

Then the developed antennas are presented according to the following categories: sectorial and microstrip antennas. Two sectorial antennas are presented: a narrowband antenna operating at 2.4 to 2.5 GHz and a broadband antenna operating at 800MHz-2.4GHz. The low cost printed antennas were designed to operate at 5 GHz, which may be used for vehicular communication. After presenting the various antennas, several prototypes of indoor/outdoor LS are implemented and analyzed.

Localization protocols are also proposed, one based on simplicity and low power, and the other on interoperability with different types of antennas and system requirements.

Table of Contents

List of Figures

List of Tables

List of Acronyms

AoA	Angle of Arrival
AR	Axial Ratio
AuT	Antenna under Test
BW	Bandwidth
CP	Circular Polarization
D(θ,φ)	Directivity
DoA	Direction of Arrival
DSN	Distributed Sensor Network
E(r,θ,φ)	Electric Field
ESPAR	Electronically Steerable Parasitic Array Radiator
FDTD	Finite-difference time-domain
FEM	Finite Element Method
G(θ,φ)	Gain
G_{abs}	Absolute Gain
GLONASS	Global Orbiting Navigation Satellite System
GNSS	Global Navigation Satellite Systems
GPS	Global Positioning System
HFSS	High Frequency Structural Simulator
IR	Infra-Red
ISM	Industrial Scientific Medical
IVC	Inter Vehicular Communications
LoS	Line of Sight
LS	Localization System
MoM	Method of Moments
MU	Mobile Unit
NA	Network Analyzer
NLoS	Non Line of Sight
OMAA	Omnidirectional Microstrip Antenna Array
P_{in}	Input Power

PEM	Planar Elliptical Monopole
Prad	Radiation Power
RF	Radio Frequency
RFID	Radio-Frequency Identification
RL	Return Loss
RP	Radiation Pattern
RSS	Received Signal Strength
RSSF	Rede de Sensores sem Fios
RSSI	Received Signal Strength Indication
RTLS	Real Time Localization System
RToF	Round-Trip Time of Flight
SA	Sectorised Antenna
SAA	Sectorised Antenna Arrays
SAR	Specific Absorption Rate
SB	Switch Beam
SL	Sistema Localização
SNA	Scalar Network Analyzer
SoC	System on Chip
TDoA	Time Difference of Arrival
TLM	Transmission Line Matrix
ToA	Time of Arrival
ToF	Time of Flight
U(θ,φ)	Radiation Intensity
UHF	Ultra High Frequency
UWB	Ultra-wideband
V2I	Vehicle to Infrastructure
V2V	Vehicle to Vehicle
VNA	Vector Network Analyzer
VSWR	Voltage Standing Wave Ratio
WLAN	Wireless Local Area Networks
WSN	Wireless Sensor Networks

Chapter 1 – Introduction

The ambition and curiosity of engineers often lead to technology leaps. This was the case on wireless sensor networks (WSN) when in 80s R. Kahn (co-inventor of TCP/IP and a key person for internet developing) desired to know if Arpanet communication (Advanced Research Projects Agency NETworking) could be extended to sensor networks. It was the origin of Distributed Sensor Networks (DSN) concept, idealized to be a large amount of spatially distributed, small size, low-cost sensing nodes, operating autonomously. These nodes could then collaborate with each other being the information routed to a desired terminal [1]. However, it was needed to wait until last 90s, around 1998, for a new research wave, initiated with the SensIT project. This research induced a considerable progress on highly dynamic ad hoc environments and resource constrained sensor nodes. It was the shift to WSN research. Its importance gained so much attention that in September 1999, on Business Week, it was referred as one of the key technologies of the 21st century [2].

Almost 15 years passed since the Business Week prediction and looking to nowadays technology we can affirm that the prediction could not be more correct. The replacement of wired connections among electronic devices with wireless networks completely revolutionized the way we organize our industrial, office and even home environments. These WSN are currently found in different fields like medical, industrial, transport systems, public safety and consumer electronics.

Among the possible applications, positioning or localization become one of the main research areas in WSN. Localization Systems (LS) have been developed through several technologies (e.g. infrared, Bluetooth, ZigBee, Radio Frequency Identification (RFID), Ultra Wideband (UWB), ultra-sounds), based on diverse techniques (e.g. lateration, angulation, scene analysis and proximity) and supported by innumerable algorithms (e.g. neural networks, k-nearest neighbors) [3]. Each of these categories has unique advantages and drawbacks making its choice dependent to the desired performance benchmarks. A short resume of some of these LS according with resolution and range is presented in Fig. 1.1.

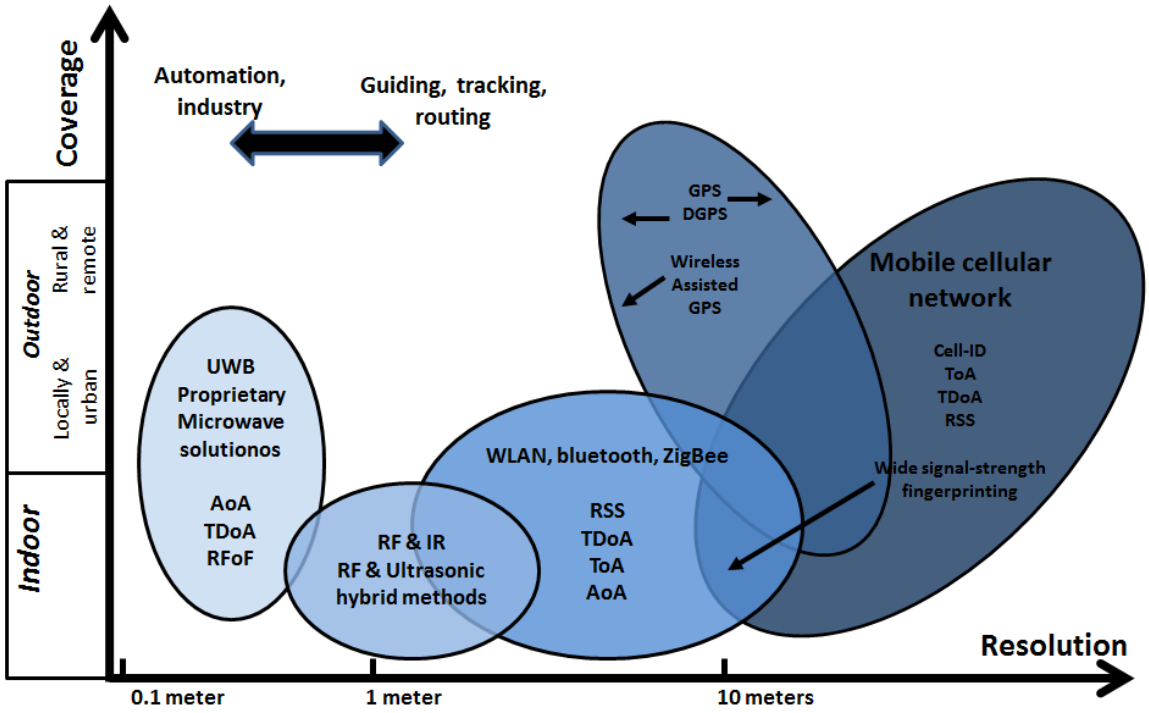

Fig. 1.1 Localization systems

Despite of the large panoply of existing Radio Frequency (RF) LS, they are highly influenced by one common factor, the antenna's performance. Reference unit antennas are commonly designed to be robust, inexpensive, impedance matched over the entire operational bandwidth, small, and highly efficient. These characteristics are important for the correct performance of the antenna, which inherently have impact on the LS performance. Nevertheless, other antenna's characteristics such as directivity, radiation pattern and polarization should be carefully chosen according to the LS approach.

LS based on WSN have been mostly integrated with omnidirectional and vertical polarized antennas [4]-[6], as presented in Fig. 1.2 A). Nevertheless, diversity of radiation pattern and polarization can significantly improves localization as well as the communication systems' performance. These benefits can be achieved using independent directive antennas such as mechanical rotated and sectorised antennas (SA) [7], as presented in Fig. 1.2. B).

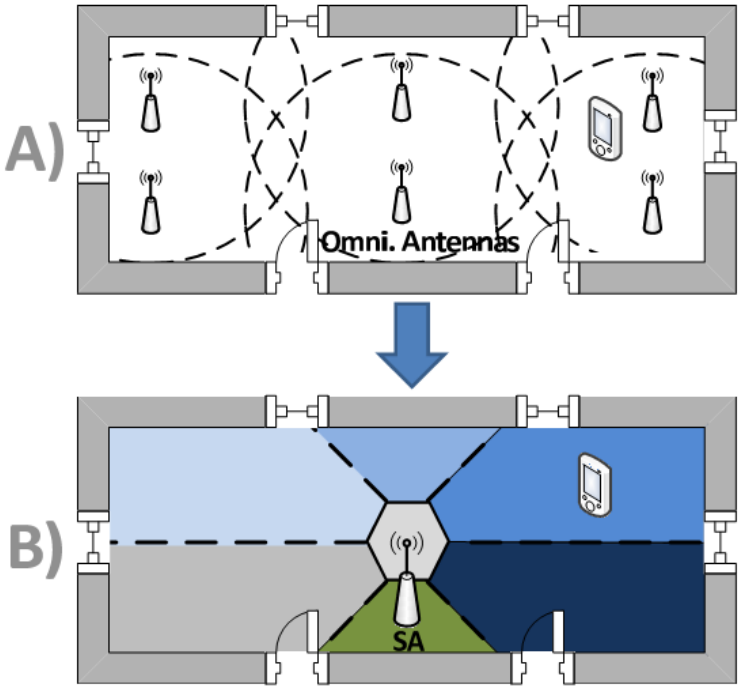

Fig. 1.2 LS models: based on WSN A) and based on SA B)

In this context, this PhD thesis studies, investigates and proposes LSs integrated with different types of antennas, with main emphasis on sectorial antennas. Presented a short introduction of this thesis, it will be now presented the motivation, objectives, thesis outline and main contributions achieved with this work.

1.1 Motivation

This thesis presents the continuation of the developed work by the same author on his master thesis "Desenvolvimento de sistema de localização indoor de baixo consumo" ("Development of indoor localization system of low power consumption") presented on 2010. In this work, it was developed an indoor localization system, based on ZigBee with the following characteristics: reduced power consumption, two modes of localization available (proximity and fingerprinting based), and development of a friendly user management application [8].The user interface is presented in Fig. 1.3 and the achieved mobile node expected life time duration in Table 1.1.

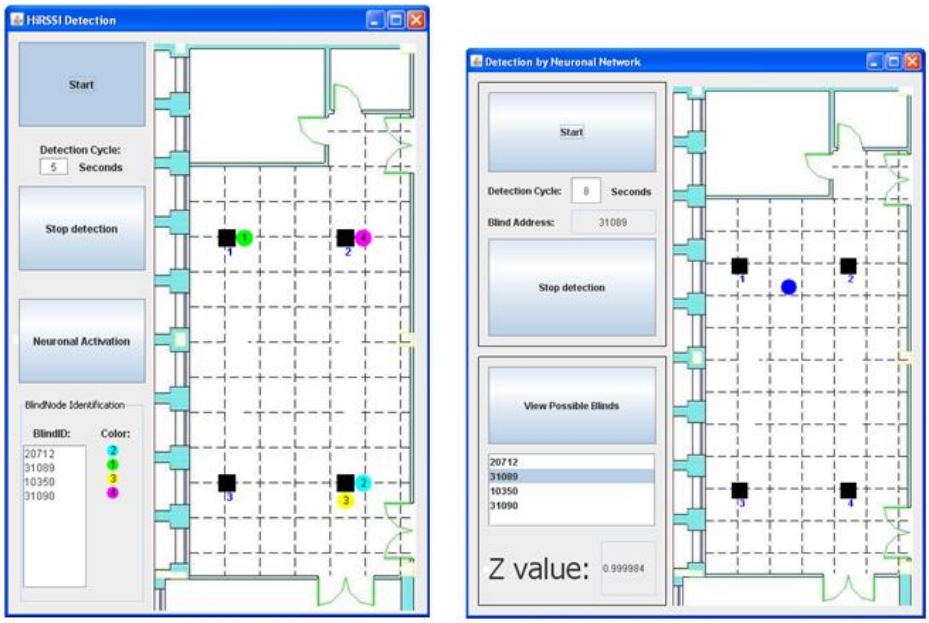

Fig. 1.3 User Interface for proximity (left) and fingerprinting (right)

One battery of 650 mAH	**Life time (days)**		
Sleep Cycle (seconds)	**1 Blast**	**5 Blasts**	**8 Blasts**
3	469,2	107,4	72,4
5	776,4	177,8	119,4
10	1529,2	353,2	237,3
20	2972,9	700,5	471,1
60	8034,1	2045,9	1386,4

Table 1.1 Mobile node expected life time duration

The low power consumption was achieved due to a simple protocol development, significantly reducing the mobile nodes communication time within the WSN [C1]. Considering the SoC CC2430/31, this was a good improvement on batteries life time comparing with other systems up to date. This system provided low power consumption and a satisfactory resolution (< 2 meters) based in Received Signal Strength (RSS) techniques. In order to improve the overall system performance it was proposed the implementation of hybrid techniques (RSS and AoA) supported by proper sectorial antennas.

1.2 Objectives

The presented PhD work led to new research areas, sectorial antenna design, hybrid localization techniques and compliant protocols. In this sense, important goals have been accomplished during this doctoral study as follows:

- Development of low cost and low power consumption LS;
- Implementation of a system based on hybrid localization techniques;
- Development of firmware and localization algorithms for LS;
- Development of antenna and RF circuits for the reference nodes to increase systems localization and communication performance;
- Proposal of a protocol compliant with different types of antennas.

1.3 Thesis Outline

After this introductory chapter this thesis in divided in more 6 chapters organized as follows. Chapter 2 presents a brief background of antenna analysis. In this chapter are described the fundamental antenna parameters, the electromagnetic simulator used and the measurement systems and procedures explaining how the presented results were achieved.

In Chapter 3 it is presented a background of LS: techniques and the antennas that best meet the needs of each LS with particular attention to systems based on RSS and AoA. This step is intended to provide a fundamental understanding of the presented work.

Then, in Chapter 4 it is presented the developed antennas divided as: sectorial antennas, (the Hive5 and the 6-SB Log Periodic Antenna) and planar antennas for diverse communication application at 5GHz (planar linear array, loop and planar elliptical array).

In chapter 5 the developed LS are presented with special attention for the systems integrated with the developed sectorial antennas and the indoor/outdoor LS combining several technologies.

In chapter 6 localization protocols are proposed, one based on simplicity and low power, another on the interoperability with different types of antennas (omnidirectional, sectorial and arrays) and system requirements (power consumption, user privacy and

accuracy). The last chapter presents the final conclusions and contributions originated from the work done for this thesis and some ideas for future work.

The work performed during this PhD led to the papers publishing/submission to prestigious scientific journals [J1]-[J5] or presented in some relevant international conferences [C1]–[C8].

1.4 Main Contributions

For the purpose of this thesis it was taken into consideration the contents of most relevant publications. The document is mainly supported on the following papers:

[J1] Bras, L.; Carvalho, N. B.; Pinho, P., Kulas L. and Nyka K.; "A Review of Antennas for Indoor Positioning Systems", *International Journal of Antennas and Propagation*, ID 953269, 2012;

[J2] Bras, L.; Carvalho, N.B.; Pinho, P.; "Pentagonal Patch-Excited Sectorized Antenna for Localization Systems," *Antennas and Propagation, IEEE Transactions on* , vol. 60, nº. 3, pp.1634-1638, March 2012;

[J3] Bras, L.; Carvalho, N. B.; Pinho, P.; "Evaluation of a Sectorised Antenna in an Indoor Localization System*" IET Microwaves, Antennas & Propagation*, vol. 7, nº. 8, pp. 679 – 685, June 2013;

[J4] Bras, L.; Carvalho, N. B.; Pinho, P.; "Evaluation of planar elliptical antenna array with inner counter-elliptical slot" *submitted in IEEE Transactions on Antennas and Propagation*;

[J5] Bras, L.; Carvalho, N. B.; Pinho, P.; "Location Protocol for WSNs compliant with Omnidirectional, Arrays and Sectorial Antennas" submitted in Elsevier Journal, Computer Communications;

[C1] Bras, L.; Oliveira, M.; Carvalho, N. B.; Pinho, P.; "Low Power Location Protocol based on ZigBee Wireless Sensor Networks", *2010 International Conference on Indoor Positioning and Indoor Navigation (IPIN),* September 15-17, 2010, Zurich, Switzerland;

[C2] Guenda, L.; Bras, L.; Oliveira, M.; Carvalho, N. B.; "Indoor/Outdoor Management System Compliant with Google Maps and Android® OS", *EUROCON 2011 and CONFTELE 2011*, April 27-29, 2011, Lisbon – Portugal;

[C3] Bras, L.; Oliveira, M.; Guenda, L.; Carvalho, N. B.; Pinho, P.; "Localization System Improvement using a Special Designed Sectorised Antenna," *IEEE AP-S International Symposium on Antennas and Propagation and 2011 USNC/URSI*, July 2011, Washington, USA;

[C4] Bras, L.; Oliveira, M.; Guenda, L.; Carvalho, N. B.; Pinho, P.; "Location System applied in Management of Emergency Scenarios", *2011 International Conference on Indoor Positioning and Indoor Navigation (IPIN)*, 21-23 September 2011, Guimarães, Portugal;

[C5] Bras, L.; Oliveira, M.; Guenda, L.; Carvalho, N. B.; Pinho, P.; "Improved Sectorised Antenna for Indoor Localization Systems", *European Microwave Conference*, October 9-14, 2011, Manchester, England;

[C6] Bras, L.; Carvalho, N.B.; Pinho, P., "Circular polarized planar elliptical antenna array," *Antennas and Propagation (EuCAP), 2013 7th European Conference on*., pp.891,893, 8-12 April 2013 Gothenburg, Sweden.

[C7] Bras, L.; Carvalho, N. B.; Pinho, P.; "Planar Omnidirectional Microstrip Antenna Array for 5 GHz ISM and UNII band" *2013 IEEE International Symposium on Antennas and Propagation*, July 7-13, 2013, Orlando, Florida, USA;

[C8] Bras, L.; Carvalho, N. B.; Pinho, P.; "Omnidirectional Printed Loop Antenna for Taxi Communications*" 2013 IEEE International Symposium on Antennas and Propagation*, July 7-13, 2013, Orlando, Florida, USA.

Chapter 2 –Antenna Analysis

This chapter provides the background on antenna analysis. In order to understand the antenna simulations and measurements presented in this thesis several concepts and procedures need to be well understood. For this reason it is presented in this chapter the antenna fundamental parameters, the electromagnetic simulator used in this thesis, Ansys High Frequency Simulation Software (HFSS), and a brief introduction to antenna measurement equipment's and procedures.

2.1 Fundamental Antenna Parameters

The main fundamental antenna parameters can be resumed as:

1) Radiation pattern;
2) Radiation intensity;
3) Directivity;
4) Efficiency;
5) Gain;
6) Bandwidth;
7) Polarization.

All the parameters mentioned are commonly used to characterize an antenna, and will be described in detail in this chapter by the introduced order.

2.1.1 Radiation Pattern

The radiation pattern (RP) of an antenna (also called antenna pattern) is defined in the IEEE Standard Definitions of Terms for Antennas as:

"A mathematical function or graphical representation of the radiation properties of the antenna as a function of space coordinates. In most cases, the radiation pattern is determined in the far field region and is represented as a function of the directional coordinates" [9].

The RP property represents the two (or three dimensional) spatial distribution of the radiated energy at a constant distance along a path (2D) or surface (3D) of constant radius and is usually measured using spherical coordinates as shown in Fig. 2.1.

According with the measured parameters the radiation pattern can be specified with different nomenclatures as:

Power pattern – spatial variation of received power along a constant radius;

Field amplitude pattern – spatial variation of received electric (or magnetic) field along a constant radius.

Field and power patterns are usually normalized with respect to their maximum value and commonly plotted on a logarithmic scale, in decibels (dB). This scale has the advantage of accentuate in more detail those parts that have very low values, commonly referred as minor lobes.

In practice 3D patterns are recorded in a series of two dimensional patterns (pattern cuts). These patterns are obtained by fixing one of the spherical coordinates (θ or φ) while varying the other.

Planes where we fix φ value ($0 \leq \varphi \leq 2\pi$) and vary θ are referred as elevation patterns. Planes where we fix a θ value ($0 \leq \theta \leq \pi$) and vary φ are referred as azimuthal patterns.

The elevation plane of φ=0º (XoZ plan), and the azimuthal plane of θ = 90º (XoY plane) are shown in Fig. 2.1.

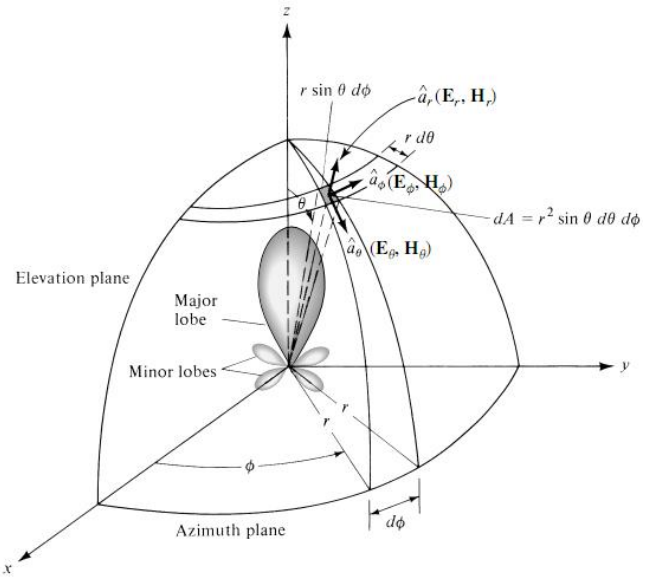

Fig. 2.1 Coordinate system for antenna analysis [10]

For linear polarized antenna, it is also common to refer to the E and H planes, defined as the planes containing the direction of maximum radiation and the electric and magnetic field vectors.

2.1.2 Radiation Intensity

The Radiation intensity in a given direction is defined in the IEEE Standard Definitions of Terms for Antennas as *"the power radiated from an antenna per unit solid angle"* [9].

The radiation intensity is a far field parameter which can be related with the electric field of an antenna as:

$$U_{(\theta,\phi)} = \frac{r^2}{2\eta}\left|E_{(r,\theta,\phi)}\right|^2 \tag{2.1}$$

Where, $E_{(r,\theta,\phi)}$ = electric-field intensity

η = intrinsic impedance of the medium

r= distance from the antenna to the analyzed point

The integration of the radiation intensity over the entire solid angle of 4π gives the total power or radiation power which can be defined as presented in (2.2).

$$P_{rad} = \oiint_{\Omega} U d\Omega = \int_0^{2\pi}\int_0^{\pi} U \sin\theta \, d\theta d\phi \tag{2.2}$$

$d\Omega$= element of solid angle =$\sin\theta \, d\theta d\phi$

For the case of an isotropic source, U will be independent of the angle θ or ϕ, thus (2.2) can be written as:

$$P_{rad} = \oiint_{\Omega} U_0 d\Omega = 4\pi U_0 \tag{2.3}$$

This equation leads to the direct relation of the radiation power with the radiation intensity given as:

$$U_0 = \frac{P_{rad}}{4\pi} \tag{2.4}$$

2.1.3 Directivity

Directivity is defined in the IEEE Standard Definitions of Terms for Antennas as:

"The ratio of the radiation intensity in a given direction from the antenna to the radiation intensity averaged over all directions. The average radiation intensity is equal to the total power radiated by the antenna divided by 4π. If the direction is not specified, the direction of the maximum radiation intensity is implied." [9].

The directivity of a nonisotropic source can be seen as the ratio of its radiation intensity in a given direction over that of an isotopic source. It can also be seen as ratio of the antenna radiated power density at a distant point to the total antenna radiated power (P_{rad}) radiated isotropically written as:

$$D_{(\theta,\phi)} = \frac{U_{(\theta,\phi)}}{U_0} \tag{2.5}$$

or

$$D_{(\theta,\phi)} = \frac{4\pi U_{(\theta,\phi)}}{P_{rad}} \tag{2.6}$$

Where, $U_{(\theta,\phi)}$ = radiation intensity (W/unit solid angle)

U_0 = radiation intensity of an isotropic source (W/unit solid angle)

P_{rad} = total radiated power (W)

When direction is not specified, it is implicitly considered the direction of maximum directivity. For antennas with orthogonal polarization components, it is defined the partial directivity of an antenna for a given polarization as "that part of the radiation intensity corresponding to a given polarization divided by the total radiation intensity averaged over all directions". For spherical coordinates the total directivity is given by the sum of the partial directivities for any two orthogonal polarizations θ and ϕ components expressed as in (2.7).

$$D = D_\theta + D_\phi \tag{2.7a}$$

$$D_\theta = \frac{4\pi U_\theta}{(P_{rad})_\theta + (P_{rad})_\phi} \tag{2.7b}$$

$$D_\phi = \frac{4\pi U_\phi}{(P_{rad})_\theta + (P_{rad})_\phi} \tag{2.7c}$$

2.1.4 Efficiency

The overall antenna efficiency (η_0) takes into account the losses at the input terminals and within the structure of the antenna itself (conduction and dielectric losses), which can be translated into two characteristics: reflection and radiation efficiency.

The mismatch or reflection efficiency (η_r) is directly related to the return loss (Γ), defined as:

$$\eta_r = (1 - |\Gamma|^2) \tag{2.8}$$

The antenna radiation efficiency (η_{cd}) is a measure of how much power is lost in the antenna due only to conductor and dielectric losses. These losses reduce the radiation in any and can be expressed as:

$$\eta_{cd} = \frac{P_{rad}}{P_{in}} \tag{2.9}$$

The overall antenna efficiency (η_0) is then given as:

$$\eta_0 = \eta_{cd}\eta_r \tag{2.10}$$

2.1.5 Gain

Gain is defined in the IEEE Standard Definitions of Terms for Antennas as:

"The ratio of the intensity, in a given direction, to the radiation intensity that would be obtained if the power accepted by the antenna were radiated isotropically. The radiation intensity corresponding to the isotropically radiated power is equal to the power accepted by the antenna divided by 4π" [9].

When the direction of radiation is not stated, the power gain is always calculated in the direction of maximum radiation and by definition defined as the ratio of the antenna radiated power density at a distant point to the total antenna input power (P_{in}) radiated isotropically:

$$G = \frac{4\pi U(\theta, \phi)}{P_{in}} \tag{2.11}$$

Or expressed by the product of the radiating efficiency by the directivity given as:

$$G = \eta_{cd}.D \tag{2.12}$$

It is important to refer that the IEEE standards state that "*gain does not include losses arising from impedance and polarization mismatches*". Some authors prefer to refer the gain as absolute gain (G_{abs}) which takes into consideration the reflection losses and is given as:

$$G_{abs} = \eta_r \, \eta_{cd} . D = \, (1 - |\Gamma|^2) \eta_{cd} . D \tag{2.13}$$

2.1.6 Bandwidth

The bandwidth (BW) of an antenna is defined in the IEEE Standard Definitions of Terms for Antennas as *"the range of frequencies within which the performance of the antenna, with respect to some characteristic, conforms to a standard"* [9].

The bandwidth (BW) of an antenna can be considered as the range of frequencies, on either side of a central frequency where the antenna characteristics (such as input impedance, radiation pattern, beam width, polarization, side lobe level, gain) are within an acceptable value of those of the central frequency

The antenna bandwidth is commonly referenced simply as "impedance bandwidth", describing the bandwidth where the antenna presents acceptable losses due to mismatch or by both "impedance bandwidth" and acceptable radiation pattern characteristics.

The impedance bandwidth can be measured directly by a Vector Network Analyzer (VNA) as it will be later explained in this chapter. Analyzing the Voltage Standing Wave Ratio (VSWR) or by the Return Loss (RL) over the frequency band it is possible to defined the antenna impedance bandwidth. Both VSWR and RL are dependent on the reflection coefficient (Γ) ("ratio of the amplitude of the reflected voltage wave (V_0^-) normalized to the amplitude of the incident voltage wave (V_0^+) at a load") given as:

$$\Gamma = \frac{V_0^-}{V_0^+} \tag{2.14}$$

VSWR is defined as *"the ratio between the maximum and minimum voltage of the standing wave created by the mismatch at the load on a transmission line"* and is given by:

$$\text{VSWR} = \frac{1 + |\Gamma|}{1 - |\Gamma|} \tag{2.15}$$

The RL is defined as *"the magnitude of the ratio of the reflected wave to that of the incident wave"*, and is defined in a logarithmic scale as:

$$RL_{(dB)} = -20log_{10}|\Gamma| \tag{2.16}$$

In RF we commonly analyze the antenna bandwidth by the scattering parameter S_{11} directly provided by the VNA, related to Γ as:

$$S_{11_{(dB)}} = 20log_{10}|\Gamma| \tag{2.17}$$

Based on previous parameters the maximum acceptable mismatch for an antenna is normally referred as 10% of the incident signal. This threshold is achieved when $|\Gamma| < 0.3162$ which can be translated according with the measuring parameter as (2.18) equations.

$$1 < VSWR < 2 \tag{2.18a}$$

$$S_{11_{(dB)}} < -10 \tag{2.18b}$$

$$RL_{(dB)} > 10 \tag{2.18c}$$

The antenna impedance bandwidth can then be expressed as absolute bandwidth, the interval between the highest (F_H) and lowest frequency (F_L) where the antenna performance is acceptable given by:

$$BW_{(H_z)} = F_H - F_L \tag{2.19}$$

According with the bandwidth the antennas can be considered narrowband or broadband. Commonly broadband antennas are defined as antennas that have a ratio of $\frac{F_H}{F_L} > 2$. For narrowband antennas, the bandwidth is often expressed by percentage related to the central frequency (F_C) defined as:

$$BW_{(\%)} = \frac{F_H - F_L}{F_C} \; where \; F_C = \frac{F_H + F_L}{2} \tag{2.20}$$

For broadband antennas the bandwidth is typically expressed as the ratio of the highest to the lowest frequency (e.g 40:1) where the antenna performance is acceptable:

$$BW = F_H/F_L \tag{2.21}$$

2.1.7 Polarization

The polarization of an antenna refers to the orientation of the electric field vector of its radiated wave and is defined in the IEEE Standard Definitions of Terms for Antennas as:

"The property of an electromagnetic wave describing the time varying direction and relative magnitude of the electric-field vector; specifically, the figure traced as a function of time by the extremity of the vector at a fixed location in space, and the sense in which it is traced, as observed along the direction of propagation" [9].

Antenna polarization can then be seen as the curve traced by the tips of the arrows representing the instantaneous electric field and observed along the direction of propagation, describing a polarization ellipse as presented in Fig. 2.2 . The polarization of an antenna is often characterized by electric field direction of rotation and its polarization ellipse (maximum magnitudes of E components and tilt angle, τ).

Antenna polarization can be divided as: linear, circular and elliptical, however linear and circular polarization can be seen as special cases of elliptical polarized antennas. Linear when the ellipse collapses into a line and circular when the polarization ellipse varies minimally becoming a circle.

The figure of the electric field is traced in clockwise (*CW*) or counterclockwise (*CCW*) sense. CW is also designed right-hand (*RH*) and CCW left-hand (*LH*) polarization.

The instantaneous electric field of a plane wave travelling in the negative z direction may be written as:

$$E(z,t) = E_x(z,t)\hat{x} + E_y(z,t)\hat{y} \tag{2.22}$$

Where the instantaneous components are defined as:

$$E_x(z,t) = E_{x0}cos(\omega t + \beta z + \phi_x) \tag{2.23a}$$

and

$$E_y(z,t) = E_{y0}cos\left(\omega t + \beta z + \phi_y\right) \tag{2.23b}$$

E_{x0} and E_{y0} represent the electric field maximum magnitudes, ϕ_x and ϕ_y are the phase angles of the x and y components, ω is the angular frequency, and β is the propagation constant.

The polarization ellipse parameters (OA major axis and OB minor axis) can be calculated by equations (2.24).

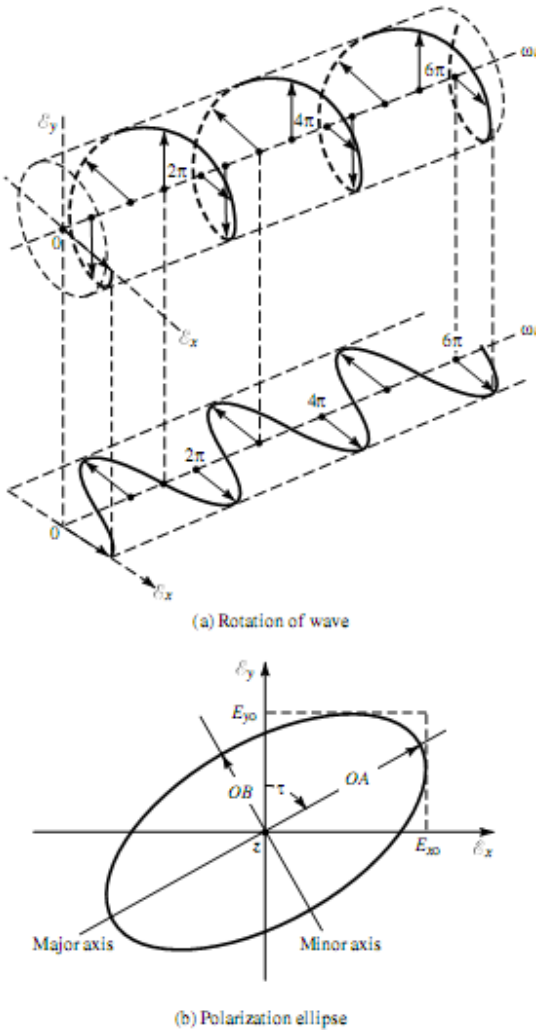

Fig. 2.2 Rotation of a plane EM wave and its pol. ellipse at z = 0 [11]

$$OA = \left[\frac{1}{2}\left\{{E_{xo}}^2 + {E_{yo}}^2 + \left[{E_{xo}}^4 + {E_{yo}}^4 + 2.{E_{xo}}^2{E_{yo}}^2.\cos(2\Delta\phi)\right]^{1/2}\right\}\right]^{1/2} \quad (2.24a)$$

$$OB = \left[\frac{1}{2}\left\{{E_{xo}}^2 + {E_{yo}}^2 - \left[{E_{xo}}^4 + {E_{yo}}^4 + 2.{E_{xo}}^2{E_{yo}}^2.\cos(2\Delta\phi)\right]^{1/2}\right\}\right]^{1/2} \quad (2.24b)$$

$$\tau = \frac{\pi}{2} - \frac{1}{2}tan^{-1}\left[\frac{2E_{xo}E_{yo}}{{E_{xo}}^2 - {E_{yo}}^2}.\cos(2\Delta\phi)\right] \quad (2.24c)$$

Where

$$\Delta\phi = \phi_x - \phi_y \quad (2.24d)$$

The performance of antenna polarization can also be characterized by its axial ratio (*AR*), defined as the ratio of the major axis to the minor axis of the polarization ellipse described as:

$$AR = \frac{major\ axis}{minor\ axis} = \frac{OA}{OB} \tag{2.25}$$

For circular polarization OA = OB (AR = 1), whereas for linear polarization AR tends for infinite.

2.2 Electromagnetic simulators

Nowadays there are several software packages available on the market for antenna simulation (e. g. IE3D, CST Microwave Studio, FEKO, XFDTD and HFSS) implemented with different time and frequency domain methods (e.g. Method of Moments (MoM), Finite Element Method (FEM), Finite-difference time-domain (FDTD) and Transmission Line Matrix (TLM)), each with their own advantages and disadvantages. The comparisons of the simulators performance it is out of the scope of this thesis, however for a better understand of the methods a short resume is presented in Table 2.1.

	Frequency domain methods		***Time domain methods***	
	MoM	***FEM***	***FDTD***	***TLM***
Advantages	Fast as single frequency; Easily combined with other methods to deal with large problems		Broadband results is one simulation; Good for pulse-type problems;	
Disadvantages	Difficult to deal with pulse-type problems		Not suitable for electrically large systems	
Notes	Most suitable for wire-type antennas	Be careful with very thin wires	Be careful with the boundary conditions	Be careful with thin wires

Table 2.1 Comparison of the time and frequency domain methods

The knowledge of the simulation process and methods is of high importance in order to optimize the simulation time and evaluate its accuracy. In this thesis we will refer only to the used simulator for design and simulation, High Frequency Structural Simulator (HFSS) from Ansys [12].

2.2.1 High Frequency Structural Simulator (HFSS)

Ansys HFSS utilizes a 3D full-wave FEM to compute the electrical behavior of high-frequency and high-speed components [12]. A rigorous mathematical foundation of FEM was provided by Strang in 1973 [13].

FEM is a numerical method based on solving partial differential equations. It subdivides the full problem into large number of smaller regions and represents the field in each sub-region (element) expressed in terms of a number of basic functions. As simplified analysis FEM may be implemented in EM simulators in the following steps [14]:

1) Discretization of the solution region into elements;
2) Assign a basis function to each element, representing the fields on it;
3) Generation of a matrix equation that represents the interaction between each segment and every other;
4) Solve the interaction-matrix to get the coefficient of basis functions;
5) Calculate the far-field patterns and other parameters using the fields on each segment.

In HFSS the geometrical model is automatically divided into large number of tethaedra, where a single tethaedron is a four-sided pyramid and the collection of tethaedra is referred as the finite element mesh as shown in Fig. 2.3.

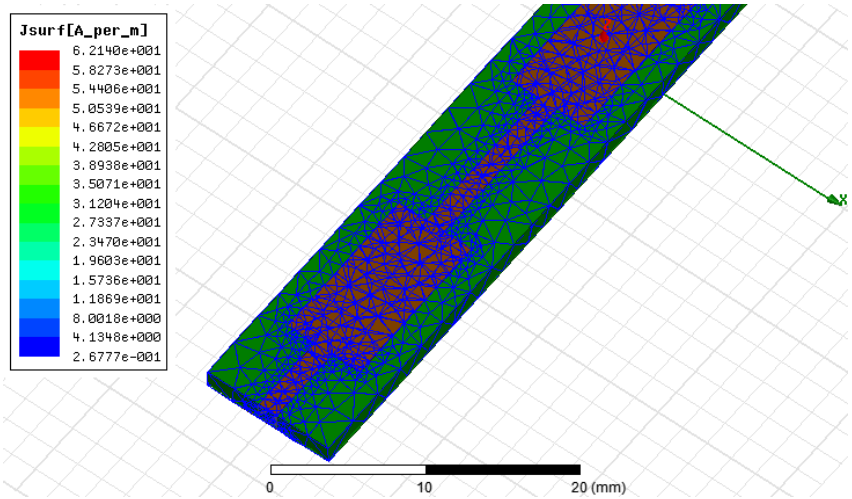

Fig. 2.3 HFSS design mesh

The simulation process of HFSS can be resumed by flow chart of Fig. 2.4 [15].

The first step starts by the parametric model where the geometry, boundaries and excitations are defined. After the analysis setup is defined, the solution setup and frequency sweeps are settled. The analysis is performed by a solve loop, and finally the results and the reports are presented.

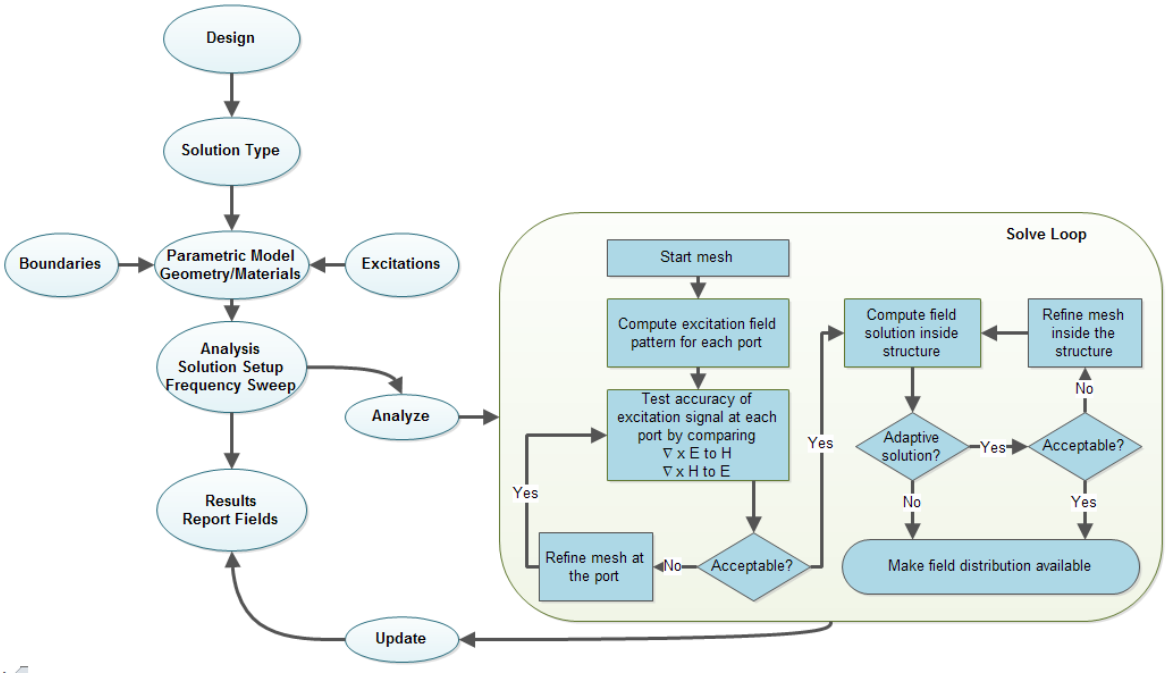

Fig. 2.4 HFSS operation flow chart

The solved loop process starts with the initial definition of this mesh. Then it is necessary to determine the excitation field pattern at each port. The field patterns of a traveling wave inside waveguide for each frequency can be solved by equation (2.26), derived by Maxwell's equations:

$$\nabla \times \left(\frac{1}{\mu_r}\nabla \times \boldsymbol{E}(x,y)\right) - {k_0}^2 \varepsilon_r \boldsymbol{E}(x,y) = 0 \tag{2.26}$$

Where:

$\boldsymbol{E}(x,y)$ is a phasor representing an oscillating electric field;

k_0 is the free space wave number;

μ_r is the complex relative permeability;

ε_r is the complex relative permittivity.

After solving this equation it is obtained the field pattern in the form of phasor solution $\boldsymbol{E}(x, y)$. It also performed an independent calculation for $\boldsymbol{H}(x, y)$ with the corresponding wave equation in $\boldsymbol{H}$.

After field computation it is performed a refinement procedure based on Maxwell equations, more specifically Ampere and Faraday equation and the derivative property of Fourier transforms which result in (2.27) equations.

$$\nabla \times \boldsymbol{H} = \sigma \boldsymbol{E} + j\omega\varepsilon \boldsymbol{E} \tag{2.27a}$$

$$\nabla \times \boldsymbol{E} = -j\omega\mu \boldsymbol{H} \tag{2.27b}$$

After $\boldsymbol{E}$ and $\boldsymbol{H}$ are calculated, it is computed $\nabla \times \boldsymbol{H}$ and compared with the solved $\boldsymbol{E}$. Then $\nabla \times \boldsymbol{H}$ is computed and compared with solved $\boldsymbol{H}$. If the result falls within an acceptable tolerance, the solution is accepted, if not the mesh network is refined.

Achieved the accepted field solution at defined port (or ports) it is computed the field solution inside the simulation structure where a similar refinement procedure is performed. Finalized this process all desired reports can be provided.

2.3 Antenna Measuring System

Once an antenna is designed and constructed, it is essential to validate the design with proper measurements. In this thesis the antennas were validated by measuring the impedance bandwidth, radiation pattern, antenna gain and polarization.

The antenna measurement system used in this thesis is shown in Fig. 2.5 and includes the following equipments:

1) Tapered far field anechoic chamber with proper absorber materials to reduce unwanted reflected energy;
2) Test positioner (3 axis) to provide elevation and azimuthal rotation of the antenna under test (AUT);
3) Polarization positioner (2 axis) to provide polarization rotation;
4) Positioner controller for rotation control;
5) VNA for transmitting and receiving signals;
6) Antennas with standardized gain for correct gain reference (used a linear polarized horn antenna);
7) Computer with proper application for data processing.

Not all antennas can be measured in this system which is limited mainly by VNA bandwidth, sensitivity; dynamic range and anechoic chamber size, defining a minimum valid testing frequency defined by far field conditions. For a better understanding of this limitation, far field condition, anechoic chambers and radio absorbers are next briefly described.

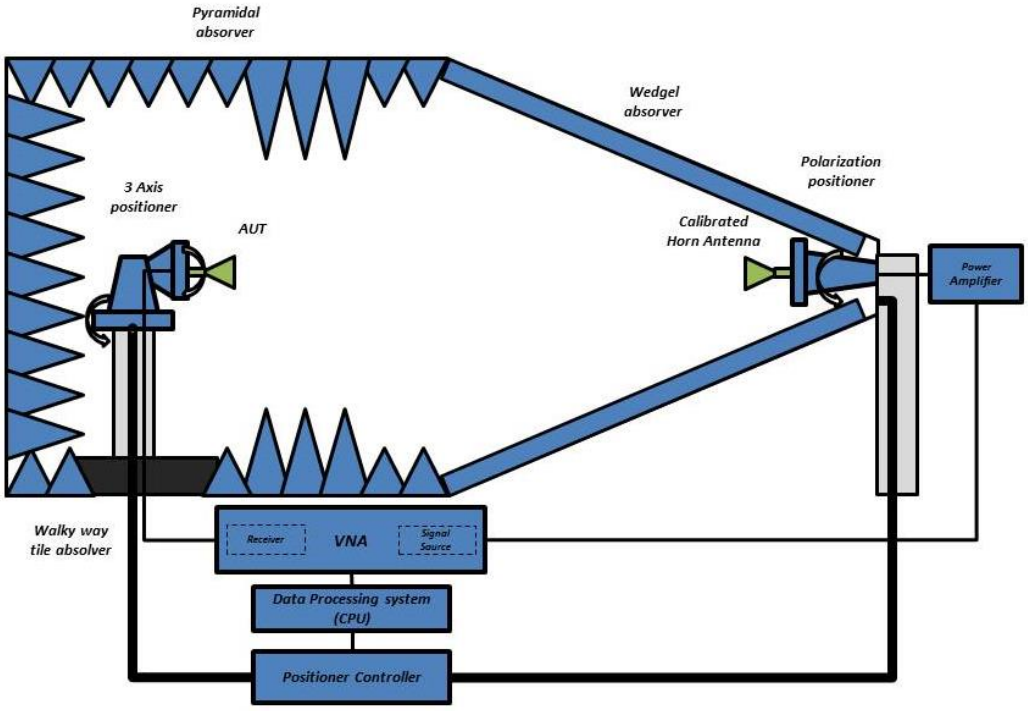

Fig. 2.5 Antenna measuring system

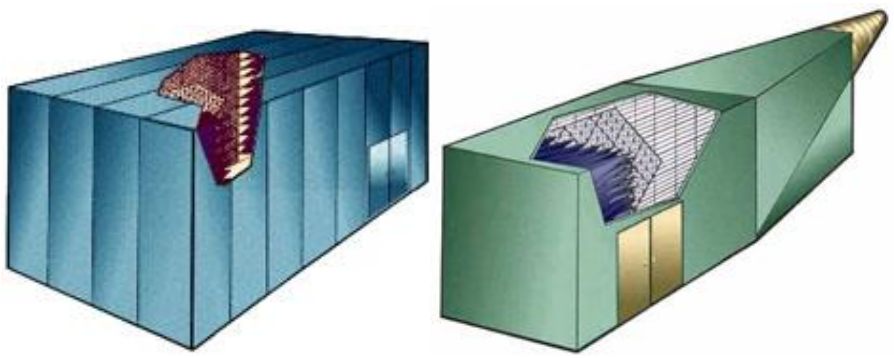

Fig. 2.6 Tapered (left) and Rectangular (right) Anechoic Chambers [19]

There are two main kind of anechoic chambers, rectangular and tapered chambers.

Tapered anechoic chambers have a form of pyramidal horn, starting with a tapered chamber leading to a rectangular configuration at the test zone. Rectangular chamber, as the name suggests, has a rectangular shape as shown in Fig. 2.6.

In the tapered chambers we can move the source near the apex in order to provide a nearly constructive interference with the direct rays at the test location. The direct and reflected waves near the test antenna region are vector added (due to in phase waves) providing a relatively smooth amplitude variation [18]. This smoother variation makes these chambers more suitable for radiation pattern measurements using low-gain antennas.

For higher frequency, it becomes harder to place the source antenna sufficiently close to the apex that the phase difference between the direct and specular reflected waves can be maintained below an acceptable level. For these cases, it is common to use a high gain antenna whose radiation towards the walls is minimal, suppressing the reflections from the walls of the chamber. Also the source antenna is usually moved from the apex to a place closer to the end of the tapering section, simulating a rectangular chamber. This is the case of the used anechoic chamber in Aveiro University.

This kind of chamber exhibits better low frequency performance, and provides significant cost saving as a result of less surface area, and also use of less expensive absorbers. Despite all referred advantages, these chambers exhibit several disadvantages compared with rectangular anechoic chambers.

In tapered chambers there is a multipath effect which implies a simulation of not exactly a free-space environment (Quasi-free space). Because of this, the power density in the chamber will deviate from the distance (R) dependence l/R^2; being dependent of the path difference and the reflection coefficient at the walls [20].

Tapered anechoic chambers can't be used for measurements involving absolute field strength since they provide different path loss comparing to the one of free space, although relative gain measurements can be performed.

This kind of anechoic chamber is also not suitable for measurements involving several sources or moving sources, or bistatic radar cross section. This is because only one source can be placed at the apex and the multipath effect provides deviated measurements for absolute gain results [20].

When a dependency of l/R^2 is demanded or a more uniform testing chamber is preferred, the use of rectangular chambers (although they demand more space) is needed,

obviously bigger costs are involved. According with the anechoic chamber type and its placement different type of radio absorbers can be more suitable. A resume of those absorbers are described in next section.

2.3.1 Wave Absorbers

Radio wave absorbers in anechoic chamber are the materials which provide the absorption of radio waves that try to enter or exit the anechoic chamber. There are several common types of absorbers such as pyramidal, wedge, walkway foam absorbers and ferrite tiles. The use of these materials is not new, being its origins related to the efforts to build aircraft which absorbed or scattered radar signals during the World War II which provided radar camouflage [21].

The performance of the selected absorber is determined by the reflection coefficient (Γ), which is the relation between the magnitude of reflected (Er) and incident (Ei) electric-fields of plane waves, or alternatively, the absorber performance can also be described by reflectivity (R) in decibels, given by:

$$R = 20log_{10}(|\Gamma|)[dB] \tag{2.28}$$

The smaller the value of *R* (dB), better the absorber performance.

The reflections from absorbing material represent constructive or destructive interference at the receiving antenna of anechoic chamber, being the reason they should be minimized.

2.3.3.1 Urethane Pyramidal Absorber

Pyramidal absorbers are one of the most common materials used for absorption in anechoic chambers, being constitute in majority of urethane foam and loaded with carbon. These pyramids exhibit dimensions typically higher than λ/2.

The effective impedance presented in this kind of absorbers is essentially 377Ω at the tip, changing gradually over the height *h* till impedance in the base of typically:

$$Z = \frac{377}{\sqrt{2 - j1}} = 245.24 + j57.97\ \Omega \tag{2.29}$$

This happens because the pyramidal have μ_r=1 being a non magnetic material and ε_r=2-j1, low permittivity with losses. Like this it becomes electrically lossier with deepness. Due to this long taper, the signal will be progressively absorbed. For example, if we do not have the taper, the reflective coefficient would be of -12.4dB, where acceptable values are typically smaller than -30/-40dB.

$$|Z| = \left|\frac{Z_L - Z_0}{Z_0 - Z_L}\right| = 0.24\ or\ -12.4dB \tag{2.30}$$

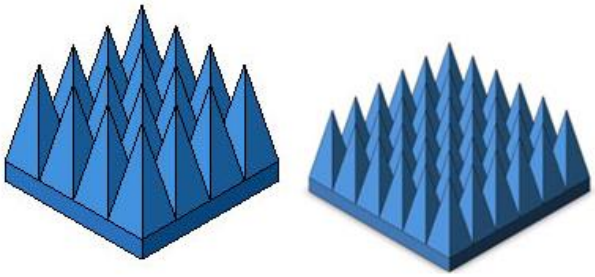

Fig. 2.7 Pyramidal absorber examples [19]

The degree of carbon loading in the urethane foam is an important factor when producing these kinds of absorbers. Being the reflectivity greatly dependent on the quantity of carbon introduced in the foam. These variations of reflectivity versus thickness of carbon coating in the foam in relation with the frequency are described Fig. 2.8.

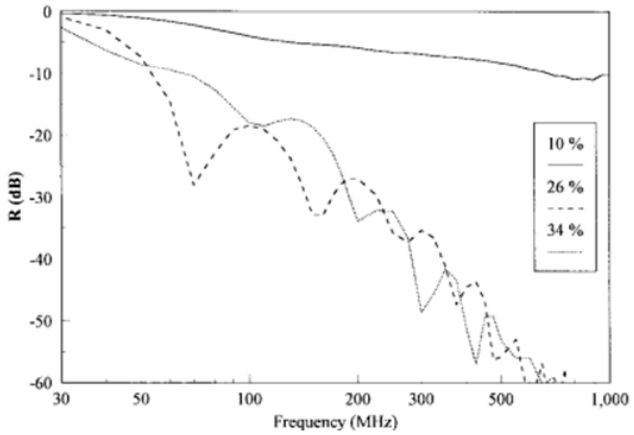

Fig. 2.8 Normal-incident *R* for 1.22m urethane for diferent carbon loadings [22]

It is seen that the better carbon loading for 1.22 meters pyramids is 34% and the better loading for the 2.44 meters pyramids is 26%.

The pyramids act as impedance matching networks, being the amount of carbon loading determinant for the effective characteristic impedance of the pyramids. If the carbon

loading is too high, the impedance between free space and the absorber will be too abrupt, causing the incident wave to be reflected from the region near the pyramid tips. On the other hand, if the loading is too low, the incident wave that penetrates the pyramids will not be absorbed being reflected by the metallic chamber wall. By other words, it would be expected that a material of higher loss tangent and higher dielectric constant to provide adequate loss at reduced thickness, although, a material with these characteristics would lead to impedance different from free space, and consequently to higher front-face reflection.

Usually pyramidal absorbers as standard, are painted with blue latex based paint because provides a good light reflectance from external lightning, reducing the requirements for lighting within the chamber. As a safety standard, this referred paint is treated with fire-retardant chemicals. Although, typically for bigger dimension pyramidal absorbers, the tips are not painted, providing a bigger absorption. It is important to consider that the paint provide some degradation of absorber reflectivity [22].

The performances of pyramidal absorbers are commonly specified as the reflectivity at normal incidence. A typical table describing its performance relating thickness versus frequency is shown Fig. 2.9.

	Height	Weight	Tips per	Normal Incidence Reflectivity, GHz									
Type	(cm)	(kg)	piece	0.12	0.3	0.5	1.0	3.0	6.0	10.0	18.0	36	50
P-4	10.9	1.4	144					30	35	42	50	50	50
P-6	15.2	1.6	100					32	40	45	50	50	50
P-8	20.3	2	64				30	37	45	50	50	50	50
P-12	30.5	2.7	36				35	40	45	50	50	50	50
P-18	45.7	5.4	16			30	37	40	45	50	50	50	>45
P-24	61	7.7	9		30	35	40	45	50	50	50	50	>45
P-36	91.4	10.9	4		35	37	42	50	50	50	50	50	>45
P-48	121.9	17	2	28	35	40	50	50	50	50	50	50	>45
P-72	182.9	23	1	33	40	45	50	50	50	50	50	50	>45

Note: Base dimensions are 2ft x 2ft

Fig. 2.9 General Pyramidal Absorber Performances [22]

2.3.3.2 Twisted urethane pyramids

This kind of pyramid is similar to standard pyramid, with the change of being rotated 45º, presented in Fig. 2.10. These absorbers have the advantage of being constructed using less material exhibiting tips that droop less with age comparing with standard pyramids.

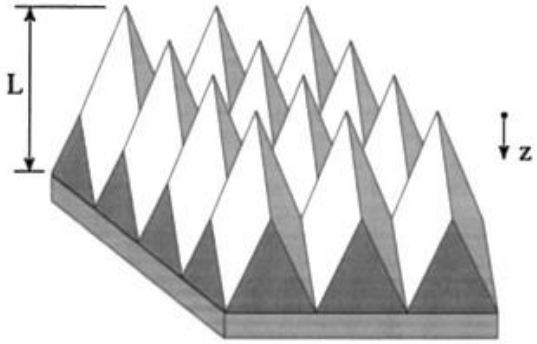

Fig. 2.10 Twisted urethane pyramid [22]

This kind of absorber does not perform as well as standard urethane pyramids referred before, although, using different geometries and carbon loadings, these materials can be optimized to achieve reflectivity low as those archive with standard pyramids.

2.3.3.3 Wedge Absorber

Wedge absorbers have a shape of triangular prisms, they provide lower reflectivity at normal incident angle than typical pyramidal absorbers, but in counterpart they provide better backscattering absorption.

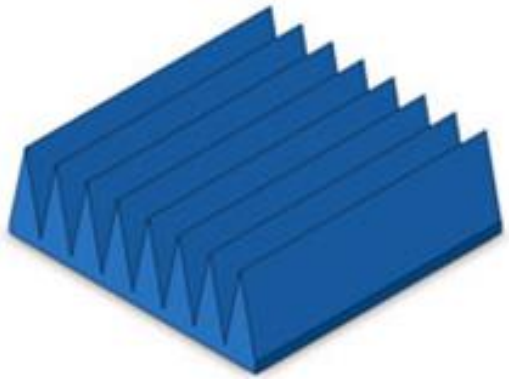

Fig. 2.11 Wedge Absorber example [19]

When an incident wave strikes the absorber wall by an oblique angle to normal vector, two erroneous signals are generated: a forward going reflected signal and a back-scattered signal. As referred in [23], the backscattering strength of wedge absorber is lower than pyramid absorber. So, to prevent back-scattered signal wedge absorbers are preferred.

When the inclined angle of incidence is large, the relevance of back-scattered signal become also larger, so the focus in these situations should be more turned to prevent

electromagnetic wave from entering into quiet zone (receiver antenna position) by backscattering instead of the absorbing capabilities of material reducing reflected signal.

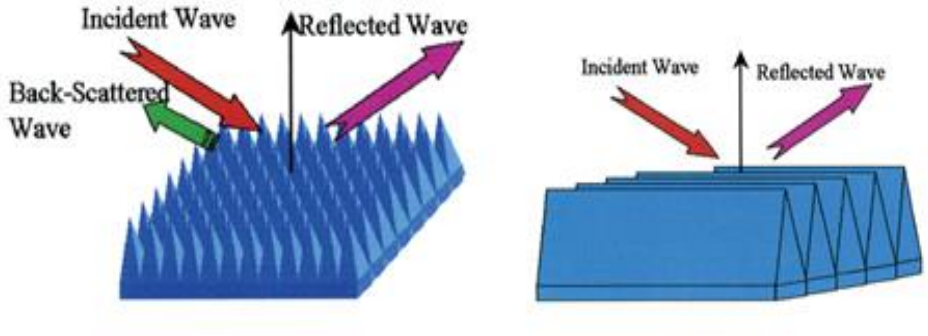

Fig. 2.12 Pyramidal and Wedge reflection comparison [24]

2.3.3.4 Ferrite Tiles and Grids

Ferrite tiles absorbers have much smaller thickness (*in order of mm*) than pyramidal absorbers and are mainly used due to its flat shape. They provide a very attractive alternative to typical bulkier walky-way tiles which are low-density rigid polystyrene foam used to encapsulate a standard pyramidal or wedge absorber. Normally is also incorporated with a thin sheet of semi-rigid polyvinyl chloride foam adhered to the top to provide a walking surface [25].

From Maxwell's equations is shown that a medium with complex permeability equal to its complex dielectric constant would have no reflection for radiation at normal incidence angle, because this medium would have impedance equal to free-space (377Ω). Ferrite shown to have these desired characteristics although for a narrow frequency range.

With a big research in this area, ferrite based absorbers can provide nowadays reflectivity of 10 to 25dB in 30 to 1000MHz.

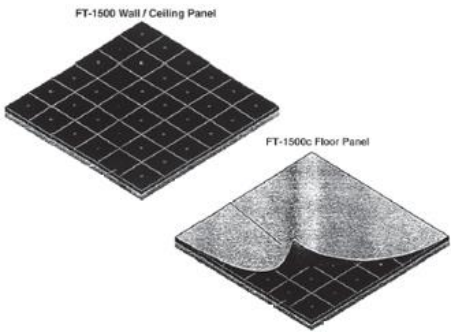

Fig. 2.13 Ferrite tiles [25]

It is also common used ferrite grid (or waffle) instead of typical ferrite tiles. This kind of tile is constituted by a grid of square air sections cut into a ferrite tile.

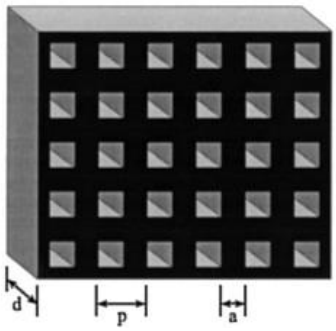

Fig. 2.14 Grid or waffle ferrite tile geometry [22]

The reflectivity of the ferrite grid is very dependent of the filling factor ($g=a^2/p^2$), being *a*, the periodic ferrite length in the grid and *p* the periodic ferrite plus the air section length in the grid. The advantage of the implementation of ferrite grid geometry over the standard solid tile is the addition of a new parameter (the filling factor) that can be varied in order to minimize the reflectivity at a desired frequency. So, ferrite grid can be designed to have a reduced reflectivity in a desired frequency band providing better performance over that of the standard solid tiles by appropriately choosing the tile thickness and filling factor.

Ferrite tiles perform well from 30 to 600 MHz [22] being a useful material for low frequencies, where the use of pyramidal tiles are size and cost inadequate.

2.3.3.5 Hybrid Absorber

As previous mentioned urethane pyramids provide low reflectivity above few hundreds of MHz, and ferrite tiles provide good reflectivity below several hundred MHz. Due to these materials characteristics they are usually combined to achieve a compact wideband absorber that performs well from 30MHz until dozens of GHz frequency range.

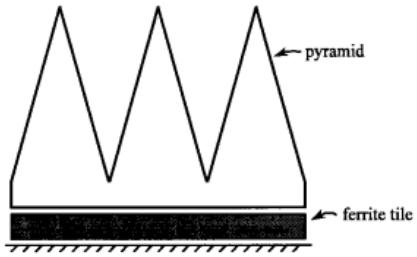

Fig. 2.15 urethane-pyramid and ferrite-tile hybrid [22]

2.3.3.6 Improvement with dielectric layer

The responsive bandwidth performance of ferrite can be improved dramatically by adding a dielectric layer (spacer) between the ferrite tiles and the metal wall, as describe in Fig. 2.16. This is also applied for urethane pyramid absorbers or hybrid absorbers. One of the most typical spacers used is wood.

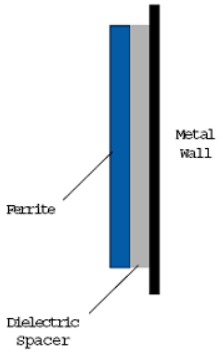

Fig. 2.16 Dielectric spacer between ferrite tile and metal wall [26]

Like this, the absorber can be tuned to a desired frequency by varying the ferrite tile and/or dielectric layer thickness. This ability of being able to tune the absorber can be important when we are trying to eliminate undesirable resonances that may occur in certain room sizes. Although, we need to take in attention that to improve some certain frequency range zones with ferrite/dielectric, we will degrade the reflectivity in other frequency range. This is evident analyzing Fig. 2.17.

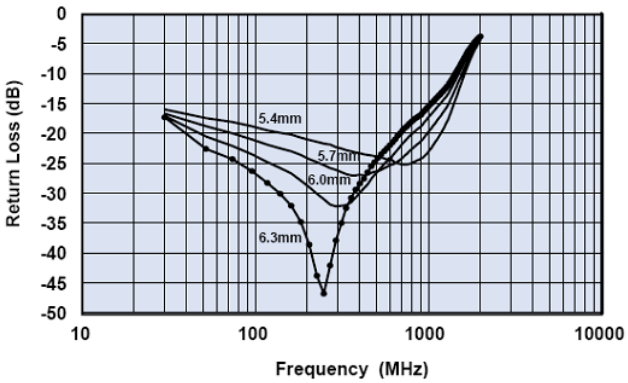

Fig. 2.17 Reflectivity of varying dielectric spacer length [26]

2.4 Antenna Measurements Procedures

Having understood the antenna measuring system it is now possible to correctly measure the antenna. In this section the procedures for impedance bandwidth, radiation pattern, gain, directivity, efficiency and polarization are described.

All measurements assume the use of the previous equipments, a VNA and a far field anechoic chamber.

2.4.1 Impedance bandwidth

As previous described the antenna impedance bandwidth refers to the frequency band that presents a mismatch lower than 10% of the incident signal.

This mismatch can be measured by the VSWR, RL or by the forward reflection coefficient (S_{11}) having the threshold values resumed as in (2.18), here again referred:

$$1 < SWR < 2 \tag{2.31a}$$

$$S_{11_{(dB)}} < -10 \tag{2.31b}$$

$$RL_{(dB)} > 10 \tag{2.31c}$$

These measurements are commonly performed by a VNA but can also be performed by a SNA. The standard measurement procedure can be resumed as:

1. Select a suitable cable (low loss and phase stable) for the measurement and properly connect it to the VNA;
2. Select the measurement frequency range and suitable number of measurement points;
3. Perform the one-port calibration and ensure that the cable is not moved;
4. Conduct the measurements in an environment with little reflection (recommended in an anechoic chamber);
5. Perform the measurements according with the desired parameter, VSWR, RL or S_{11} and analyze the frequency band below the threshold.

2.4.2 Radiation Pattern

Radiation pattern measurements always refers to electric field or the power (which is proportional to the electric field squared) analysis. When in a linear scale, the field and power pattern may look very different, however, when the patterns are plotted on a logarithmic scale (dB plot), both the normalized field and power patterns are the same since $10\ log_{10}(P/Pmax)$ is equivalent to $20\ log_{10}(E/Emax)$. Thus, in practice, we often plot the patterns in dB scale.

The RP can be measured by the transmission coefficient (S_{21}) between the source and testing antennas. The S_{21} measures the voltage gain which has the same value of power gain and can be analogue to E gain given as:

$$S_{21}(dB) = 20log_{10}\left|\frac{V_t}{V_r}\right| \tag{2.32a}$$

$$= 10log_{10}\left|\frac{P_t}{P_r}\right| \tag{2.32b}$$

$$= 20log_{10}\left|\frac{E_t}{E_r}\right| \tag{2.32c}$$

The field pattern is then given by the normalization of the total field pattern described by the vector sum of the two orthogonally polarized radiated field components:

$$E_{(\theta,\varphi)} = \sqrt{\left|E_{\theta\,(\theta,\varphi)}\right|^2 + \left|E_{\varphi\,(\theta,\varphi)}\right|^2}\ (V/m) \tag{2.33}$$

For a practical explanation let's consider for instance the Fig. 2.18 where two planes are desired to be measured: $E_{(\theta,\varphi=0)}$, the elevation plane of φ =0º, and $E_{(\theta=90,\varphi)}$, the azimuthal plane of θ = 90º.

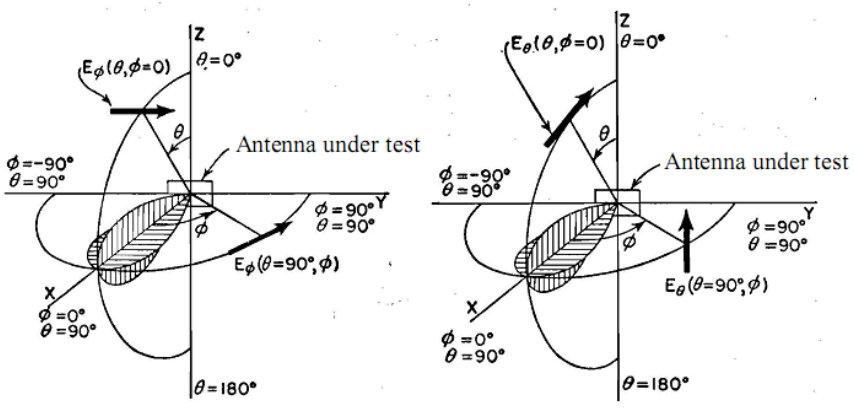

Fig. 2.18 Antenna system reference

To measure the field radiation pattern with the antenna range measurement system previously described, the measuring procedure in a VNA can be defined as:

1. Measure the $S_{21,}\frac{P_t}{P_r}$ between AUT and source antenna in φ for θ = 90º (azimuthal plane of θ = 90º). Perform the measurements with source antenna in vertical polarization $E_{\theta\,(\theta=90,\varphi)}$and then with horizontal polarization $E_{\varphi\,(\theta=90,\varphi)}$.
2. Measure the $S_{21,}\frac{P_t}{P_r}$ between AUT and source antenna in θ for φ = 0º (elevation plane of φ = 0º). Perform the measurements with source antenna in vertical polarization $E_{\theta\,(\theta,\varphi=0)}$and then with horizontal polarization $E_{\varphi\,(\theta,\varphi=0)}$.
3. **a)** Calculate the non-normalized RP for azimuthal plane of θ = 90º based on S_{21} magnitude given as

$$\mathrm{RP}_{S_{21}(\theta=90,\varphi)} = \sqrt{\left|S_{21\theta\,(\theta=90,\varphi)}\right|^2 + \left|S_{21\varphi\,(\theta=90,\varphi)}\right|^2}\ \text{(linear)} \tag{2.34}$$

3 b) Calculate the non-normalized RP for elevation plane of φ = 0º based on S_{21} magnitude given as

$$\mathrm{RP}_{S_{21}(\theta,\varphi=0)} = \sqrt{\left|S_{21\theta\,(\theta,\varphi=0)}\right|^2 + \left|S_{21\varphi\,(\theta,\varphi=0)}\right|^2}\ \text{(linear)} \tag{2.35}$$

4 a) Pattern normalization of azimuthal plane of θ= 90º in logarithmic scale given as:

$$\overline{\mathrm{RP}_{(\theta=90,\varphi)}}_{(dB)} = 20\log_{10}\frac{\mathrm{RP}_{S_{21}(\theta=90,\varphi)}}{\max\left(\mathrm{RP}_{S_{21}(\theta=90,\varphi)}\right)} \tag{2.36}$$

4 b) Pattern normalization of elevation plane of φ = 0º in logarithmic scale given as:

$$\overline{\mathrm{RP}_{(\theta,\varphi=0)}}_{(dB)} = 20\log_{10}\frac{\mathrm{RP}_{S_{21}(\theta,\varphi=0)}}{\max\left(\mathrm{RP}_{S_{21}(\theta,\varphi=0)}\right)} \tag{2.37}$$

2.4.3 Gain Measurements

There are several techniques that can be employed to make gain measurements. These techniques are described in detail in [20].

A brief overview of each method will be described in this section. There are two main methods of gain measurements: absolute-gain and gain comparison (gain-tranfer).

The absolute gain measurements are based on Friis transmission formula and can be performed by the two-antenna method and three-antenna method.

Absolute measurements are not very accurate into a tapered anechoic chamber. For accurate measurements a rectangular anechoic chamber need to be used and the following criterions need to be fulfilled:

- The antennas need to be well matched in terms of impedance and polarization;
- Far field condition need to be verified;
- The antennas are aligned for boresight radiation;
- The system needs to be stable.

2.4.3.1 Two-antenna method

Two-antenna method is used when we have two identical test antennas whose gain is unknown, one as transmitter and the other as receiver.

The measuring steps can be resumed as follows:

1) Calibration of the system loss;

2) Correct positioning in terms of polarization matching;

3) Measurement of S_{21} between antennas, $S_{21} = 10log_{10}\left(\frac{P_r}{P_t}\right)$;

4) Calculation of path loss (PL), $PL = 20log_{10}\left(\frac{4\pi l}{\lambda}\right)$;

5) Calculation of antennas gain by the:

$$(G)_{dB} = \frac{1}{2}\left[20log_{10}\left(\frac{4\pi l}{\lambda}\right) + 10log_{10}\left(\frac{P_r}{P_t}\right)\right] \quad (2.38)$$

2.4.3.2 Three-antenna method

Three antenna method is used when the antennas we want to measure are not identical. For this method three antennas must be employed and three measurements must be made.

The measuring steps can be resumed as follows:

1) Calibration of the system loss;

2) Correct positioning of antennas in terms of polarization matching;

3) Calculation of path loss (PL), $PL = 20log_{10}\left(\frac{4\pi l}{\lambda}\right)$;

4) Perform following set of measurements with a VNA:

a) Antenna 1 as transmiter and antenna 2 as receiver

$$(G_1)_{dB} + (G_2)_{dB} = 20log_{10}\left(\frac{4\pi R}{\lambda}\right) + 10log_{10}\left(\frac{P_{r2}}{P_{t1}}\right) \quad (2.39)$$

b) Antenna 1 as transmiter and antenna 3 as receiver

$$(G_1)_{dB} + (G_3)_{dB} = 20log_{10}\left(\frac{4\pi R}{\lambda}\right) + 10log_{10}\left(\frac{P_{r3}}{P_{t1}}\right) \quad (2.40)$$

c) Antenna 2 as transmiter and antenna 3 as receiver

$$(G_2)_{dB} + (G_3)_{dB} = 20log_{10}\left(\frac{4\pi R}{\lambda}\right) + 10log_{10}\left(\frac{P_{r3}}{P_{t2}}\right) \quad (2.41)$$

5) Calculate the gain of each antenna by solving the following equations.

$$(G_1)_{dB} + (G_2)_{dB} = A \quad (2.42a)$$

$$(G_1)_{dB} + (G_3)_{dB} = B \quad (2.42b)$$

$$(G_2)_{dB} + (G_3)_{dB} = C \quad (2.42c)$$

$$(G_1)_{dB} = \frac{-A + B + C}{2} \quad (2.42d)$$

$$(G_2)_{dB} = \frac{A - B + C}{2} \quad (2.42e)$$

$$(G_3)_{dB} = \frac{-A + B + C}{2} \quad (2.42f)$$

2.4.3.3 Gain-Comparison

Gain comparison method is used when we have a gain standard (with a known gain) match on measuring frequency. This is the techniques used for antenna gain measurement in this thesis which can be performed into a tapered anechoic chamber.

The measuring steps can be resumed as follows:

1) Place the AUT in receiving mode, and measure its received power (P_{AUT})

2) Replace AUT by a standard antenna and measure received power (P_{GS}) (The geometrical arrangement need to be kept intact)

3) The two measures lead to following system of equations:

$$G_{AUT\,dB} + G_{0\,dB} = 20log_{10}\left(\frac{4\pi R}{\lambda}\right) + \ 10log_{10}\left(\frac{P_{AUT}}{P_0}\right) \tag{2.43}$$

$$G_{GS\,dB} + G_{0\,dB} = 20log_{10}\left(\frac{4\pi R}{\lambda}\right) + \ 10log_{10}\left(\frac{P_{GS}}{P_0}\right) \tag{2.44}$$

Where,

$G_{AUT\,dB}$ is the gain of the test antenna;

$G_{GS\,dB}$ is the gain of the gain standard; and

$G_{0\,dB}$ is the gain of the transmitting antenna.

4) Resolving the equations results in (2.45).

$$G_{AUT\,dB} = G_{GS\,dB} + \ 10log_{10}\left(\frac{P_{AUT}}{P_0}\right) - 10log_{10}\left(\frac{P_{GS}}{P_0}\right) \tag{2.45a}$$

$$= G_{GS\,dB} + \ 10log_{10}\left(\frac{P_{AUT}}{P_{GS}}\right) \tag{2.45b}$$

If the test antenna is elliptically polarized (also circular polarized) its gain is measured by analyzing its partial gains at two orthogonal orientations, for example the horizontal and vertical orientation. First we measure (use comparison method) the gain in the vertical orientation GTV. Then rotate the antenna about its axis through 90º and measure its gain in the horizontal orientation GTH. The total gain of the antenna GT related to an isotropic antenna with same polarization given by:

$$(G_T)_{dB} = 10log_{10}(G_{TV} + G_{TH}) \tag{2.46}$$

2.4.4 Directivity

The directivity is directly related to the pattern measurements. Once the pattern is found over the sphere, the directivity can be determined.

Directivity is defined as the ration of antenna radiation intensity ($U_{(\theta,\varphi)}$) in a given direction over the radiation intensity of an isotropic source which is often expressed in dBi given as:

$$D = \frac{U}{U_0} \tag{2.47a}$$

$$= \frac{U}{P_{rad}/4\pi} \tag{2.47b}$$

Where, U = radiation intensity (W/unit solid angle)

U_0 = radiation intensity of an isotropic source (W/unit solid angle)

P_{rad} = total radiated power (W)

The radiation power can be found by integrating the radiation power pattern $U_{(\theta,\varphi)}$ over a full sphere. Substituting this integrated expression for P_{rad} in (2.47a)) it results in:

$$D = \frac{U_{max}}{\frac{1}{4\pi}\int_0^{2\pi}\int_0^{\pi} U_{(\theta,\varphi)}.\sin(\theta)\,.d\theta\,d\,\varphi} \tag{2.48}$$

The numerical equivalent is given as:

$$D_{(\theta,\varphi)} = \frac{U_{max}}{\frac{1}{4\pi}\sum_{j=1}^{M}\left[\sum_{i=1}^{N} U_{(\theta_i,\varphi_j)}.\sin(\theta_i)\Delta\theta.\Delta\varphi\right]} \tag{2.49}$$

Or in terms of relative radiation intensity as in (2.50):

$$D_0 = \frac{1}{\frac{1}{4\pi}\sum_{j=1}^{M}\left[\sum_{i=1}^{N} U_{(\theta_i,\varphi_j)}.\sin(\theta_i)\Delta\theta.\Delta\varphi\right]} \tag{2.50}$$

Where N and M are the number of points in the θ and φ plane respectively.

With gain and directivity measured it is then possible to calculate the antenna efficiency as $\eta = G/D$.

2.4.5 Circular Polarization Measurements

To characterize the circular or elliptical polarization properties of an antenna it is often analyzed in terms of circular polarization purity which can be discriminated by the polarization ellipse, tilt angle and its sense of rotation.

In order to measure the purity of LH and RH components it is performed a field transformation of magnitude of vertical and horizontal E components (E_θ and E_φ) to magnitude of right and left hand CP E components (E_{RHCP} and E_{LHCP}).

$$E_{RHCP} = \frac{1}{\sqrt{2}}(E_\theta - jE_\varphi) \tag{2.51}$$

$$E_{LHCP} = \frac{1}{\sqrt{2}}(E_\theta + jE_\varphi) \tag{2.52}$$

And the calculation of the phase angle is given by $\Delta\gamma = angle(\boldsymbol{E_\varphi}) - angle(\boldsymbol{E_\theta})$, where $\boldsymbol{E_\varphi}$ and $\boldsymbol{E_\theta}$ are the E field components in complex form. If

$$\Delta\gamma > 0 \Rightarrow LH\ Polarization$$

$$\Delta\gamma < 0 \Rightarrow RH\ Polarization$$

We can now represent the radiation pattern in LHCP and RHCP components.

To perform the calculation of the polarization ellipse (major component, minor component and tilt angle) we just need to perform the following calculations.

$$OA = \left[\frac{1}{2}\left\{{E_\theta}^2 + {E_\varphi}^2 + \left[{E_\theta}^4 + {E_\varphi}^4 + 2.{E_\theta}^2{E_\varphi}^2.\cos(2\Delta\gamma)\right]^{1/2}\right\}\right]^{1/2} \quad (2.53)$$

$$OB = \left[\frac{1}{2}\left\{{E_\theta}^2 + {E_\varphi}^2 - \left[{E_\theta}^4 + {E_\varphi}^4 + 2.{E_\theta}^2{E_\varphi}^2.\cos(2\Delta\gamma)\right]^{1/2}\right\}\right]^{1/2} \quad (2.54)$$

$$\tau = \frac{\pi}{2} - \frac{1}{2}arctan\left[\frac{2E_\theta E_\varphi}{{E_\theta}^2 - {E_\varphi}^2}.\cos(2\Delta\gamma)\right] \quad (2.55)$$

The AR can now be easily calculated given by $AR = \frac{OA}{OB}$. An antenna is considered with circular polarization with $AR_{dB} < 3dB$, the relation between polarization ellipse components can be smaller than $\sqrt{2}$.

2.5 Summary of this chapter

This chapter provides the background of antenna analysis, a short explanation of EM simulators and the description of antenna measuring equipments and procedures.

The knowledge of simulator and measuring system limitations are of high importance. It can provide an optimization of simulation time and the knowledge of the measuring system and equipments is essential to correctly perform the desired measurements and to know its level of accuracy. This chapter intends to guide antenna engineers in fundamentals, simulators and measuring systems.

Chapter 3 – Indoor LS techniques and requirements

Indoor positioning systems have attracted researchers' interest over the last decade. These systems can provide navigation, tracking or monitoring services where Global Navigation Satellite Systems (GNSS), such as Global Positioning System (GPS) [27], Global Orbiting Navigation Satellite System (GLONASS) [28], and Galileo [29] are unfeasible solutions.

Indoor localization systems can be categorized as token or token-less according to whether or not the mobile unit carries any device used for the localization process [30]. Token localization presents a wider variety of technologies and systems that have been developed by different companies, research centers and universities. These systems have been implemented based on several technologies: infrared (IR) [31],[32], Bluetooth [33] radio-frequency identification (RFID) [34], wireless local area networks (WLAN) [35]-[38], Ultra-wideband (UWB) [39]-[43], ultra-sound [44]-[47], magnetic positioning [48] and audible sounds [49],[50].

On indoor localization systems, devices have been categorized by their role in the system, although, according to different technologies, applications or authors, several nomenclatures have been presented in the literature. For a coherent reading of this thesis, localization system devices are categorized into two groups: reference and mobile units. Reference units refer to the devices in known positions relative to the system, behaving as a reference and localization support for tracked units. Mobile units refer to the devices in unknown positions and desired to be estimated.

Nowadays a wide variety of antennas has been applied for wireless communications although not all are suitable for localization systems.

This chapter explains the main localization techniques used in indoor localization systems and intends to guide antenna designers toward developing reference unit antennas suitable for indoor localization.

3.1 LS Techniques

In this section, each of the main localization techniques applied for token systems can be divided in: triangulation (lateration and angulation), received signal strength (RSS) scene analysis (fingerprinting) and proximity based [3].

3.1.1 Triangulation

Triangulation is a technique that uses the geometric properties of triangles to estimate the target localization and can be divided into two derivations: lateration and angulation.

Lateration or range measurement technique, estimates the position of a mobile unit according to its distances from multiple reference units. The distance is mainly derived by computing the measured RSS, or derived by the signal propagation time of flight, ToF, typically divided as time of arrival (ToA), time difference of arrival (TDoA) and round-trip time of flight (RToF). The other derivation of this technique is the angulation, commonly called angle of arrival (AoA) or even direction of arrival (DoA). The sub-categories of triangulation will be now described.

3.1.1.1 Time of Arrival (ToA)

ToA technique derives the distance between two devices by measuring the one-way propagation time between them, knowing a priori the signal propagation speed. The distance between these device d, is given by $d = s\,(t_2 - t_1)$, where t_1 is the transmitting time of the signal, t_2 the time needed for the signal to arrive at the receiver and s is the signal propagation speed. The calculated relative distance between the devices together with the knowledge of the reference units absolute positioning provides the chance to calculate the localization of mobile units.

The estimation of the localization can ideally be seen as the interception point of circumferences (or spheres on 3D plane) centered on reference units and radius (Rx) of estimated distance to the mobile unit as shown in Fig. 3.1.

For the correct position estimation based on ToA techniques, a precise synchronization of all networks devices (mobile and reference units) is required, also as the timestamp information (sent on the transmitted packet). ToA techniques provide high accuracy although at a cost of higher hardware complexity.

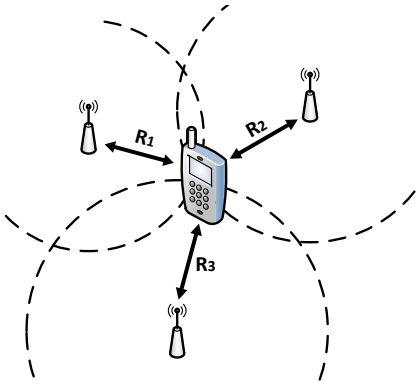

Fig. 3.1 Representation of ToA localization technique

3.1.1.2 Time Difference of Arrival (TDoA):

TDoA technique determines the relative position of the units based on two different approaches: difference in the propagation time of a transmitted signal between a single unit and three or more reference units; Difference in the propagation time of multiple signals from a single source unit and three or more reference units.

The first described approach requires precise synchronization of reference units. TDoA can after be estimated performing the correlation between received signals for each pair of measuring units. The TDoA refers to the time value which maximizes the cross-correlation function. By this reason only reference units (rather than all units for ToA methods) need to be synchronized. The distance estimated to the mobile unit by the TDoA between two reference units is given by a hyperboloid function [8]. Based on the chosen TDoA pairs, the interception of two hyperboloids gives the position of the mobile unit, as in Fig. 3.2

These relative coordinates, along with the knowledge of reference units' position, provides a base to estimate the localization of mobile units.

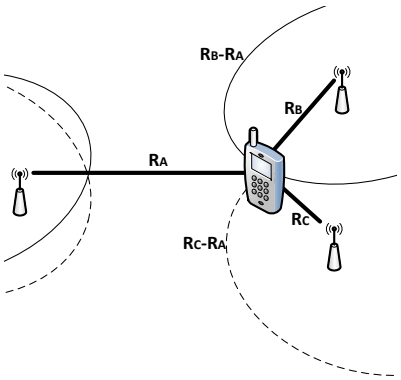

Fig. 3.2 TDoA localization technique representation

In the second case the mobile units need to be equipped with extra hardware capable of sending two types of signals simultaneously. These signals must have different propagation speeds, like radio/ultrasound [44] or radio/acoustic [50]. Knowing at priori the position of three reference units and the TDoA between the two signals, the localization of the mobile units can be estimated. This approach does not require synchronization of the infrastructure, although they need extra hardware to send the second signal, which typically has limited range. TDoA localization systems also provide high accuracy.

3.1.1.3 Round Trip Time of Flight (RToF):

RToF technique or ToA two-ways ranging, measures the complete trip ToF of the signal between the transmitter and the receiver units. These systems do not demand precise clock synchronization as systems based on ToA, nevertheless it is crucial to know the exact processing time of the "responder", typically measured in a calibration phase. Errors on this measurement have significant impact for the system localization resolution, critical for small range systems. The representation of this technique is presented in Fig. 3.1 although the measured RToF represents the propagation time of the signal to cross distance Rx twice with the incremental time processing delay.

3.1.1.4 Received Signal Strength Indication (RSSI):

RSSI represents the receiver measured RSS and can be used to estimate the distance between devices based on signal attenuation models, typically log-normal [51]. This technique has the advantage of simplicity of implementation and low cost mainly because wireless system receivers are commonly integrated with RSS measurement capabilities, which were initially used for other purposes such as automatic gain control or even transmit power control.

In real environments such as indoor environments where it is difficult to find the LoS (Line of Sight) between units, the RSSI is highly affected by multipath fading, shadowing and even antenna type, making it challenging to develop a mathematical model of the channel that matches with the real propagation, resulting in inaccurate distance estimations. Other parameters such as Link Quality Indicator (LQI), Packet Reception Ratio (PRR), Signal-to-Noise Ratio (SNR) and Response Rate (RR) can be used to support the localization process. When low cost is in priority over accuracy, these systems provide a suitable solution. Converting the RSSI into distance, the estimation of mobile unit

localization can be performed by the interception of three circumferences centered on the reference units.

3.1.1.5 Angle of Arrival (AoA)

Angulation is other derivation of the triangulation technique, commonly called angle of arrival (AoA) or even direction of arrival (DoA). It estimates the unit localization computing angles relative to multiple reference points. This angle can be related to its own unit, to an electronic compass or even to a second signal received by the unit. The estimation of the AoA is done by the use of several directive or antenna arrays described in Fig. 3.3.

The main advantage of this technique it that if the mobile unit orientation is known, only two measurements of non collinear reference nodes are needed for 2-D localization (three for 3-D localization) and there is no need for time synchronization between units, [52]. The disadvantages of this technique rely on the need or large and complex hardware requirements.

The localization based on these systems relies on accurate angle measurements which becomes less precise as the unit moves further away from the measuring unit and are, highly affected by multipath or even by directivity of the measuring aperture.

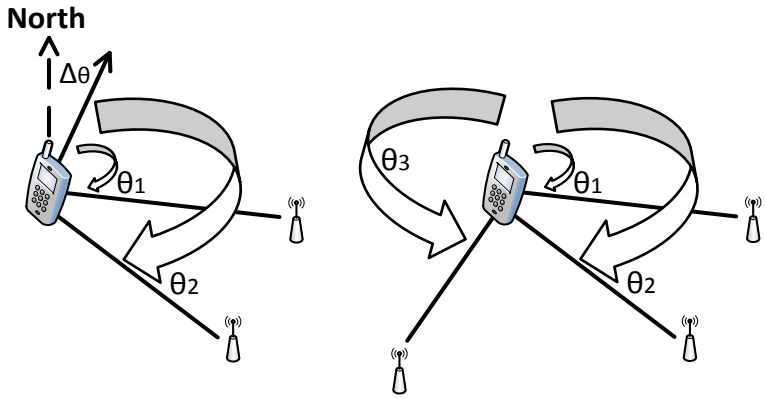

Fig. 3.3 AoA with known orientation A) and without known orientation B)

3.1.2 RSS Scene Analysis

RSS scene analysis is a localization technique that estimates the mobile unit position matching the online scene collected features (fingerprints) with the closest fingerprints saved a priori on a database, as presented in Fig. 3.4

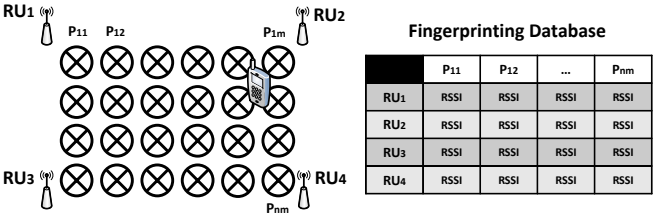

Fig. 3.4 RSS fingerprinting representation

This technique is performed in two phases: offline and online. During the offline phase, the position coordinates and respective RSS collection from nearby reference units is gathered. During the online phase, localization fingerprinting algorithms uses the observed RSS collection to estimate the mobile units' position.

Positioning with signal strength fingerprinting algorithms is usually based on deterministic and probabilistic approaches, neural networks and decision trees. A comparative survey of WLAN location fingerprinting can be found in [53].

The main drawbacks to this technique are the consuming time calibration, which needs to be updated in case of localization environment changes, and the need of high computational cost and space to store network information.

3.1.3 Proximity

The proximity method simply provides symbolic relative localization information. If a mobile unit is detected by a single reference unit, the mobile position is associated to it. In case of more reference units' detection, the mobile unit position is related to the unit that detects the strongest signal. This technique is commonly applied to localization systems based on infrared, RFID or even cell identification, where positioning is related to the cellular network cell that the device is using at a given time.

3.2 Antennas for Localization requirements

According to the technology, technique and nature of the signals being processed, different antennas have been applied for radio frequency (RF) localization systems. The infrastructure of the localization system, formed by reference units, has been mainly integrated with omnidirectional radiation pattern antennas. Nevertheless, diversity of radiation pattern starts to become a desired feature for performance enhancement of these

systems, which is possible due to sectorised antenna arrays (SAA), multiple directive antennas with different discrimination zones, phased arrays or even adaptive arrays, also called Smart Antennas [54].

The use of omnidirectional, directive, SAA, phased arrays and Smart Antennas can be applied to localization systems reference units based on different models of localization as presented in Fig. 3.5. One common model is based on a set of omnidirectional antennas distributed over the localization scenario, as presented in Fig. 3.5-A. This model is typically implemented for lateration and fingerprinting techniques and it is widely implemented in WSNs. Another model passes by the use of directive antennas for a more confined localization based on proximity, widely implemented on RFID systems. This localization model is presented in Fig. 3.5-B as an access control system with directive antennas over the room doors. SAA/Phased/Smart Antennas can also be used for the localization process, which when well implemented, can provide higher coverage, higher accuracy, increased system capacity, signal-to-noise ratio improvement, multipath rejection and the reduction of needed reference units leading to reduced system cost.

However, these antennas inherently imply a larger and more complex implementation comparing with previously described antennas. The localization process of systems integrated with these antennas can be performed based on: analysis of the signal received by the elements of one or more antenna arrays with appropriate signal processing algorithms support; or even performing a sweep of the radiation beam for the DoA estimation. SAA can be used to analyze the signal received by multiple directive elements or even by the sweep of fixed number of radiation beams, six in the case presented in Fig. 3.5-C. Phased arrays or smart antennas can provide higher directivity and higher number of radiation beams making it suitable for single tracking and sweep of the radiation beam, as shown in Fig. 3.5-D. Notice that Fig. 3.5-C and D are only presented with one single antenna array although several arrays can be applied. Despite of its benefits, the paradigm of localization based on these antennas demand proper modifications of the medium access control layer and routing techniques [55].

Besides the radiation pattern, antenna bandwidth and polarization are two important characteristics to consider when designing antennas for localization systems.

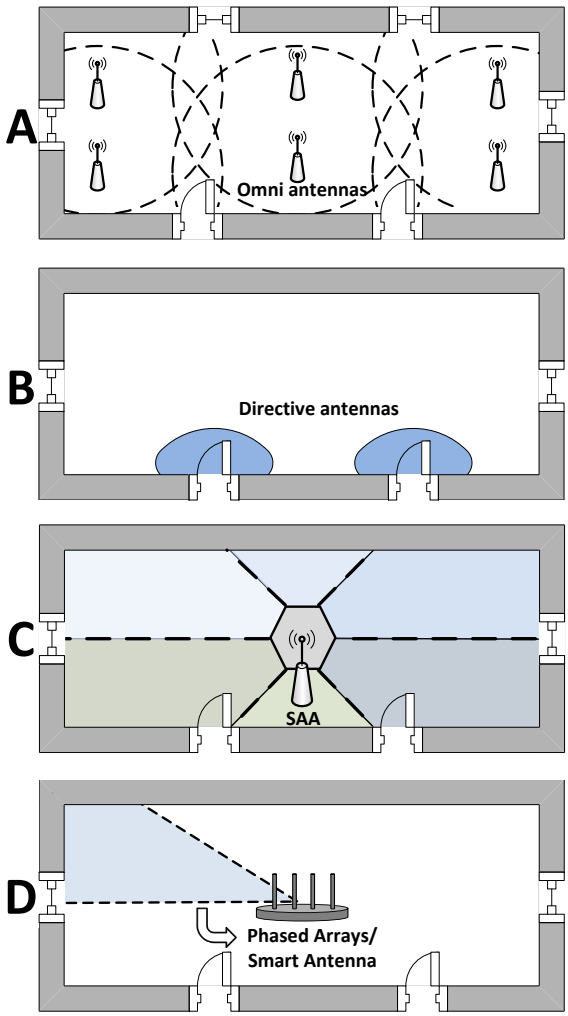

Fig. 3.5 LS models: based on omni antennas A); single directive antenna B); with SAA C) and with phased/smart antenna D)

Different localization techniques demand antennas with different bandwidth requirements and a proper polarization which can improve the quality of measurement signals. These antenna requirements will be discussed further in this chapter.

Indoor localization systems have been widely implemented with a large variety of antennas. In this section an overview of antennas for localization system will be presented focusing on the ones integrated on reference units. This section is divided according to the nature of the measurements for the localization process as: RSS; ToF and DoA.

3.2.1 Antennas applied for RSS

RSS localization systems can be divided based on: RSS lateration, fingerprinting and proximity techniques. The performance of these systems is related to RSS measurements which in indoor environments are highly affected by several factors such as [6]:

- Multipath fading and shadowing;
- Interference of other electrical field sources;
- Transceiver hardware inaccuracies on RSS measurements;
- Low probability of LoS path availability;
- User mobility.

Besides previously referred factors, the used antennas have a significant impact of localization system performance that demands careful implementation according to several factors such as: radiation pattern, polarization, gain, bandwidth and efficiency.

As it is standard for all antennas integrated with reference units, they are designed to be robust, inexpensive, impedance matched over the entire operational bandwidth, small and highly efficient. These characteristics are important for the correct performance of the antenna which inherently affects the system localization errors. Nevertheless, other antenna characteristics such as radiation pattern and polarization should be carefully chosen according to different localization systems, as will be discussed next.

Antennas applied for RSS lateration: antennas used as reference units for RSS lateration technique are desired with a perfect isotropic radiation pattern providing a homogeneous signal transmission over 3-D dimensions. Unfortunately, these antennas do not exist. Due to this limitation, a simple and common solution passes by the implementation of antennas with omnidirectional pattern over the azimuthal plane.

The mobile units, are widely carried by users for its localization, move and rotate according to the human motion profile, mainly over azimuthal plane with reduced rotation over elevation. Considering that this human movement and rotation profile is known a priori, the vertical polarized omnidirectional antennas on clear LoS are desired. To achieve these characteristics, antennas of mobile units should be applied on human heads providing a clear LoS or even on the shoulders, although this would provide impractical solutions for the user and specifically regarding human specific absorption rate (SAR). A possible

solution to achieve these desired characteristics can be achieved by the use of wearable antennas [56],[57]. Considering a case where polarization orientation of the antenna on the user is guaranteed, co-polar linear vertical polarized antennas on reference and mobile units are preferred.

Omnidirectional pattern with vertical polarization can be achieved with a correct design of a wide variety of antennas, although simplicity and cost make half-wavelength dipole or quarter-wavelength monopoles (in case of ground plane availability) the most used antenna types. For applications with higher azimuthal range needs, omnidirectional antennas with a higher gain and vertical polarization antennas can be implemented by the use of slot arrays or collinear arrays of half-wavelength dipoles can also be used [54].

In case of the mobile units that do not provide guaranteed polarization orientation, such as the use of localization devices as bracelets where the natural body movement cause change over time, reference units are desired with circular polarization (CP). The use of these antennas as reference units provide a solution less dependent on mobile unit orientation, although at the cost of localization range considering the typical linear polarized tracker antennas.

Several systems based on simple RSS lateration have been presented in literature, mainly with commercial linear omnidirectional antennas [4],[6], [58].

Antennas applied for RSS fingerprinting: localization systems based on RSS fingerprinting rely on an offline calibration phase which should be as similar as possible to the online phase conditions. These conditions refer not to the localization scenario and environmental conditions, but also to the network units' characteristics during the calibration phase. Considering that calibration conditions are maintained, the system performance ideally does not depend on the antenna characteristics. However, the exact calibration conditions are not always guaranteed, but the less variance of the measurements when compared with the calibration results is of primordial importance. This variance in measurements can result from several interference sources or even by user movement and rotation.

Antennas with omnidirectional radiation pattern lead to smaller RSS variances than directional antennas over the entire radiation pattern making its use preferable for fingerprinting. Another point of interest is its polarization orientation, depending on

whether or not the polarization of antenna mobile units is guaranteed with vertical polarization, vertical polarized or circular polarized antennas should be preferred. The last approach provides less RSS variance with the tracker rotation, leading to smaller errors based on fingerprinting techniques.

Localization systems based on fingerprinting have been widely applied for WLAN, WSN and RFID, commonly integrated with commercial monopole and dipole antennas [34]-[37]. These characteristics are mainly justified once again by the omnidirectional radiation pattern, robustness, size and cost. A wider quantity of fingerprinting based localization systems have been presented in literature, nevertheless, antenna characteristics during calibration and online phase is often omitted. For a correct analysis and validation of results this information should be mentioned regarding radiation pattern and polarization.

Antennas applied for proximity: localization systems based on proximity cannot be considered real time localization systems (RTLS), in the sense that the mobile node localization is only performed if the mobile unit passes near reading zones and not constantly tracked over the localization scenario. Due to this different approach the antenna requirements also change in order to optimize the performance of these systems. This localization technique is mainly applied for Ultra High Frequency (UHF) and microwave passive RFID widely used in security/access control, asset management, transportation and animal tracking.

These systems are generally implemented for localization of large quantities of RFID tags (RFID mobile units) under diverse localization scenarios where size, cost, efficiency and reliability are the main restrictions. Being an antenna a main component of a tag it is crucial to be inexpensive, with reduced dimensions and high efficiency [59]. The huge variety of RFID applications commonly without availability of ground plane makes dipole or dual dipoles for reduced orientation dependency, the most used tag antennas [60]. On these localization systems, due to cost and size, the located tag is typically a device with linear polarization and no uniformity of orientation. Impedance matching over operation bandwidth and mechanical robustness requirements are a key point. The antennas for the passive UHF RFID readers (RFID reference units) are mainly designed with high quality circular polarization to mitigate the problem of tags orientation sensitivity, high gain and

low side lobes for high directive range applications. Wide bandwidth is also desired for universal UHF RFID compatibility (840−960 MHz). Although, if tags orientation is guaranteed, linear readers can be more suitable for creating a focused and oriented electromagnetic field used for greater range and deeper penetration. According to the localization scenario and desired application, omnidirectional radiation pattern antennas could be more suitable. A representation of a RFID system implemented with directive antenna is presented in Fig. 3.6.

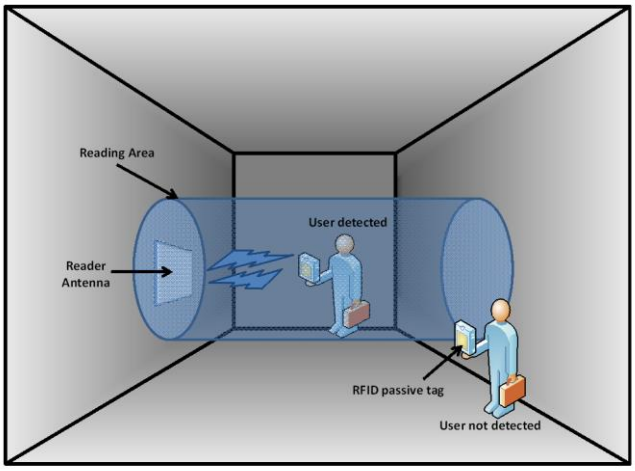

Fig. 3.6 RFID System working with proximity technique

Several studies also have been performed on multi band RFID reader's antennas, although, antenna characteristics uniformity over the bands are harder to guarantee which can affect the performance of the localization system.

Several reader antennas useful for RFID proximity systems have been implemented such as: microstrip patch, dipole, slots, spiral and helical antennas. A wide study has been presented for RFID reader antennas [61]-[68]. A comparison of handheld UHF RFID reader planar antennas and the reading range has been performed, [61], where fractal implementations were also analyzed. Unidirectional dual band antennas, with advantage of RFID operation over two bands, UHF and microwave RFID also have been presented [62]. UHF RFID reader antenna with CP and high Tx/Rx isolation is discussed in [63] or even with different exciting techniques suitable for compact CP antennas [64]. Reader antennas covering the entire UHF RFID band (860-960MHz) and a suitable CP have been reported, with helical, spiral shapes and two corners truncated patches respectively [65]-[67]. A

discussion of the propagation aspects of passive RFID systems and suitable tag antennas has also been presented [68].

3.2.2 Antennas applied for ToF

As previously mentioned, ToF system can rely on the measurements of DToA between two different speed propagation signals or even based on the ToA of ultra-short electromagnetic pulses. RF ToF localization systems can be efficiently implemented using UWB technology, mainly because of a high time resolution. UWB technology occupies a minimum bandwidth of 500 MHz or at least 20% of the cental frequency, demanding for a wide spectrum allocation for these applications (3.1-10.6 GHz) [69].

Indoor localization systems based on Impulse Radio UWB are commonly characterized by low power consumption and transmission of low data rate using very short-pulses spread over a wide bandwidth [70]. The high data spreading rate, due to low data over a large bandwidth allows not only the transmission over reasonable distances for indoor localization, but also improves the robustness to interference from narrowband interferers (jammers) and/or other UWB devices. Furthermore, a large absolute bandwidth allows very precise ranging, since the ranging accuracy is proportional to the bandwidth of the emitted signal [71].

UWB have been proven to be useful for indoor localization which made IEEE 802.15.4a Working Group regard UWB as the first choice for high accuracy indoor localization [72],[73].

The availability of synchronization in UWB systems combined with short transmitted pulses provides a chance to avoid multipath fading by reducing the overlap on the original signal. Nevertheless, there is always a chance of false-alarms (identification of LoS as Non LoS (NLoS)) which degrade the localization accuracy [74].

Mainly due to the strong research over UWB transmission techniques over the last years, UWB, in general, is now considered better than conventional narrowband modulation and multiple access techniques at meeting the WSN requirements (low cost, low power consumption, robustness, localization accuracy) [75].

Once again, the antennas play a crucial role in the performance of these localization systems however, the design of UWB antennas are much more challenging than narrow

band antennas [76]. The main desired characteristics of the reference unit antennas for localization systems based on RF ToA can be described as:

- Bandwidth coverage of the operational channel (minimum 500MHz for 802.15.4a) and ideally covering the entire UWB band;
- Omnidirectional radiation pattern (for uniform coverage);
- Antenna uniformity over entire operational bandwidth (radiation pattern, gain, polarization and impedance matching);
- Reduced dimensions and cost requirements (for integration with several equipments or printed circuit boards);
- High radiation efficiency due to the extreme low power transmitted signal, typically >70%;
- Linear phase in the time domain (constant group delay is desired to prevent pulse distortion);
- Physically compact with low profile (preferably planar due to easier manufacture and implementation).

Conventional UWB localization systems based in ToF (more than three reference units) are commonly used as unidirectional TDoA systems needing only precise synchronization of the infrastructure reference units [39]. Unidirectional ToA or bidirectional RToF techniques can also be applied. On ToA technique the transmission time of the mobile unit need to be known, demanding synchronization of the entire network; for the RToF less demands of synchronization are required but an additional calibration phase should be performed [41],[77].

Several interesting UWB antenna approaches have been presented in literature with different planar formats (e.g. rectangular, triangular, elliptical, spiral, fractal geometries) for high bandwidth, omnidirectional patterns and/or polarization concerns [78]-[80]; different feeding techniques (e.g. simple, two-branch, trident strip) that can improve polarization purity [81]; different geometries (step-shaped, cross-square, U-shaped, rolled, cross-plate) for stability of radiation pattern across the UWB band [82]; and integrated with suitable band-notches to reduce interference over specific bands [83]-[85].

Another desired characteristic for UWB reference unit antennas is its implementation with CP over the entire band, making it suitable to detect targets for which polarization is unknown [86]. A good example of UWB CP antenna is presented in [86], a spiral antenna with axial ratio below 3dB from 3 to 14.5 GHz and return loss better than 10 dB from 3.75 to 18.6 GHz. This antenna also provides reduced pulse distortion and the feeding structure is performed by the integration of a tapered microstrip balun making its construction completely planar.

3.2.3 Antennas applied for DoA

Localization based on DoA technique relies on accurate angle measurements, although, the accuracy of these systems is highly influenced by multipath reflections, shadowing or even the directivity of the measuring aperture.

The estimation of the DoA can be achieved by the use of antenna arrays or directional antennas that improve the system in terms of capacity, connectivity and spectrum efficiency. Different approaches have been proposed and applied to localization systems based on DoA, usually integrated with RSSI and ToF measurements.

Several different antenna implementations as reference units have been reported for positioning integrated with DoA approaches, some of them can be described as follows:

- Narrowband SAA estimates the localization based on DoA algorithms considering RSSI and/or phase measurements of antenna elements [87];
- UWB SAA estimates DoA based on amplitude difference of the received UWB pulse between each antenna elements [88],[89];
- UWB mono-pulse radar systems estimates localization based on DoA (difference of signal phase and amplitude at receivers) and RToF to measure the distance [90],[91];
- Switch beam, phase antenna array or mechanical rotation of a directive antenna performing a sweep of the beam over the localization area (typically at a constant angular speed) to estimate DoA and the distance based on RSSI and/or phase measurements [92]-[96];
- UWB uniform linear array estimates localization based on DoA algorithms [97].

According to the previously mentioned approaches, one or several reference units are required and appropriate MAC protocols need to be developed in order to potentiate the correct localization environment coverage and localization resolution [55].

Antennas suitable for localization based on DoA are required with different requirements according to previous approaches for DoA estimation. For narrow band systems, reference units are typically desired with narrow beam width to provide higher accuracy and higher range, CP to mitigate polarization diversity problems and reduced coupling between neighbor antennas to avoid radiation pattern distortions; for DoA based on UWB systems, the requirements are similar to UWB ToF systems with the addition of shorter beam width and reduced coupling between the neighbor antennas. Both approaches are desired to be applied as printed circuit boards providing manufacture and implementation cost advantages.

Antennas suitable for DoA with possibility of independent localization zones have been presented. SAA over a semi dodecahedron shape with CP and designed for ISM 2.4 GHz systems are presented in [87], although [J2] presents higher gain by the use of patch excited horn antenna array.

In [88],[89] and [98] SAA for UWB applications are presented. Antennas implemented for azimuthal coverage by the use of six directive antennas into prismatic structures are presented in [88],[89] and in [98] with seven multilayer microstrip antennas integrated into a semi-spherical polyhedral antenna array configuration. DoA also can be obtained by other switch beam UWB antennas such as double square loop antennas [99] and linear arrays implemented with beam forming networks [100]. UWB radar systems based on DoA and RToF have been presented in [90][91]. Similar implementations have been presented for narrowband WSN based on sectorial sweeper or tracking systems. The distance of these systems is not based on RToF but instead on RSSI measurements. In [92],[94] the systems are based on linear antenna arrays and in [95] in a rotating directive antenna.

Circular monopole antennas have also been applied to DoA finding based on sector switching, obtained by two main topologies [101],[102]:

- One central monopole operating as main antenna for emitter/receiver connection while surrounding peripheral circular array may be switched connected as

different reactive loads, usually called electronically steerable parasitic array radiator (ESPAR).

- No central monopole is present and the circular symmetry is broken by connecting specific antenna elements to the emitter/receiver, where the others are connected to some reactance or short-circuited to the ground plane.

Several ESPAR antennas based on monopoles have been presented, mainly for 2.4 GHz ISM band with different number of parasitic elements [103]-[106] or even for UWB [107].

This previous topology of switch beam based on parasitic elements also has been reported with other antenna types such as slot and planar microstrip antennas [108]-[113].

For a more clear description of the antennas implemented for DoA we divided the antenna arrays into three main blocks, ESPAR antennas, Linear/Planar Arrays and SAA. Each of the previous antenna arrays can be connected to different beam control networks according to the DoA estimation approach, as presented in Fig. 3.7 afterwards.

The first antennas block provides the beam control by the integration and control of the reactance of parasitic elements, being here defined as ESPAR antennas. Different antenna types can be used as radiating and parasitic elements such as monopoles, microstrip or even slot antennas. Each of these approaches can even be integrated with or without a central radiating element.

The second antenna block is described as linear and planar arrays, where the gain/phase control of each element provides the chance to manipulate the array radiating beam. These arrays can be performed with different antenna types and format, linear or circular arrays or even diverse planar forms.

The last antennas group described in this paper for DoA calculation is referred as Sectorised or Sectorial Antenna Array (SAA) and represent the antenna group based on a set of directive antennas in different directions. These solutions are typically designed with prismatic implementations providing azimuthal coverage or with polyhedral implementation for a semi-spherical coverage. These antennas can be implemented with any directive antenna elements, although, they are typically implemented with planar formats due to size and cost constrains.

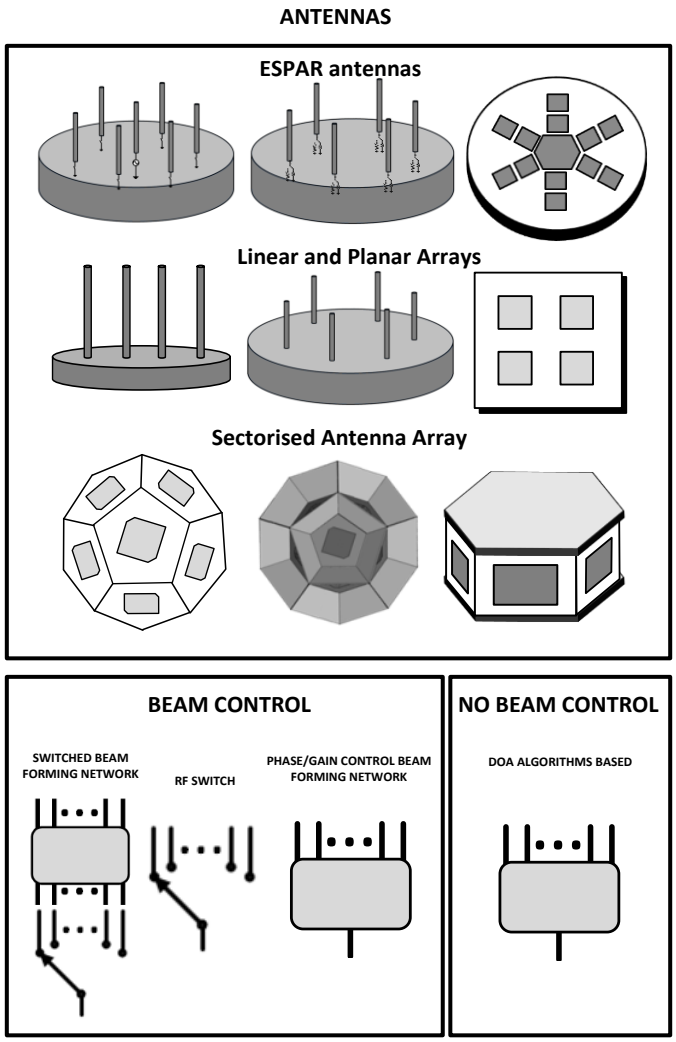

Fig. 3.7 Antennas and beam control networks for DoA

According to the implemented DoA localization approach, previous referred antennas can require a radiation beam control which can be performed by several possible techniques, such as: switched beam forming networks (i.g. Butler and Blass Matrix), switch control of radiating antenna elements or even by a phase/gain control for each antenna element. Although, localization based on DoA can also be performed without beam control, using the antenna arrays received signals and appropriate signal processing algorithms (i.g. MUSIC, ESPRIT [114]-[116]).

Mechanical rotation of a directive antenna can also be performed to control the radiation beam, and like this, be used for DoA estimation.

3.3 Concluding Remarks

This chapter presents the main types and requirements of reference unit antennas for indoor LS are present based on three different measurements: RSSI, ToF and DoA.

The RSSI approach typically relies on narrow band omnidirectional with linear or circular polarized antennas according to polarization orientation on mobile units. ToF approaches are mainly designed with similar needs, although with larger bandwidth requirements which lead to new design constrains such as: uniformity of antenna characteristics over the entire operational bandwidth and linear phase in the time domain.

DoA provided a much complex and wider arrangement of antennas that can be used as an arrangement of sectorised antennas elements or by a rotative or switch beam over the space. Several antenna approaches for localization such as: linear and planar antenna arrays, SAA, ESPAR antennas have been presented.

Based on the signal nature for the localization estimation, different reference unit antennas can be more suitable than others, as previously explained. For demonstration purposes consider a localization system based on fingerprinting. The choice of several omnidirectional antennas with CP would be preferred over a single or few SAA considering the same number of antenna elements. Due to the reduced distribution of SAA elements over the localization system, they also would become more susceptive to variations on localization system environment. However, if we consider a conference amphitheater, typically with a high ceiling, providing a good probability of LoS with the mobile units, the use of a central or few SAA would be preferable reducing mounting efforts of the LS to fewer devices, with expected similar results.

Non continuous low power localization systems could also benefit from high efficient SAA/Smart antennas compared with omnidirectional antennas, being more suitable for energy harvesting capabilities during the non-localization intervals [117].

LS performance can highly benefit from the use of appropriate reference unit antennas according to the localization technique. The antennas not only have a direct impact on system accuracy but also on: availability, number of reference units, portability, size, cost and power consumption. Based on these principles two sectorial antennas were developed described in next chapter. Other antennas were also developed, mainly for communication purposes at 5 GHz. These antennas present cheap solution based on FR4 with different characteristics in impedance bandwidth, polarization and gain.

3.4 Summary of this Chapter

This chapter explains the main localization techniques used in indoor localization systems and intends to guide antenna designers toward developing reference unit antennas suitable for indoor localization.

According with the signal nature for the localization estimation different antennas can be more suitable. This chapter explains the difference of LS requirements according with the signal measurements and their suitable antennas.

The study presented in this chapter was published in the International Journal of Antennas and Propagation [J1].

Chapter 4 –Developed Antennas

A possible solution to increase WSN Localization Systems (WSN-LS) resolution can be achieved integrating RSS and AoA measurements, similarly to the solution in [118].

In WSN-LS mobile nodes typically correspond to a high number of elements where size, cost and omnidirectional radiation pattern are the three main concerns. By these reasons they are commonly integrated with monopoles, dipoles, ceramic chip antenna and recently with wearable antennas [119].

On the other hand few fixed or reference nodes are usually integrated with higher complexity level which is typically inversely proportional to the required number of nodes for the localization process. For systems based on angle measurements, the correct discrimination of the AoA demands a carefully control of a directive beam. A cost effective solution to control the radiation pattern can be achieved with the use of switch beam antennas or sectorial (or sectorised) antennas (SA).

In this chapter it is analyzed and measured the developed sectorial antennas, a narrowband antenna for 2.45 GHz and UWB covering the 800– 2500 MHz band. Then it is presented three antenna approaches for communication purposes operating at 5.8 GHz.

4.1 Sectorial Antennas

The sectorial antennas are described in this section, divided as Hive5 a narrowband antenna with CP and a UWB antenna, the 6-SB Log Periodic Antenna.

4.1.1 Hive5 Antenna

In this thesis one of the objectives is to study a low-cost high effective antenna for LSs which could be used for implementing Angle of Arrival (AoA) techniques combined with RF fingerprinting techniques, defining the antenna requirements for the system as:

- Optimized radiation pattern for AoA discrimination;
- Possibility of integration of the two localization methods: RSS and AoA techniques;

- Circular polarization solution;
- Practical and low cost;
- Reduced required number of reference nodes;
- Small complexity of the RF control circuit.

The CP provides advantages on mitigating multipath effects on reflective environments [120] and improving significantly the performance of RSS algorithms.

From the antennas solutions available in the literature, none were suitable for our system requirements. This led us to the development of the Hive5, a SA integrated with patch-excited structures presented in [C3] and analyzed in [C5]. This section presents a resume of the publish paper in IEEE Transactions on Antennas and Propagation, [J2].

To guarantee the uniform characteristics of all antennas on the Hive5 a semi-platonic structure was developed, in this case, based on a semi-dodecahedron.

The proposed solution is designed to reduce the coupling between neighbor antennas and increase antennas directivity, guarantying at the same time a maximum of 3dB variation over the entire semispherical radiation pattern. The result is an improved SA with approximately semispherical radiation pattern which can discriminate six independent areas.

The design of this antenna structure was inspired on a wasp hive as presented in Fig 4.1. The internal structure of the hive is formed by a dense matrix of hexagonal prismatic cells, as resemblance, our developed support is also formed by cells, although, with a pyramidal pentagonal (PP) shape. These cells arrangement similarity and the pentagonal shape are the reasons why we called our antenna, the Hive5 antenna.

Fig. 4.1 Wasp hive and Hive5 antenna structure

In LSs exclusively based on RSS measurements the number of reference nodes increases very fast for a satisfactory accuracy, this can lead to costly systems due to the high number of reference nodes. The Hive5 antenna when strategically placed provides a solution to reduce the overall number of reference nodes and high coverage due to improved antenna gain. Having the PP cells fixed angles and coverage areas, a simple RSS comparison of each cell can discriminate an approximate AoA between the Hive5 and the mobile node.

To control the radiation beams of the Hive5, a RF switch circuit can be integrated allowing a sequentially discrimination of six areas, resulting in an omnidirectional coverage with maximum variation of 3dB as illustrated in Fig. 4.2 .

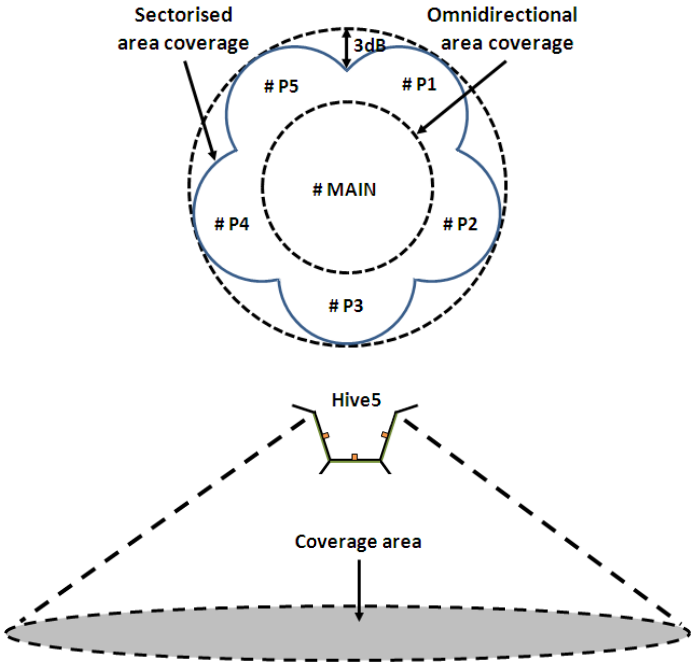

Fig. 4.2 Hive5 azimuthal (upper) and elevation (lower) planes coverage

The Hive5 radiation pattern, polarization and gain are significantly dependent on the flare angle and size of the hollow structure. Platonic solids present fixed flare angle depending of the structure dihedral angle. The dodecahedron structure has a dihedral angle of 116º 34’ leading to a fix flare angle of approximately 32º. The fix flare angle constrains make the Hive5 optimization parameters based on the patch dimensions and the hollow structure tap length.

The main objectives for the implementation of the Hive5 antenna can be resumed as:

- SA with semispherical radiation pattern and maximum variation of 3dB beam width over the radiation pattern;
- Reduced coupling between neighbor antennas;
- Increased multipath rejection;
- Resulting CP for patches inside the Hive5 structure;
- Low bandwidth (2.4-2.5 GHz);
- Practical and low cost design with small tap length.

4.1.1.1 Hive5 Simulations

Following the requirements and main objectives suitable for RSS and AoA localization several simulations were performed using the HFSS [12]. The simulations were divided into three main groups: patch antenna, PP patch-excited cell and Hive5 antenna.

Patch antenna design

Our system demands were low bandwidth and CP, thus a patch antenna is a suitable choice due to its versatility, and simplicity of construction. The presented patch antenna was optimized for implementation on the final Hive5 antenna.

Our antenna design result in simple cut corners patch with ellipsoidal polarization, as presented in Fig. 4.3. It was designed for 2.45 GHz with Left Hand Elliptical Polarization using FR4 with $\varepsilon r = 4.3$, $\tan \delta = 0.02$ of 3.2mm. Elliptic polarization was chosen in order to guarantee that it will become circular when inserted into the Hive5 structure.

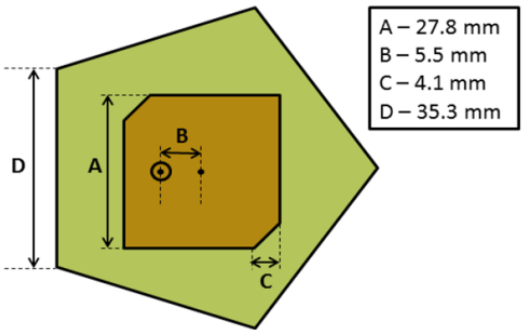

Fig. 4.3 Patch antenna design

The simulated patch antenna presented a gain of 4.54dBi, with bandwidth confined to 150 MHz (from 2.38 to 2.53 GHz)and a minimum AR of 3.57dB as can be seen in Fig. 4.4.

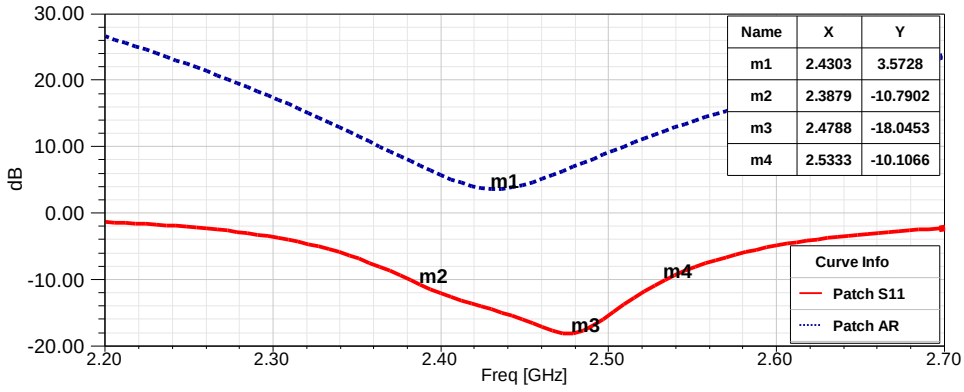

Fig. 4.4 Simulated Patch antenna S_{11} and AR

Pentagonal Pyramidal Patch-excited cell

Before designing the Hive5 structure the impact of several parameters were analyzed based on the PP patch-excited cell presented in Fig. 4.5.

Simulations confirmed an expected gain variation related to the tap length (T) from the patch antenna, flare angle (θ) and consequently aperture size (A) as shown in Fig. 4.6. The gain increases with the tap length and the optimal flare angle decreases with the increase of the tap length.

One of the main objectives of our implementation is to increase antenna gain to provide a maximum variation of 3dB beam width over the entire radiation pattern. Table 4.1 presents the PP patch-excited antenna tap length relation with the gain and beam width over XoZ and YoZ planes for 2.45 GHz.

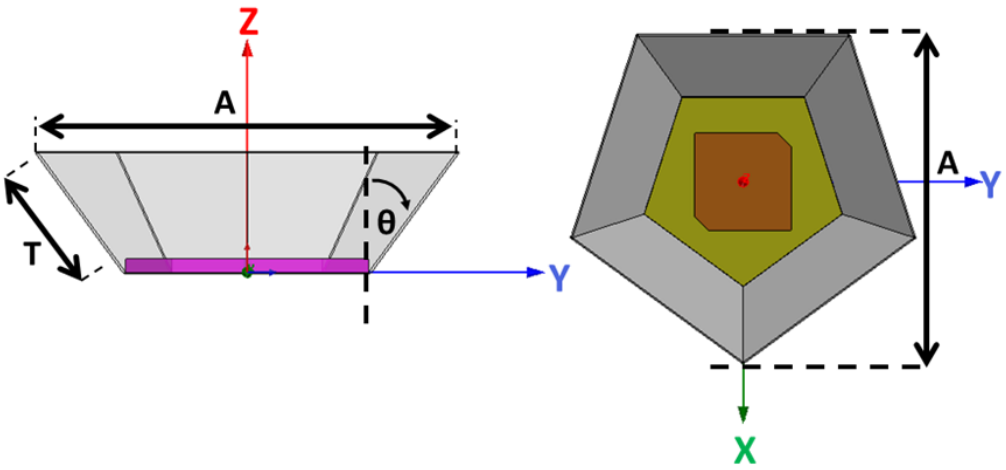

Fig. 4.5 PP Patch-excited antenna design on YoZ (left) and XoY (right) planes

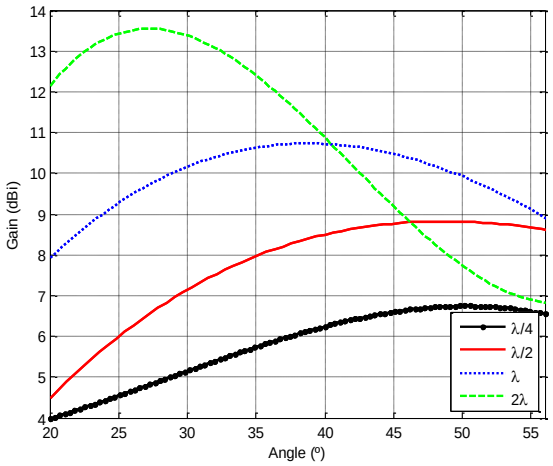

Fig. 4.6 PP Patch-excited gain relation with flare angle for several tap lengths

Tap Length (T)	Aperture Size (A)	beam width below 3dB (XoZ & YoZ planes)	Max Gain(dBi)
No Tap	-	93º,95º	4.54
λ/4	0.78λ	68º, 69º	5.40
λ/2	1.07λ	54º, 55º	7.57
λ	1.67λ	38º, 40º	10.49
2 λ	2.85λ	26º, 28º	13.08

Table 4.1 PP Patch-excited cell Beam Width & Gain relation with Tap Length

Hive5 Antenna

After the study of the PP patch-excited cell, the entire Hive5 antenna presented in Fig. 4.7 (made by six PP patch-excited cells) with tap length of λ/4 was analyzed. For the simulations we considered that all but one patch antenna are inactive and are terminated with 50Ω matched loads.

A comparative analysis of return loss (S_{11}) and AR on patch, PP patch-excited cell and Hive5 main antenna are presented in Fig. 4.8 and Fig. 4.9.

Analyzing Fig. 4.8 we can verify a significant but similar impact of the PP structure and the Hive5 main cell on the S_{11} of the patch antenna. All the three analyzed cases present return loss greater than 10dB over the band of interest, however PP and Hive5 structures provide optimized matching.

The AR of the patch antenna also suffered significant impact with the integration of the two analyzed structures as presented in Fig. 4.9. With the integration of patch antennas on

the PP and Hive5 structures we can verify an AR variation greater than 3dB. Although, between both it is verified a negligent variation of 0.15dB on minimum AR.

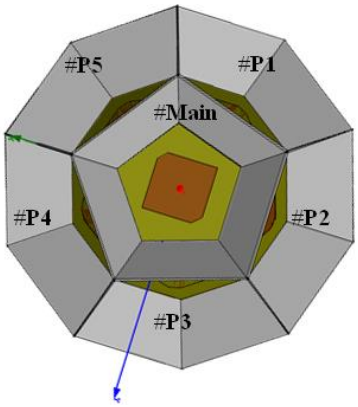

Fig. 4.7 Hive5 antenna design

The next step on our analysis was to perform a comparison between S_{11}, AR and gain of all the elements of the Hive5 antenna as presented in Fig. 4.10 and Fig. 4.11. We can notice similar return loss of all the lateral antennas and a maximum AR variation of 1.25dB between the most deviant lateral cell and the main Hive5 cell.

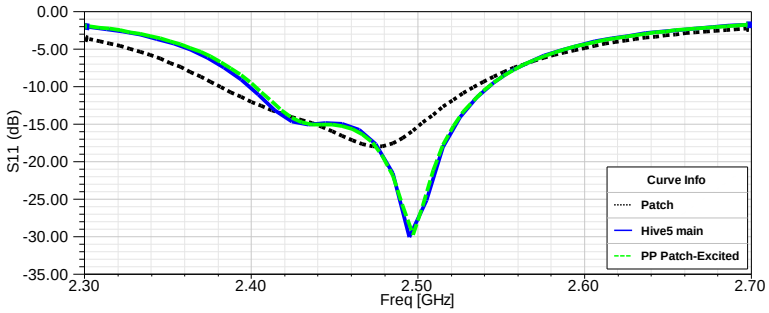

Fig. 4.8 S_{11} comparison for patch, Hive5 main and PP patch-excited cell

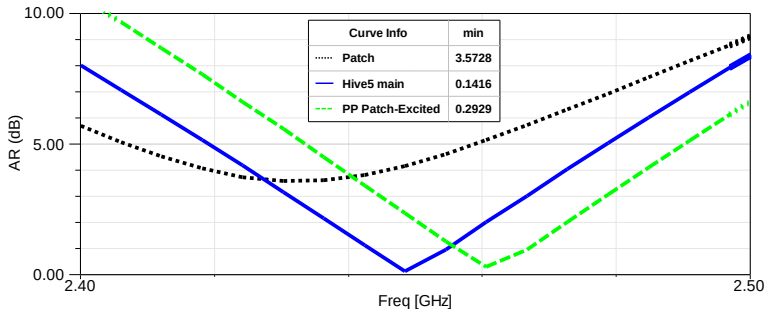

Fig. 4.9 AR comparison for patch, Hive5 main and pentagonal horn cells

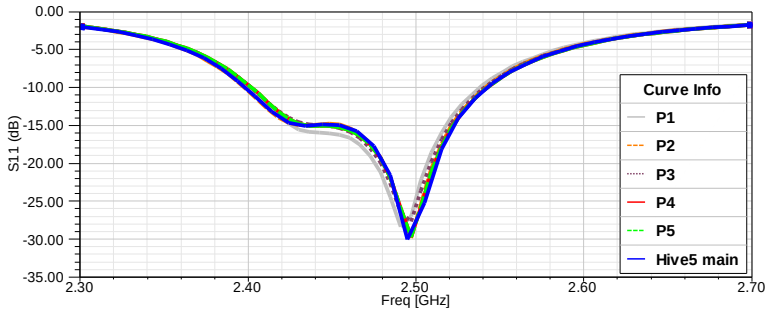

Fig. 4.10 S_{11} comparison between Hive5 Elements

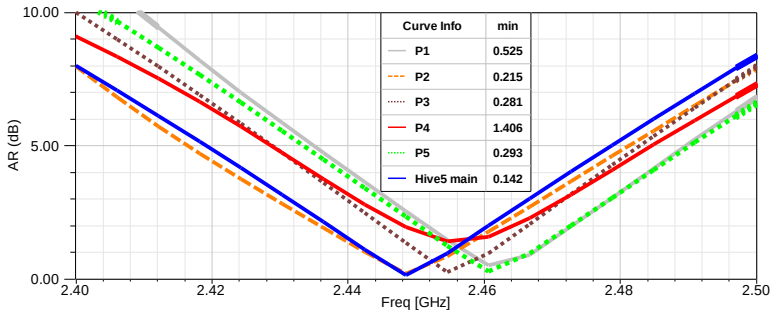

Fig. 4.11 AR comparison between Hive5 Elements

The Hive5 simulation results were very promising, with a gain of 5.31dBi, beam width below 3dB of 68º and 70º over XoZ and YoZ planes, bandwidth of 140 MHz from 2.4 GHz to 2.54 GHz and an AR below 3dB from 2.435 GHz to 2.468 GHz.

The gain of lateral cells of the Hive5 antenna for 2.45 GHz varied between 4.89 and 5.12dBi with a beam width of few degrees larger than the Hive5 main cell.

Hive5 Measurements

The first implementation of the Hive5 antenna is shown in Fig. 4.12. For its correct analysis we measured S parameters of each antenna element of the Hive5, between main and lateral elements, two consecutive and two non-consecutive lateral elements. All other antennas were terminated with 50Ω matched loads. The measured S parameters are presented in Fig. 4.13 and Fig. 4.14.

As can be seen by measurements Hive5 elements presented a bandwidth around 140 MHz, from 2.43 to 2.57 GHz. All measured elements presented similar results with a shift of around 30 MHz related to the simulated results which can be justified by some errors in the considered permittivity of FR4 or by mechanical implementation deviation.

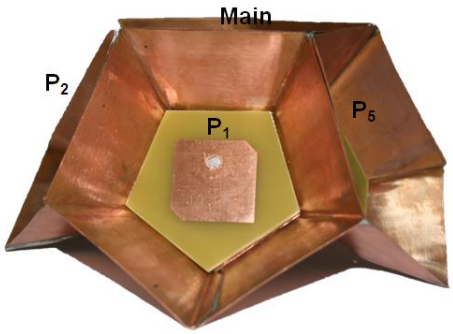

Fig. 4.12 Implemented Hive5 antenna

The isolation between Hive5 elements is well noticed, main and lateral elements isolation is presented in 4.13, two consecutive lateral and non-consecutive lateral elements are presented in Fig. 4.14.

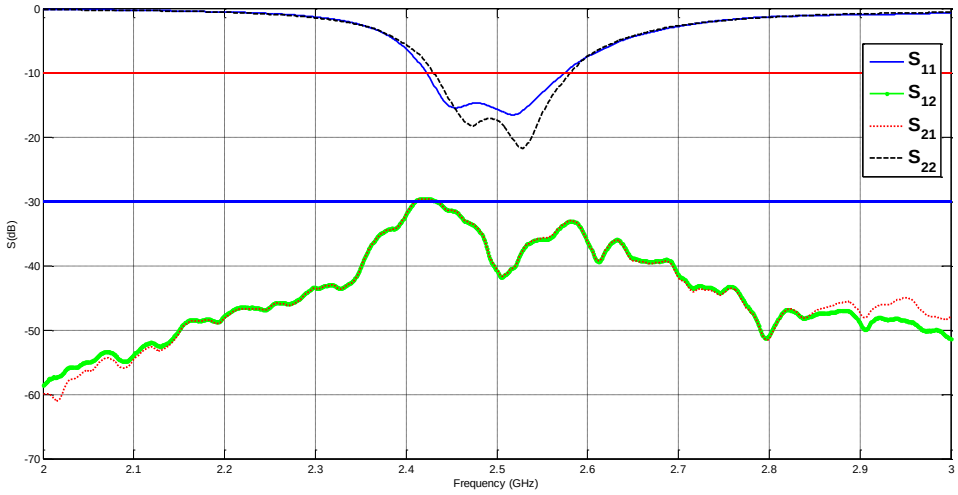

Fig. 4.13 S parameters between Hive5 main and lateral elements

Then we measured the Hive5 elements AR and radiation pattern where similar behavior with small deviance between elements was achieved. Fig. 4.15 presents the AR measured in three situations, patch antenna without any mechanical structure, PP patch-excited element and Hive5 main cell.

The best obtained result was achieved with the Hive5 main cell with a measured AR of 0.43dB. This is predictable since the simulation and optimization was related to the Hive5.

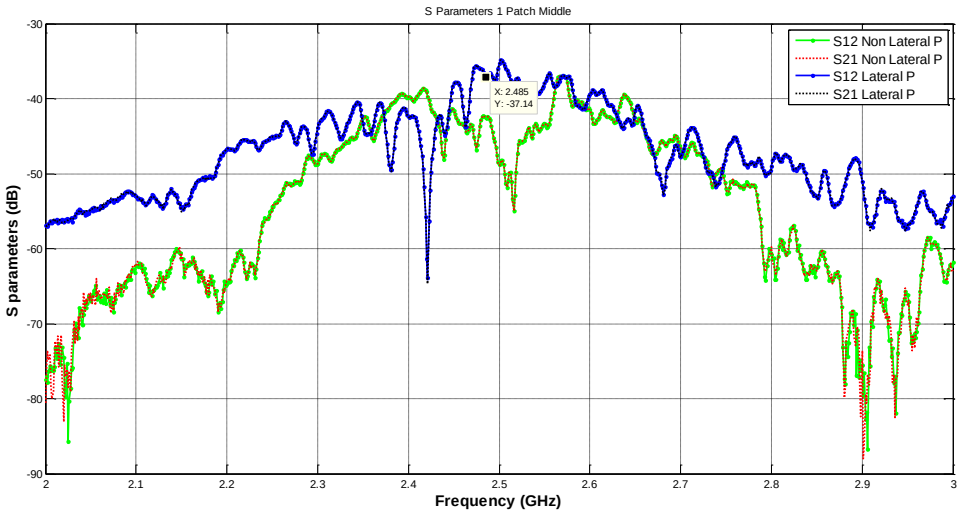

Fig. 4.14 Isolation between Hive5 consecutive and non-consecutive lateral elements

It can be seen that the Hive5 antenna presents good results and has CP for 2.485 GHz.

The measured gain of the Hive5 was of 5.52dBi with a beam width below 3 dB of 69º and 72º for XoZ and YoZ planes. The radiation pattern of the Hive5 main element was also measured and can be seen in Fig. 4.16.

Some deviations between measurement and simulation were observed which are mainly justified by manual construction of the Hive5. Nevertheless they are within the expected results.

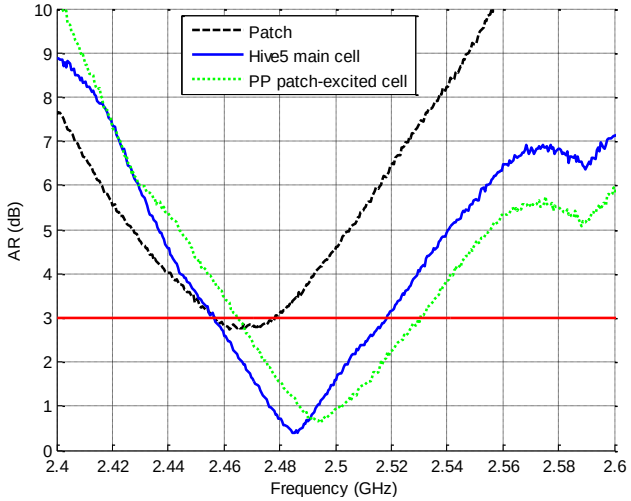

Fig. 4.15. AR measurements with different structures

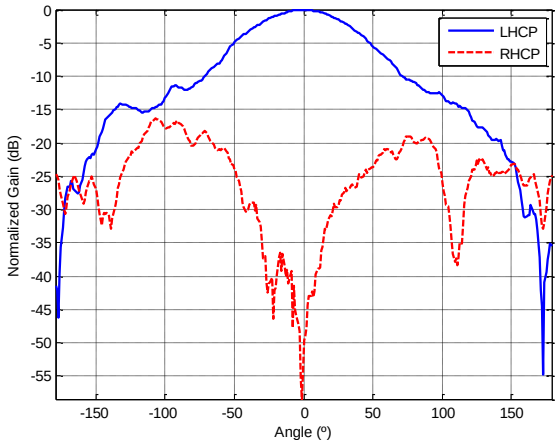

Fig. 4.16 Hive5 main element radiation pattern for LHCP and RHCP

4.1.2 SB-6 Log Periodic Antenna

The 6-SB Antenna is UWB switch beam antenna based on commercial log-Periodic dipole arrays (LPDA), model HG824-11LP-NF [122]. This antenna is designed to operate from 800 MHz to 2500 MHz being suitable for GSM/CDMA/PCS/3G/4G/WLAN applications. This antenna is presented in Fig. 4.17.

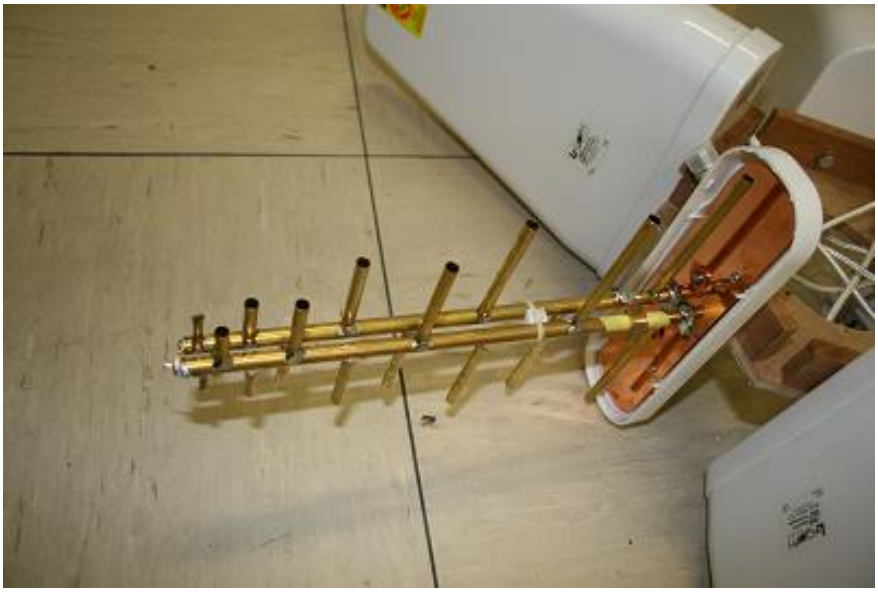

Fig. 4.17 Log-Periodic Antenna (HG824-11LP-NF)

This antenna has dimensions 330x215x62mm, linear polarization and is matched for 50 Ω. By the datasheet provided the antenna parameters can be resumed as:

At 800-960 MHz is it characterized by:

- Gain, 9.5 dBi;
- Horizontal Beam Width, 80º;
- Vertical Beam Width, 60º;
- Front to Back Ratio >= 20 dB.

And at 1710-2500 MHz by:

- Gain, 11 dBi;
- Horizontal Beam Width, 60º;
- Vertical Beam Width, 50º;
- Front to Back Ratio >= 20 dB;

To design the switch beam antenna we need to consider the entire azimuthal coverage, the 360º. Looking to the worse case of analysis, (highest frequency 2500 MHz) the horizontal beam width is 60º. In order to guarantee the 360º coverage easily we can conclude the requirement of 6 antennas for a circular switch beam approach as presented in Fig 4.18.

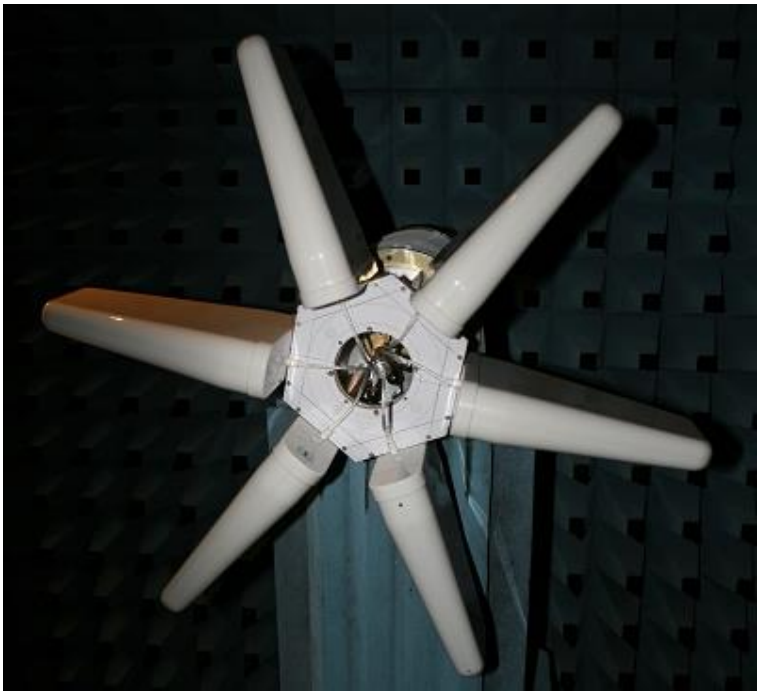

Fig. 4.18 SB-6 Log Periodic Antenna

SB-6 Log Periodic Measurements

Will the help of a VNA the S_{11} was measured as shown in Fig. 4.19.

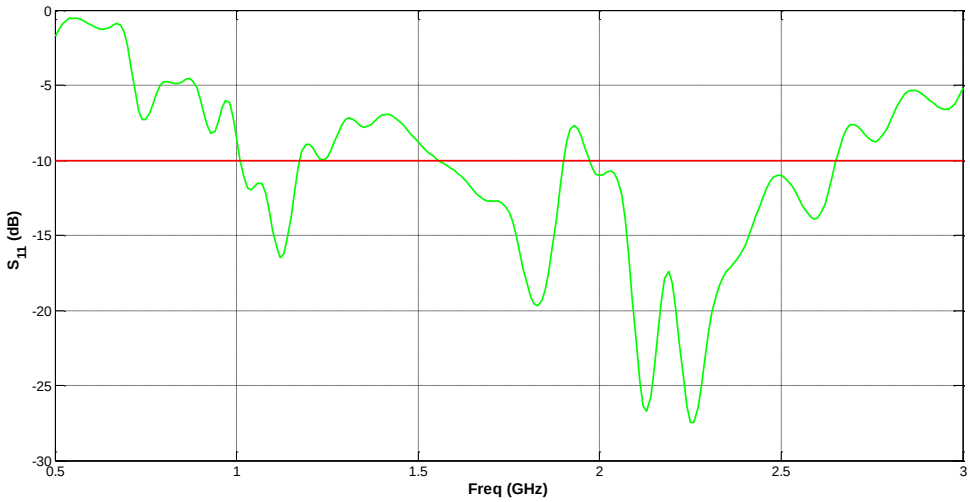

Fig. 4.19 S_{11} Measurement

The radiation pattern of a single Log Periodic antenna was also measured in an anechoic chamber. Considering the coordinates presented in Fig. 2.1, propagation in z with E align with the XoZ plane, the radiation pattern of the Log-Periodic Antenna and the SB-6 Log Periodic was measured. They were analyzed for 900 MHz and 1800 MHz.

The plots of the radiation patterns for several frequencies around 900 MHz for E plane, (XoZ plane) and H plane (YoZ plane) are shown in Fig. 4.20, A) and B) presented the Log Periodic Antenna and C) and D) a single element of the SB-6 Log Periodic Antenna. As shown the H plane plane is wider, and the E plane is narrower.

The same analysis was performed after for the GSM upper band, 1800 MHz, shown in Fig. 4.21. At this frequency side lobs are more evident. As expected, the H plane is wider, and the plane E plane narrower. Identical effect is presented of the antenna in the switch beam approach, as presented in C) and D) graphs of same figure. The impact of the surround structure is evident.

Developed and measured the SB-6 Log Periodic with commercial antennas, a lower cost solution may be in future needed to be developed. However not yet required, the full simulation of a planar LPDA was performed in case of future implementation, presented in next section.

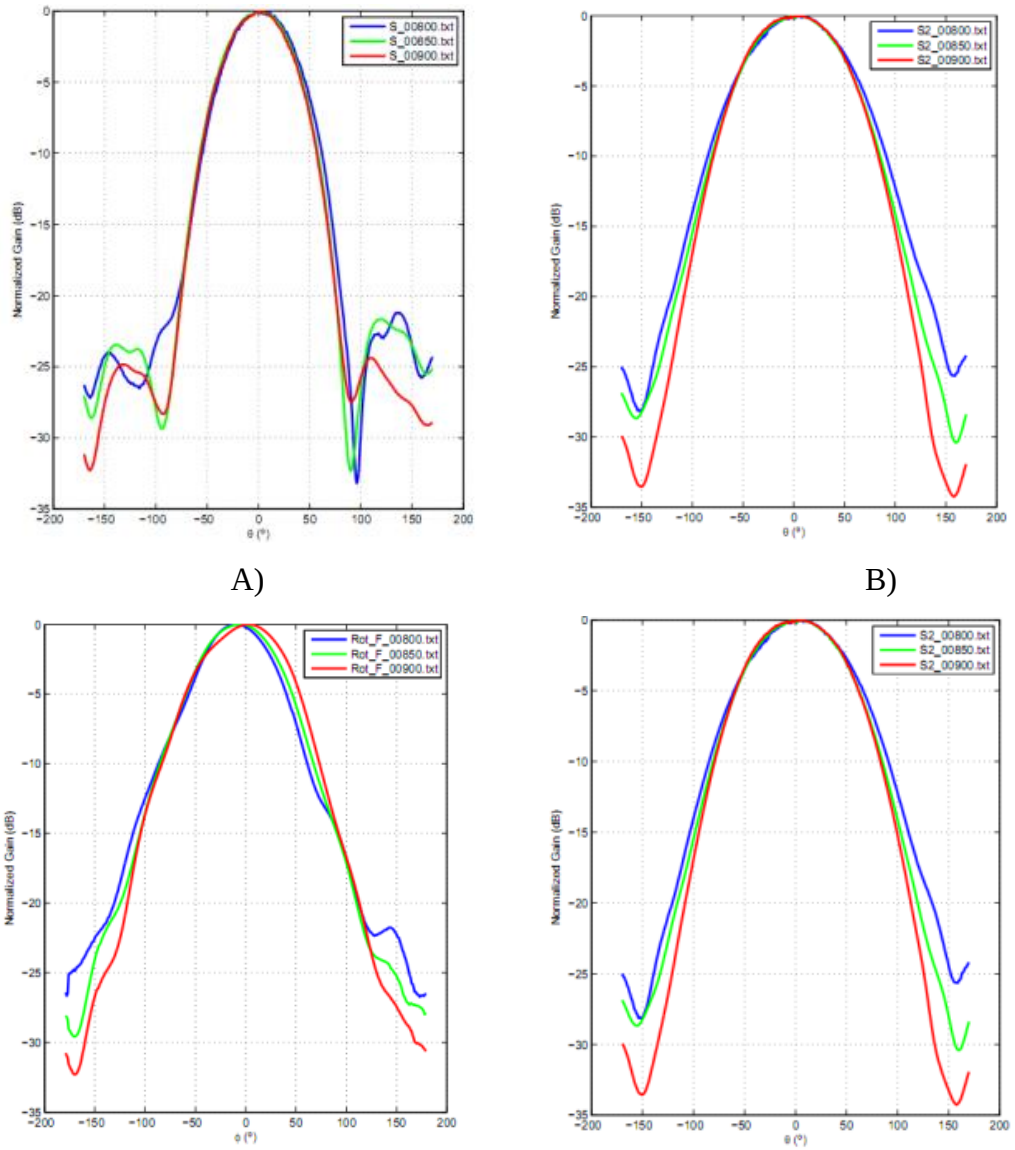

Fig. 4.20 RP at for 900 MHz for LPDA E-Plane A), and H-Plane B) and for SB-6Log Periodic E-Plane C), and H-Plane D)

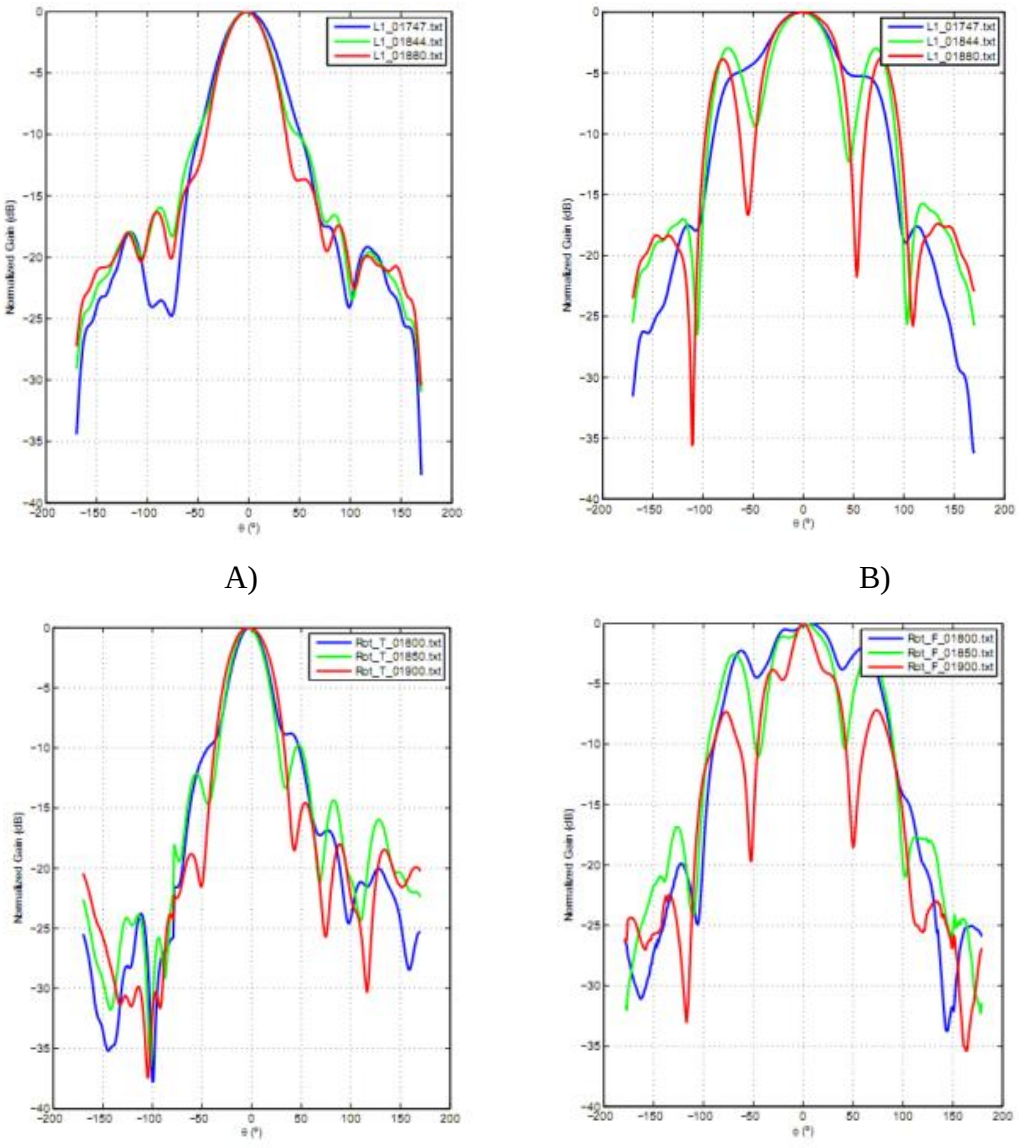

Fig. 4.21 RP at for 1800 MHz for LPDA E-Plane A), and H-Plane B) and for SB-6Log Periodic E-Plane C), and H-Plane D)

SB-6 Log Periodic Alternative

The SB-6 Log show good results, however it is based on a commercial solution. In order to reduce the system cost it was performed the simulation of a planar LPDA based on FR4. The design of the antenna is presented in Fig. 4.22. The 3D radiation patterns of the main frequencies of interest (900 MHz and 1800) are present in Fig. 4.23 and Fig. 4.24.

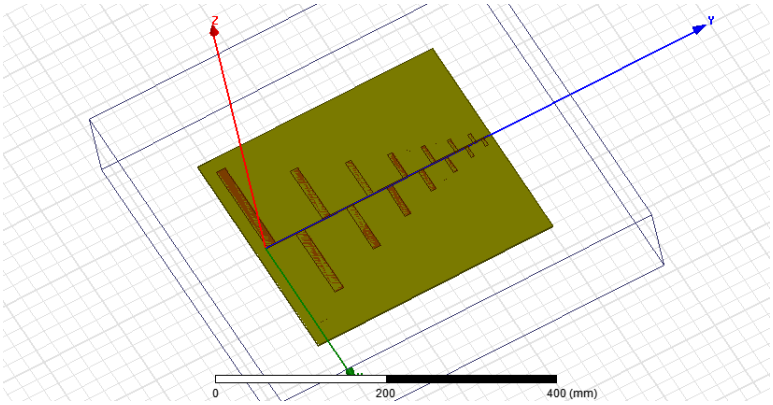

Fig. 4.22 Simulated UWB LPDA

This antenna presents a low cost with very good impedance matching, however with reduced gain compared with commercial LPDA. This is justified by the use of low cost subtract, FR4 which present significant losses.

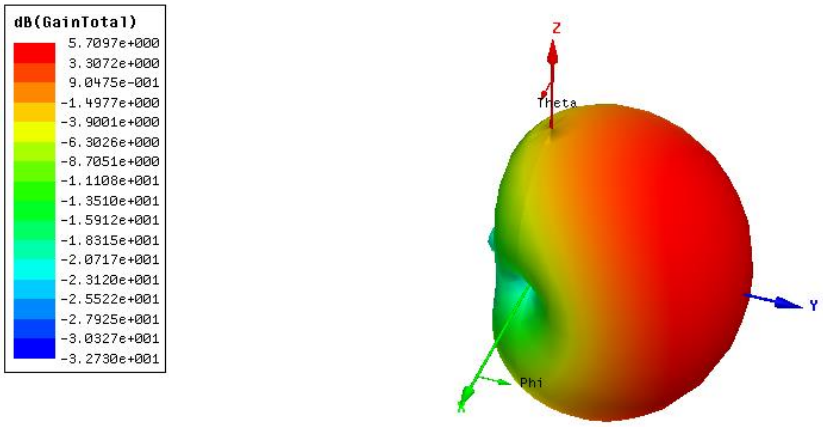

Fig. 4.23 Simulated UWB LPDA radiation pattern at 900 MHz

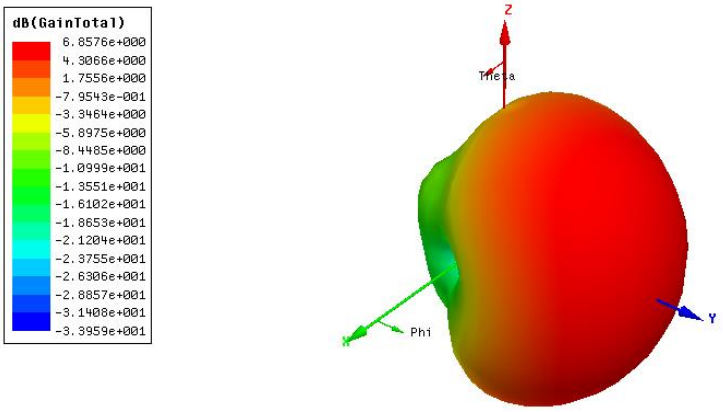

Fig. 4.24 Simulated UWB LPDA radiation pattern at 1800 MHz

The half power beam width (HPBW) of this antenna is 116º for 1800 MHz and 118º for 900 MHz which is near the 120º needed for the entire azimuthal coverage with only three antennas. Using lower loss subtracts higher gain can be achieved providing a system with higher coverage. Obviously the HPBW would be smaller being required more antennas for the entire azimuthal coverage with a maximum variation of 3 dBs.

4.2 Communication Antennas for 5 GHz

In the period of this thesis several antennas for communication purposes were also implemented. These antennas were developed to operate at 5.8 GHz or with wider band to cover the 5GHz UNII and ISM bands mainly for vehicular communications purposes. Thee planar implementations were analyzed and are presented in this section: a omnidirectional microstrip antenna array, a loop antenna and an elliptical antenna array with inner counter-elliptical slots.

4.2.1 Planar Omnidirectional Microstrip Array

WSN communication systems often require omnidirectional radiation pattern in the azimuthal plane and narrow beam width radiation in the elevation plane. One of their purposes is vehicular communications where it is desired to perform Vehicle to Vehicle (V2V) and Vehicle to Infrastructure (V2I) communications. For this purpose microstrip antenna arrays have received special attention mainly due to their low profile, light weight, and easy fabrication characteristics. Several approaches have been presented in literature such as: Hsiao [123] that proposed an omnidirectional planar antenna based on two back-to-back folded dipoles; Soliman [124] designed a dual polarized omnidirectional antenna using planar slot structures; Bancroft [125] proposed an omnidirectional antenna using planar microstrip elements; Li [126] presented another approach of omnidirectional microstrip antenna for Wimax applications; Chen [127] presented a planar slot array with the same radiation pattern. In this paper we proposed and implemented an omnidirectional microstrip antenna based on Bancroft approach. The antenna was dimensioned for higher frequency operation. The new driving point implied a new antenna design

Antenna Design

In order to implement a cheap and practical solution it was implemented an antenna with 1.6 mm-thick FR4 (εr = 4.1, tan δ = 0.02) subtract. The replacement of the driving point to the edge led to an optimization of the antenna design in order to guarantee the in phase current of all radiating elements. The design of the presented antenna, OMAA, is presented in Fig. 4.25 and parameterized in Table 4.2. The work perform in the analysis of this antenna was presented in Antennas and Propagation Symposium of 2013 [C7].

The left side of the figure presents the top layer and the right the bottom one. The radiation elements are formed as cascading impedance converters. The radiating elements have length of L1 and W1 width. The transmission line has as dimensions length L2 and width W2. In order to guarantee the in phase current of all radiating elements (top and bottom) of the OMAA, the layers are connected by a metallic via (short circuit). Considering the proposed design and an infinitesimal height antenna, the short circuit should be placed exactly in the middle of the radiating element, point of impedance 0Ω. For our antenna height (1.6 mm) and operation frequency, via size can't be neglected. By this reason the short circuit is not placed on the center of a radiation element, but instead at an offset of size L3, as shown in Fig. 4.25. The antenna driven point is placed on an antenna edge (placed at distance L5 from the first radiating element) due to practical reasons and in order to facilitate its connection with the SMA connector.

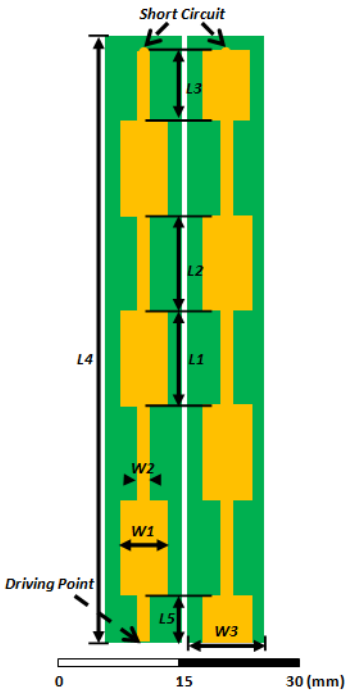

Fig. 4.25 OMAA design

Variable	***Dimension***	***Description***
L1	12mm	Radiating Element Length
L2	12mm	Transmission Line Length
L3	9mm	Upper Transmission Line Length
L4	77mm	Antenna Length
L5	6mm	Lower Transmission Line Length
W1	6mm	Radiating Element Width
W2	1.5mm	Transmission Line Width
W3	10mm	Antenna Width

Table 4.2 OMAA characterization

Measurements

The proposed antenna was simulated using ansys HFSS software package, fabricated and measured. To analyze the antenna we measured the S_{11} parameters and radiation pattern over azimuth and elevation planes. S_{11} analysis is presented in Fig. 4.26, azimuth plane in Fig. 4.27 and elevation plane in Fig. 4.28. A small deviation is present between simulations and measurements but the desired operation bandwidth is not compromised. This deviation can be mainly justified due to the FR4 characterization at this frequency.

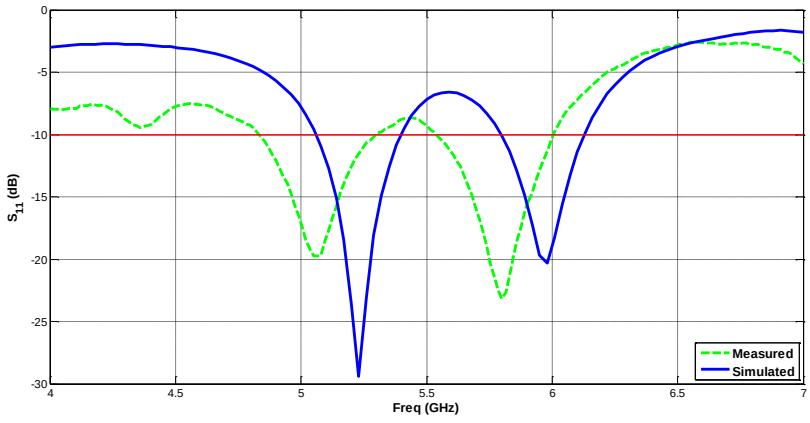

Fig. 4.26 S_{11} analysis

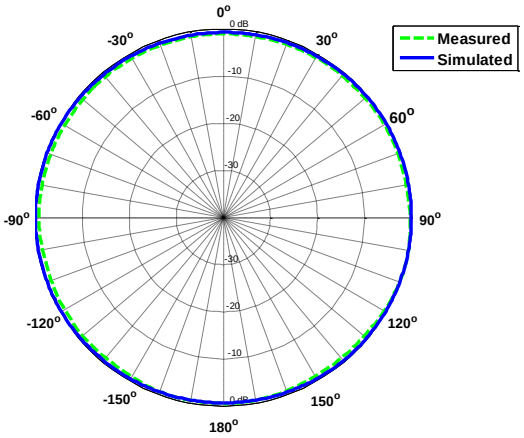

Fig. 4.27 Azimuthal plane radiation pattern

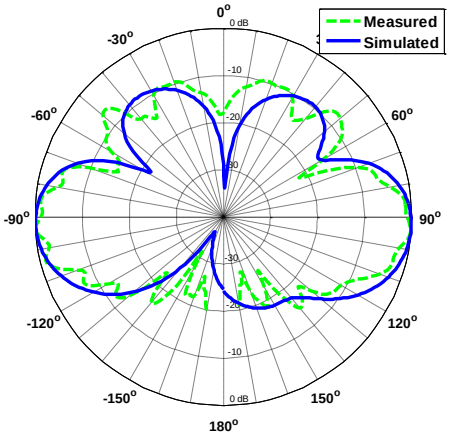

Fig. 4.28 Elevation plane radiation pattern

4.2.2 Omnidirectional Printed Loop Antenna for Taxi Communications

Inter Vehicular Communications (IVC) appears as a feasible solution to reduce road accidents, robberies and provide an auxiliary assistance for car drivers. For IVC two main communications need to be considered, vehicle-to-vehicle (V2V) and vehicle-to-infrastructure (V2I) based on the IEEE 802.11p standard. These systems have been analyzed in several fields of research since protocols, system architecture, and interference analysis [128]–[129]. Considering a roadside unit (RSU) antenna linear polarized in 45º, commonly implemented in GSM networks, onboard unit (OBU) integrated with vertical or horizontal polarized antennas can be valid solution.

For the special case of the Taxi, the integration of an antenna on the roof would imply a shadow area in the direction of the bonnet metallic components. A solution could pass by

its insertion above the bonnet, however, robustness and aesthetics constrains would be present. Nevertheless, if the antenna would be small enough and well placed inside the bonnet metal components effect could be reduced.

Taking in consideration previous considerations it is proposed a low profile planar loop antenna. This work was presented in Antennas and Propagation Symposium 2013 [C8] and the simulated antenna is shown in Fig. 4.29. Loop antennas can provide omnidirectional radiation pattern, with horizontal polarization at the same time that provide a planar solution. This antenna is based on [127], tested and re-dimensioned for 5.8 GHz, with a balun insertion. One proposal for the antenna placement is shown in Fig. 4.30, however not analyzed and discussed in this thesis.

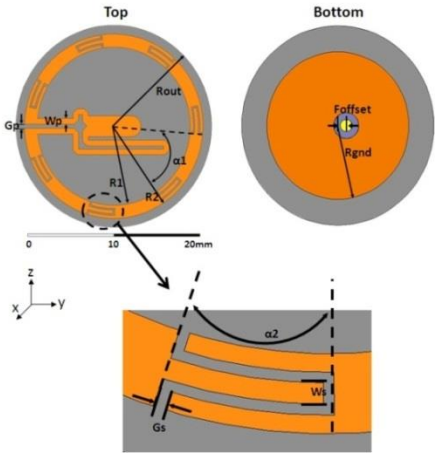

Fig. 4.29 Antenna design

Antenna Design

The basic geometry of the proposed horizontally polarized omnidirectional loop antenna is shown in Fig. 4.29 and its geometry described in Table 4.3. The antenna consists on a loop with periodical capacitive loading connected to a balun in order to allow direct unbalanced feed by a SMA connector. It was considered as subtract a 0.787 mm-thick Arlon CuClad217 ε_r 2.17, tan δ 0.0009).

Fig. 4.30 Taxi antenna placement proposal

Variable	***Dimension***	***Description***
Foffset	2mm	Feed offset to the loop center
R1	9mm	Loop inner radius
R2	10.5mm	Loop outer radius
Rgnd	8.5mm	Loop gnd radius
Rout	11.5mm	Dielectric radius
Gp	0.5mm	Gap between feed lines
Gs	0.2mm	Gap between interlaced lines
Wp	0.65mm	Width of feed lines
Ws	0.4mm	Width of center interlaced line
α1	360/7º	Angle per section
α2	9.3º	Angle for coupling lines

Table 4.3 Antenna Design characterization

Periodical capacitive loading is realized by inserting interlaced coupling lines along the loop. These interlaced coupling lines periodically introduce series capacitance to the loop, providing a small phase correction between the adjacent sections in order that the current along the loop is kept uniform and in phase, even with size comparable to the operating wavelength. Therefore, the antenna can be considered close to a magnetic dipole to achieve a horizontally polarized omnidirectional radiation pattern.

Simulations

The antenna was simulated, being S_{11} analysis presented in Fig. 4.31. Radiation pattern over azimuth and elevation planes are presented in Fig 4.33. The antenna shows gains around 2.5 dBi, omnidirectional radiation pattern over the azimuthal plane and horizontal polarization.

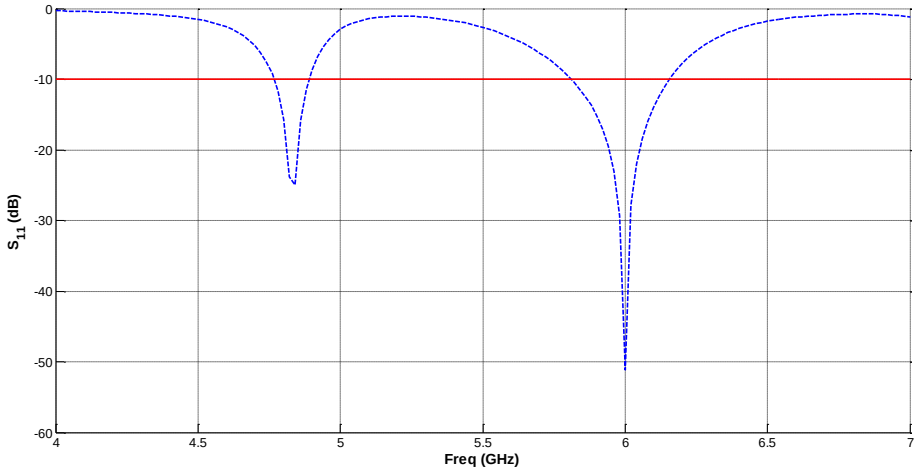

Fig. 4.31 S_{11} analysis

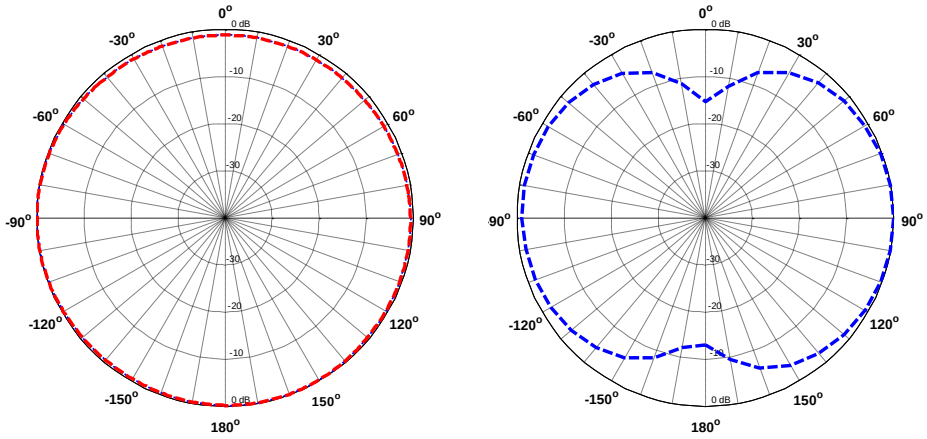

Fig. 4.32 Radiation pattern over azimuth plane(Left) and elevation (Right)

4.2.3 Planar elliptical antenna array with inner counter-elliptical slot

Nowadays with the "everywhere" availability of wireless technologies and wide electromagnetic spectrum use, it is fundamental to use single wide band antennas that accommodate different communication systems. According to the application, front-back

radiation patterns can be preferred to simple omnidirectional or single beam directivity antennas. This can be easily understood for scenarios where wireless communication is mainly in a single direction, such as in: communication inside tunnels, corridors, or even inter-vehicular communications.

Wide band antennas with CP are highly desired. Wide band antennas can accommodate different communication systems and CP presents several advantages in reflective environments since it allows signal transmission/reception in all planes; it overcomes out of phase problem, which can cause dead-spots; and it is more resistant to signal degradation due to adverse weather conditions [130].

Single feed antennas CP has been induced by several approaches such as: different radiating structures (e.g. fractal, spiral, dielectric resonator) [131]; and/or modification of radiation elements geometry (e.g. slots insertion, trimming opposite corners) [132]-[137]; and/or ground plane modifications (e.g. stub insertion) [138]-[139].

When high gain is desired, arrays can be considered, however, a correct feeding network needs to be designed. A good analysis of these feeds is presented in [140].

As previously described, high gain antennas with CP over a wide bandwidth are highly desired. With the emerging technologies for vehicular communication and wide spreading of infra-structure for high data rates WiFi, we intended to design a low-profile front-back directive antenna with CP over the entire 5GHz UNII/ISM bands (5.2-5.8 GHz).

We verified that a planar elliptical monopole (PEM) with an inner elliptical slot can provide relatively wide CP covering our band of interest.

In this section it is studied a Planar Elliptical Antenna (PEM) applied into an array of three elements, leading to the development of the CP Planar Elliptical Antenna Array (CP-PEAA) here presented. This work was p presented in [C6] and deeply analyzed in [J4].

Planar Elliptical Monopole (PEM)

Planar monopoles are characterized by their wide bandwidth and can have different geometries such as: triangular, rectangular, pentagonal, circular and elliptical, as presented in [141]. However the polarization is in majority linear and the radiation pattern omnidirectional. To impose the two orthogonal current components for CP in single feed monopoles, ground plane modification (i.e. insertion of stubs) and/or changes in the feeding position are common used techniques.

In planar elliptical monopole (PEM) CP can be induced without changing the feeding position, by rotating the radiating element. For a single element both approaches (changing feeding position or rotating the radiating element) are valid, however, if we consider a series array, where ground perturbation is not available in all radiating elements for current phase correction, the first approach can't be applied. On the other hand, the second approach (rotation of the radiating element) proved to be insufficient for array implementation with CP over the entire 5 GHz bands. The solution for this problem can be overcame with the insertion of an inner slot in each radiating element providing an individual current correction factor.

Based on previous information, PEMs can be divided into three main groups of monopoles: planar circular, planar elliptical and planar elliptical with inner slot, as suggested in Fig. 4.34 A, B and C respectively.

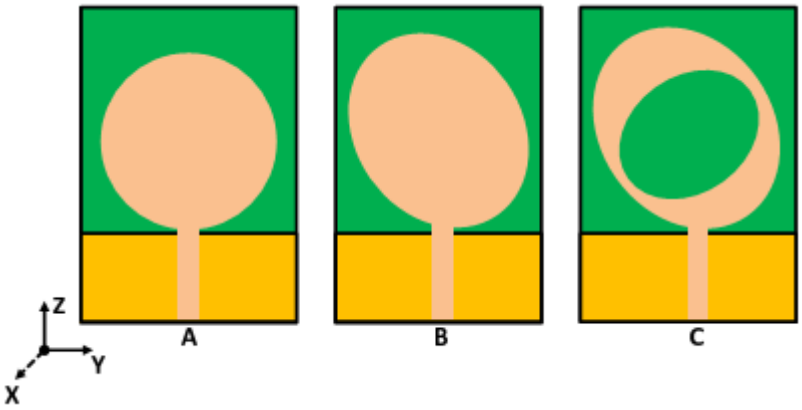

Fig. 4.34 PEM structures: A) Circular; B) Elliptical; C) Elliptical with inner slot

All the presented shapes provide wide impedance matching. The first design, a circular monopole, provides linear polarization and quasi-toroidal radiation pattern with a single optimization parameter, circular radius. Varying the circular to elliptical shape, two degrees of freedom are added, the elliptical ratio and rotation. This provides the chance to slightly change the radiation pattern and polarization. More degrees of freedom can be added with the insertion of an inner slot. For our design the slot was implemented with counter-elliptical shape. This design avoids sharp transitions and the addition of three optimization parameters (3Rs), inner major Radius, elliptical Ratio, and Rotation. All together six optimization parameters are available, three for the outer ellipse plus three for

the inner elliptical slot. This inner slot provides a way to tune CP over the desired bandwidth. The characterization of each PEM group is presented in Table 4.4.

Variable	***A***	***B***	***C***
RP	Q-Toroidal	Q-Toroidal	Q-Toroidal
Polarization	Linear	Linear/CP	Linear/CP
Wide	Wide	Wide	Wide
Parameters	1	3	6

Table 4.4 PEM characterization

The analyzed PEM is dimensioned according to the lower radiating element of the CP-PEAA are described in Table 4.5.

To design the CP-PEM with the inner counter-elliptical slot, it is important to know the influence of its three design parameters: major radius, elliptical ratio and rotation (3Rs). The dependency of S_{11} and AR with the 3Rs in presented in Fig. 4.34, Fig. 4.36 and Fig. 4.37 . It is clearly verified that while inner elliptical ratio and rotation slightly shift the AR, the radius variation has a main impact on polarization matching.

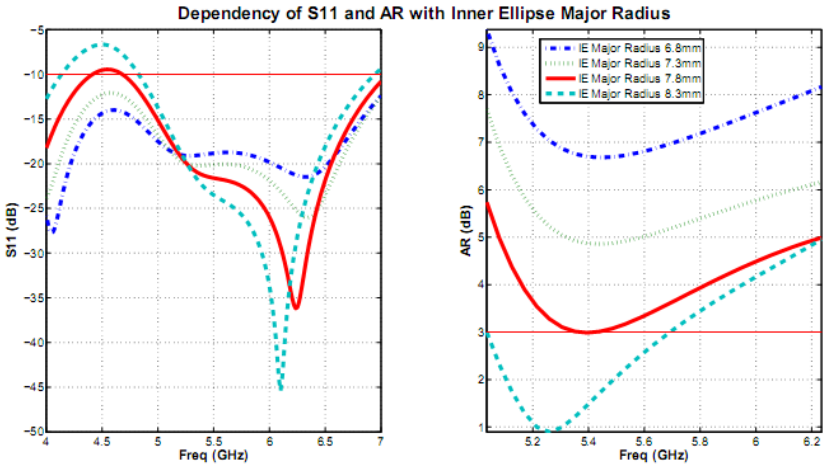

Fig. 4.34 S_{11} and AR dependency with IE Major Radius

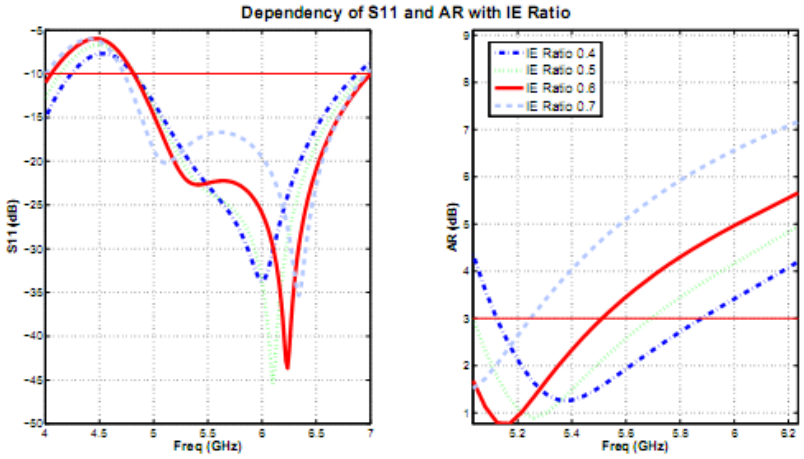

Fig. 4.36 S_{11} and AR dependency with IE Ratio

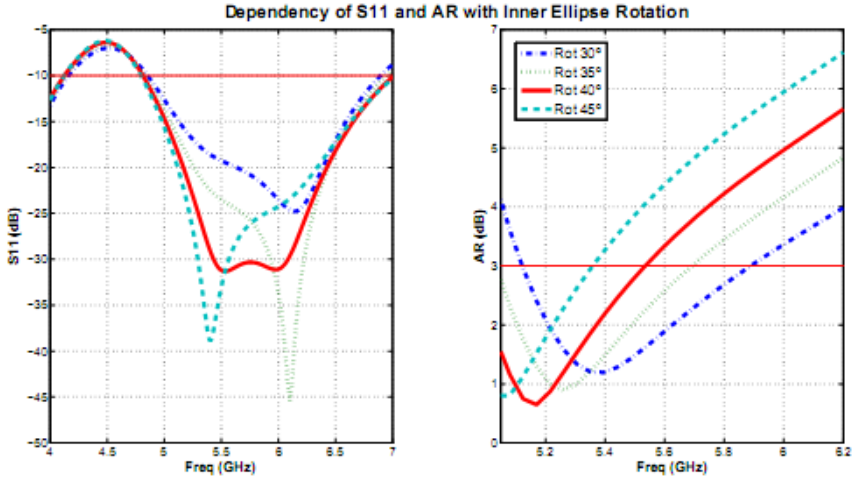

Fig. 4.37 S_{11} and AR dependency with IE Rotation

For the analyzed variation, it can be seen that the three parameters significantly influence the impedance and polarization matching. Controlling these 3Rs parameters a well matched PEM can be designed, providing the base for the CP-PEAA presented in the next section. The PEM approach presented CP over the band of interest, however with a gain of ~2 dBi which does not satisfy our requirements. In order to improve the gain the PEM approach was analyzed into an series array.

CP-Elliptical Antenna Array (CP-EAA)

To improve and achieve the desired gain a series array of three elements is analyzed, as shown in Fig. 4.38. The antenna dimensioning after optimization is presented in Table 4.5.

Variable	***Dimension***	***Description***
CL_L	17.25mm	Connecting Line Length
$E3_L$	100mm	Antenna Length
FL_L	12mm	Feed Line Length
FL_W	1.7mm	Feed Line Width
Gnd_L	5.5mm	Ground Length
Gnd_W	28mm	Ground Width
IE_NRad	8.3,8.3,8.3mm	Inner Ellipse N Major Radius
IE_NRatio	0.5,0.5,0.5	Inner Ellipse N Ratio
α_N	35º,5º,20º	Inner Elipse N Rotation
OE_NRad	8.5,8.5,8.5mm	Outer Ellipse N Major Radius
OE_NRatio	1.25,1.25,1.25	Outer Ellipse N Ratio
β_N	60º,60º,60º	Outer Elipse N Rotation

Table 4.5 CP-PEAA Dimensioning

The antenna is printed on 0.787 mm-thick FR4, εr=4.1, tan δ = 0.002) substrate with 100x28mm^2.

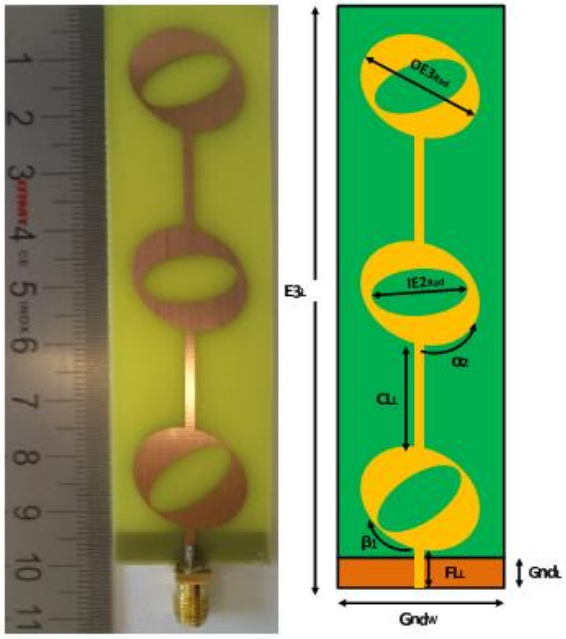

Fig. 4.38 CP-PEAA antenna design

As a starting point for comparison there were considered all the array elements with the parameters (major radius, elliptical ratio and rotation) identical to the CP-PEM presented before. With these characteristics a good impedance matching was achieved, although with poor CP over the band of interest, 5.2-5.8 GHz.

In order to improve the AR, a rotation of the inner elliptical elements 2 and 3 was performed for optimization. The impact of these parameters on S_{11} and AR is presented in Fig. 4.39 and Fig. 4.40. For this analysis all the other parameters (ground, feed and connecting lines) are described in Table 4.5.

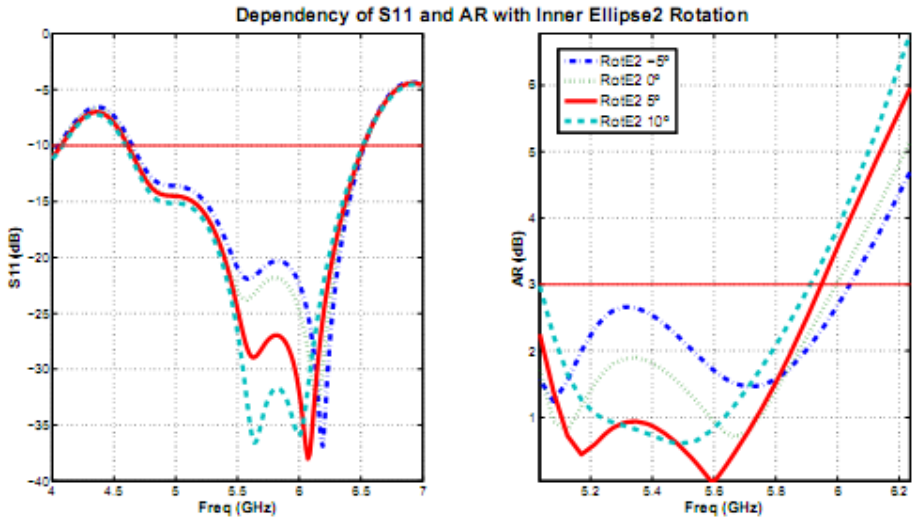

Fig. 4.39 S_{11} and AR dependency with IE2 Slot Rotation

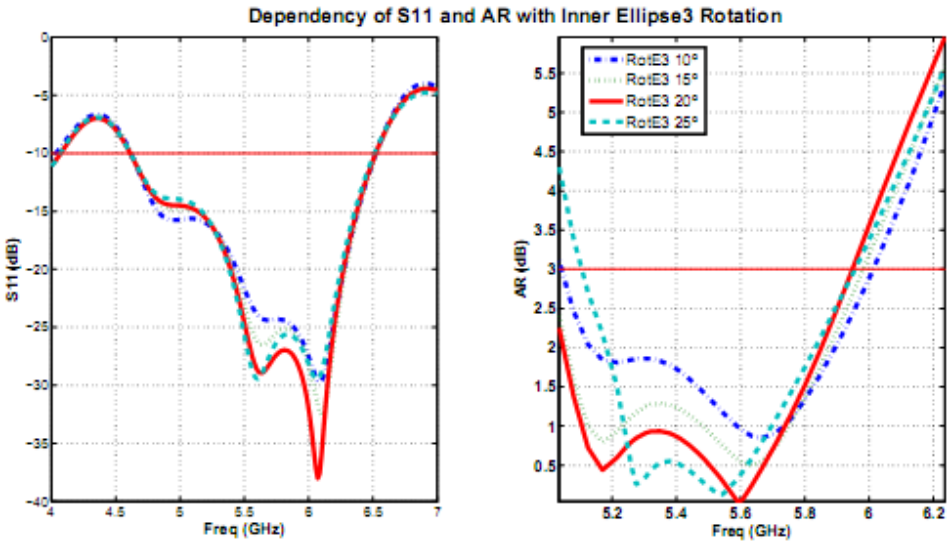

Fig. 4.40 S_{11} and AR dependency with IE3 Slot Rotation

After a careful analysis of the simulation an antenna for testing was developed, presented in next section.

Measurements

This section presents a comparison of simulated and measured results.

Fig. 4.41 presents the antenna S_{11} comparison analysis. Next we analyze the XoY plane left and right hand circular polarization (LHCP and RHCP) radiation pattern for 5.2 and 5.8 GHz, presented in Fig. 4.42 and Fig. 4.43. The 180º presents the front side of the antenna, radiating RHCP and de 0º the back side.

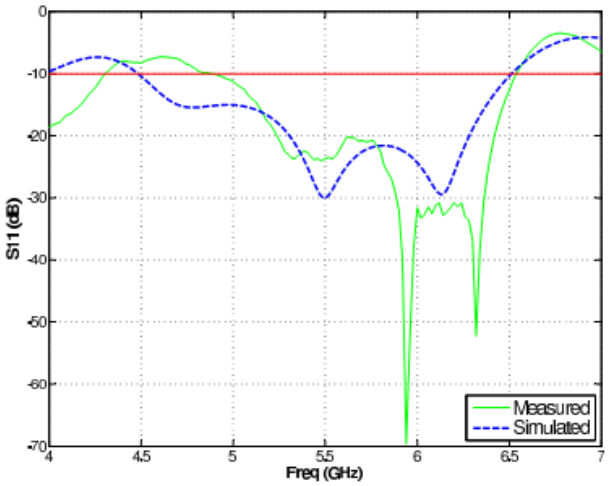

Fig. 4.41 S_{11} Comparison

The YoZ plane is presented in Fig. 4.44 and Fig. 4.45, where 90º represents the upper side of the antenna.

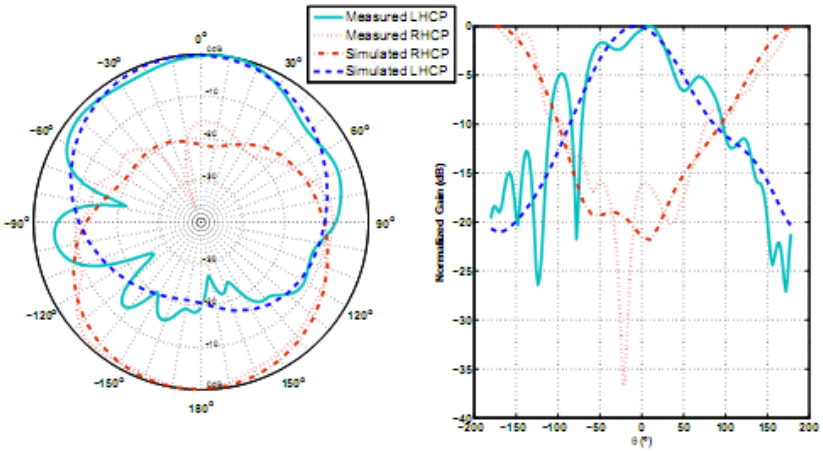

Fig. 4.42 XoY Plane, LHCP/RHCP radiation pattern for 5.2 GHz

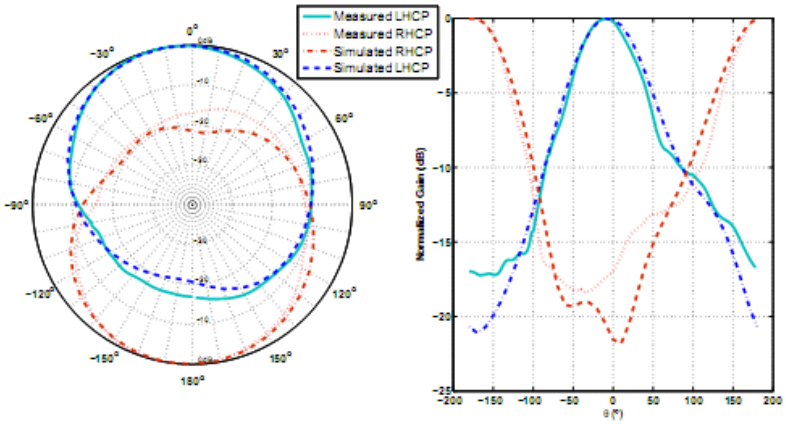

Fig. 4.43 XoY Plane, LHCP/RHCP radiation pattern for 5.8 GHz

The measured gain for XoY plane was 7.1 dBi and for upper side of YoZ plane was 6 dBi with vertical polarization.

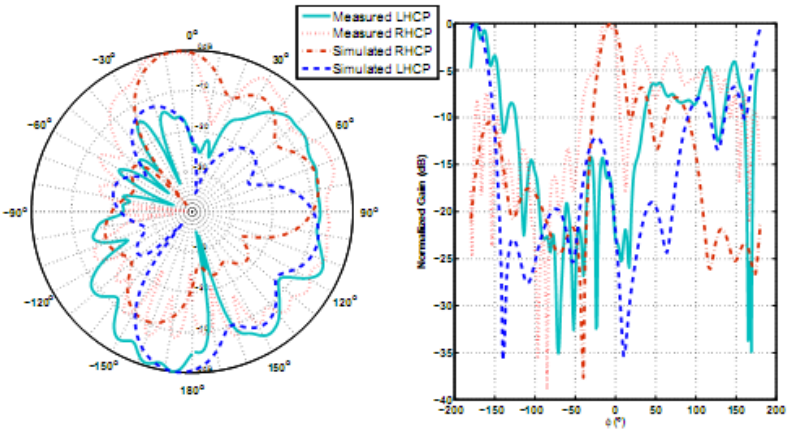

Fig. 4.44 YoZ Plane, LHCP/RHCP radiation pattern for 5.2 GHz

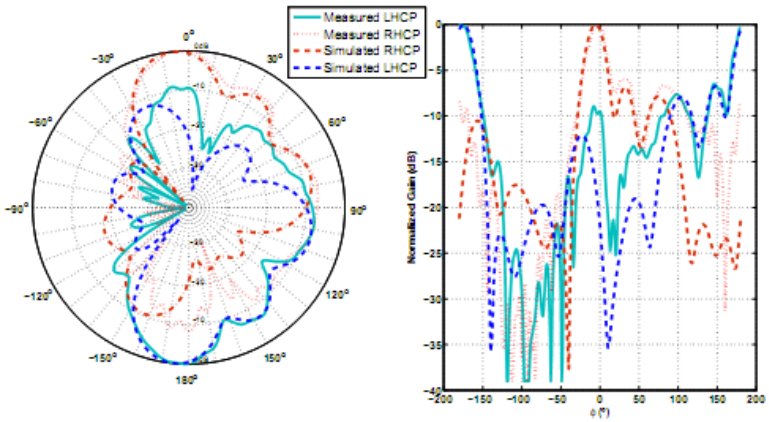

Fig. 4.45 YoZ Plane, LHCP/RHCP radiation pattern for 5.8 GHz

The AR over the operation band for the front and back sides is also analyzed, shown in Fig. 4.46. The similarities between simulation and measured results are obvious, although, some deviation can be seen, which can be partially justified by the FR4 characterization.

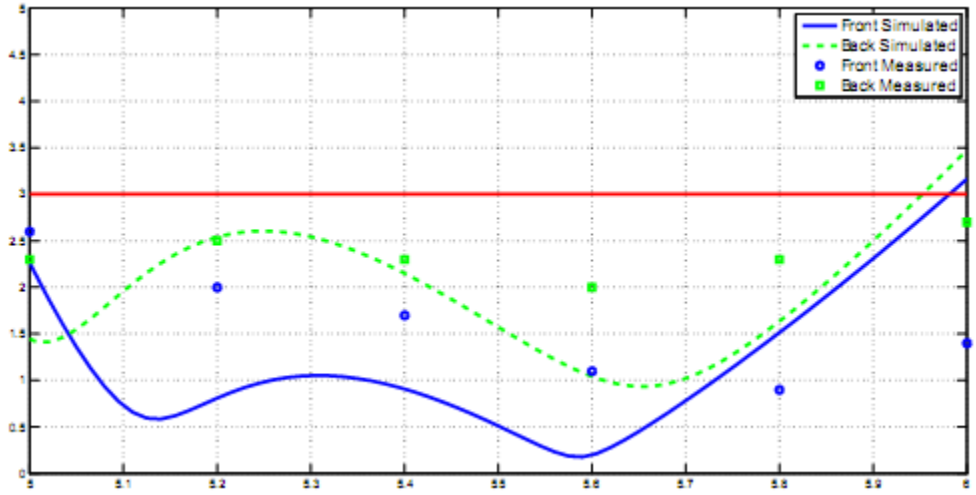

Fig. 4.46 AR over the operation bandwidth

4.3 Concluding Remarks

Two sectorial antennas are presented in this chapter.

The Hive5, a new SA constituted by PP patch-excited antennas, provides a solution for 2.4-2.5 GHz LSs with approximately semispherical radiation pattern and a maximum variation of 3dB beam width over the radiation pattern; reduced coupling between neighbor antennas; increased multipath rejection; CP of all Hive5 cells and finally a practical and low cost design suitable for LSs based on RSS and AoA. The simulations are concordant with the measurements which validates the presented proposal.

The SB-6 Log Periodic, a UWB SA provides a wide bandwidth covering the GSM-900/1800 bands and gain around 10 dBi for long distance communication purposes. Measurements prove the concept of operation can be applied. The preparation for future development of planar LPDA is also presented.

Three antennas operating at 5 GHz for communication purposes are presented in this chapter.

A new approach for OMAA antennas is presented. Based on Bancroft antenna, an OMAA optimized for 5 GHz ISM and UNII band with an edge feed was redesigned. Considering the edge driven point implies a new position for the metallic via which is here

presented. The simulations and measurements present a small deviation, however impedance matching for the desired bandwidth is not compromise.

An Omnidirectional Printed Loop Antenna for Taxi communications is proposed. The in phase and uniform current over the loop allows omnidirectional radiation pattern even with loop dimensions comparable to the operating wavelength.

A new printed planar microstrip antenna with elliptical elements is lastly presented. The operating bandwidth of the antenna with usable radiation pattern is about 20%. A new way to match PEM with CP is proposed by the insertion of an inner counter-elliptical slot. This technique provides wide band in polarization for single feed monopoles and can be easily integrated into arrays named here PEAA.

To compensate the mismatch of polarization inherent to the array implementation, rotation of the inner counter-elliptical slot can be used as an easy way of optimization.

The proposed antenna provides two main directive radiation components (front and back) with gain higher than 7dBi, and CP over the 5 GHz bands with three radiating elements. Higher gain is possible with the integration of more radiating elements.

This antenna can be suitable for performing both inter-vehicular and proximity WiFi communication.

4.4 Summary of this Chapter

This chapter presents the developed antennas during this PhD work.

A cost effective solution to control the radiation pattern can be achieved with the use of switch beam antennas. For this purpose two SA were developed, the Hive5 for 2.45 GHz and the SB-6 Log Periodic Antenna for UWB sectoring.

Low cost antenna for communication at 5.8 GHz are highly desired which can be used for example, for vehicular communications. Several antennas were studied and implemented for this frequency. It was developed a planar omnidirectional microstrip array based on Bancroft approach, a printed Loop for Taxi communications and a planar elliptical antenna array with inner counter-elliptical slot.

This work led to the publication of several articles, [J4], [C6], [C7] and [C8].

Chapter 5 – Developed Systems

After the development of the antennas it was performed their integration into LS or simple testing prototypes. The description of the LS developed during this PhD period is presented in this chapter. Firstly it is presented the LS with the Hive5 for indoor localization. Next it is described the developments performed for NaPis LS, a full management localization system integrated with several technologies. Finally it is presented the prototype of the SB-6 Log Periodic Antenna and its control application. This antenna is intended to operate for maritime communications in order to increase the cellular network range and provide data communication on board. The system for future implementation is also described.

5.1 LS with Hive5

In this section it is presented the developed firmware and management application of an LS integrated with the Hive5 previous described. This work was previous published in [J3]. This LS performance is then compared to a typical Wireless Sensor Network (WSN) LS based on four nodes. Both solutions are analyzed within the same localization environment and compared to the same supporting fingerprinting algorithm, an Artificial Neural Network (ANN). Results show that LSs integrated with the Hive5 present clear benefits when compared to the WSN of four nodes in terms of resolution and obvious reduction of required reference units. This work was published in the international journal IET Microwaves, Antennas & Propagation, [J3].

5.1.1 The system

The Hive5 can be used either as a switch beam antenna, or as an SAA with appropriate signal processing algorithms, although, in this way, at the cost of a more complex system. The switched beam antenna approach provides a simpler and cheaper solution making it more suitable for low cost LSs. Besides the Hive5 antenna, this approach also requires the following components: a measuring RSS module, an SP6T RF switch, and low loss RF cables as presented in Fig. 5.1.

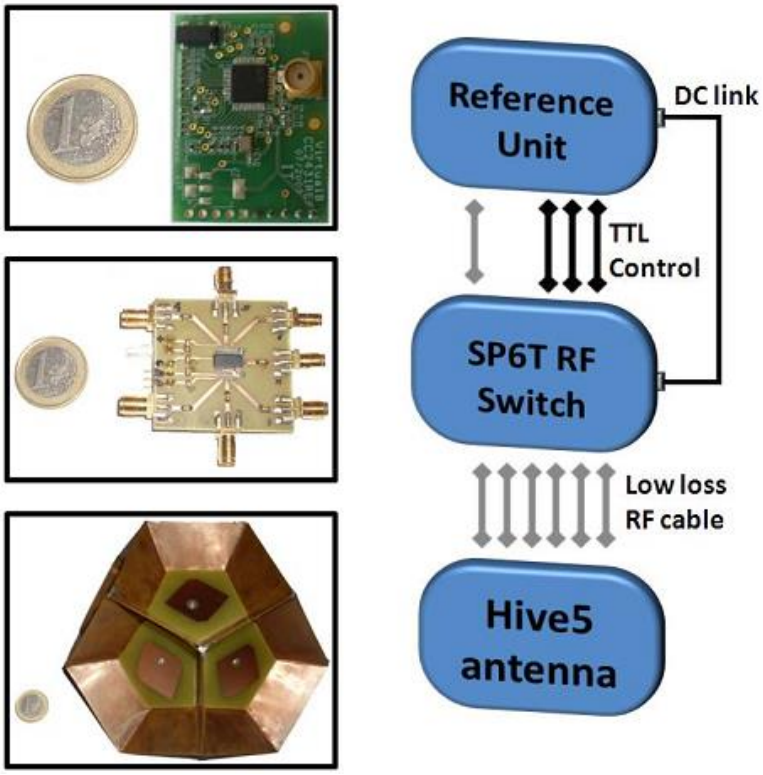

Fig. 5.1 Implementation of Hive5 in a LS

For the presented test a commercial System on Chip (SoC) was considered on the reference unit [142] a SP6T as the RF Switch [143] and semi-rigid cables of 18 and 23 cm with a measured transmission loss below 0.32 dB for considered lengths. These cables are used for the Hive5, RF-Switch, and reference unit interconnections.

5.1.2 The protocol

The Hive5 is an antenna suitable for LSs that requires a single reference unit. Nonetheless it needs to be integrated into a high and central position on the localization scenario for the system to achieve efficient performance.

The developed protocol consists of a simple network of three elements: a mobile unit (MU) or node (MN), which is the element to be located; a reference unit (RU) or node (RN), which is the controller of the Hive5; and a coordinator, which is the gateway to the PC running the LS application.

5.1.2.1 The Mobile Node (MN)

After registering into the network, the MN sends a localization request (MN_LOC_REQ) to the WSN waiting for acknowledgement from the RN (RN_LOC_ACK). This message may include configuration data as a payload. Then, the MN listens to the channel for Hive5 blasts (RN_LOC_BLAST) and subsequently, the end process message (RN_LOC_BLAST_END). Each of the previous messages sends the identification of the transmitter Hive5 element (PN0 to PN5) as a payload. The MN measures the RSS of each message and associates it to the Hive5's transmitter element.

After the collection of RN_LOC_BLASTs and subsequent RN_LOC_BLAST_END the RSSs and correspondent Hive5 elements' identification are sent as unicast to the coordinator (MN_RSS_COLLECT).

After the RSS collection is sent, the MN enters into a low power consumption mode (Sleep Mode) where the transceiver and MCU are turned off. The MN wakes up after a pre-defined interval and this process is cyclically repeated. The expired intervals and sleep time are configured within the reception of the RN_LOC_ACK message.

5.1.2.2 The Reference Node (RN)

The RN permanently stays into a polling mode listening for WSN messages. It can receive messages from the coordinator (RN_CONFIG and MN_CONFIG) to configure the RN number of blasts and/or transmission interval and the MN expiration or sleep intervals. For localization processes the RN initially receives a localization request from the MN (MN_LOC_RQT). After receiving this message, the RN replies with an acknowledgement (RN_LOC_ACK) which may contain configuration data. After this handshake, the RN sequentially activates each antenna element of the Hive5 to send blasts (RN_LOC_BLAST). When this process finishes, the main antenna element (PN0) is activated to send a confirmation of the transmission process ending (RN_LOC_BLAST_END).

5.1.2.3 The Coordinator

The WSN coordinator acts as a simple gateway with a PC running the LS application. The coordinator receives WSN messages and forwards them to the serial port and vice-

versa. All of the commands, selected on the application that will be described in next section, can be sent to the WSN by the intermediation of the coordinator.

A simplified representation of the localization protocol is shown in Fig. 5.2.

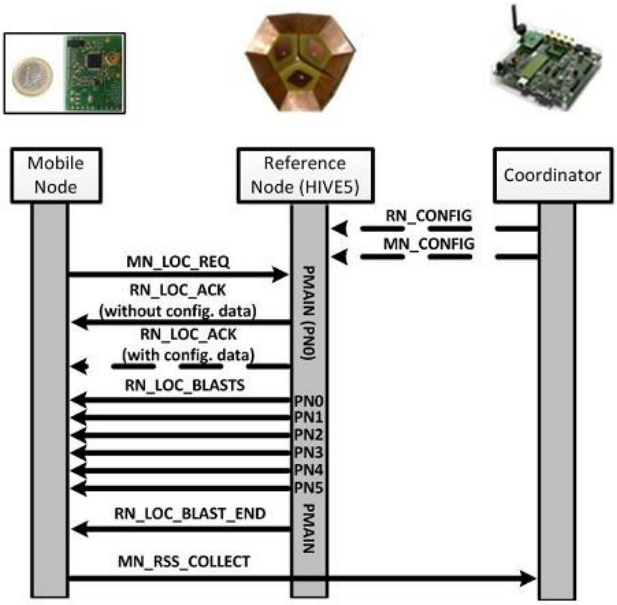

Fig. 5.2 Localization protocol description

5.1.3 The application

The management application that controls the LS was developed to perform four main operation options: detection, calibration, testing, and configuration as shown in Fig. 5.3.

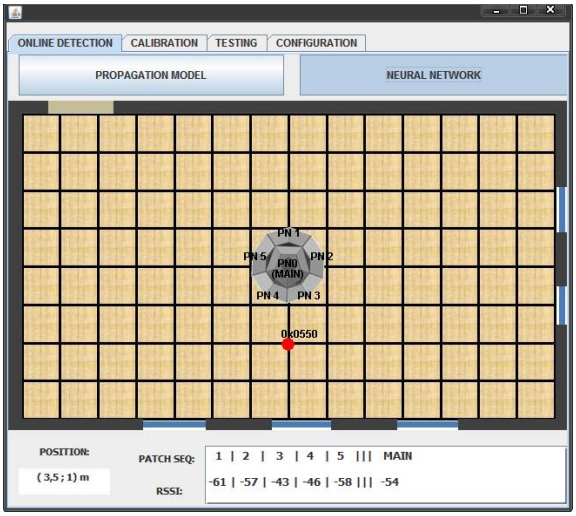

Fig. 5.3 Control Application

This application was developed using Java language due to its interoperability capabilities simplifying its implementation in different operating systems.

The first option (detection) provides an online localization based on different algorithms that can be selected by the user, such as those based on propagation models or fingerprinting, in this case, ANNs based.

Detection provides the visualization of collected RSSs and corresponding estimated localization; calibration provides the chance to record the collected RSSs for further offline calibration; testing provides the chance to analyze the response of different WSN devices; the configuration option allows for the configuration of WSN devices and an optional forwarding of the MNs position to a remote database, which is similar to the work developed in [C2].

All of the previously described options provide the basis for a correct operation and control of the Hive5 antenna according to the different localization scenarios to which it can be applied.

5.1.4 Results

In order to test the two LS solutions (using Hive5 and a typical WSN of four nodes) a testing scenario (TS) with 7m x 4m x 2.5 m was chosen, as suggested in Fig. 5.4.

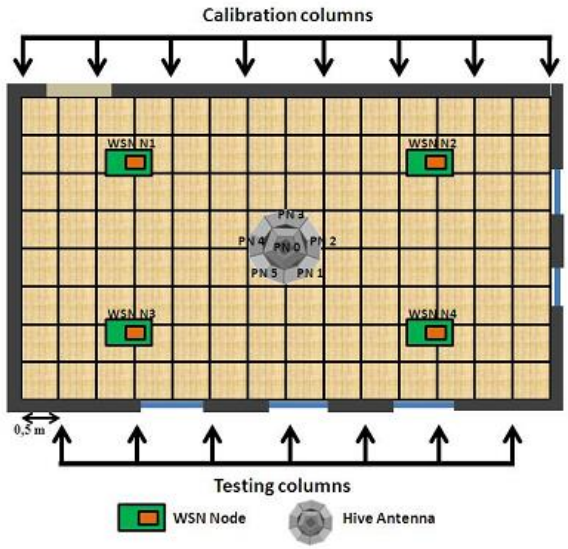

Fig. 5.4 Testing scenario (TS) representation

The Hive5 was inserted at a height of 2.3 m nearly at the center of the room and the four WSN nodes were placed on the ceiling, between 1.5 m and 1 m distant from the sidewalls. With the infra-structure settled, a MN integrated with a faced up circular polarized patch antenna was used as measuring unit. Ten RSSs measurements were made from a height of 75cm over the entire testing area. Each of the measurement points is presented by the lines intersection in Fig. 5.4.

After all the measurements were collected by the MN, an average RSS mapping of each Hive5 element was obtained, as shown in Fig. 5.5.

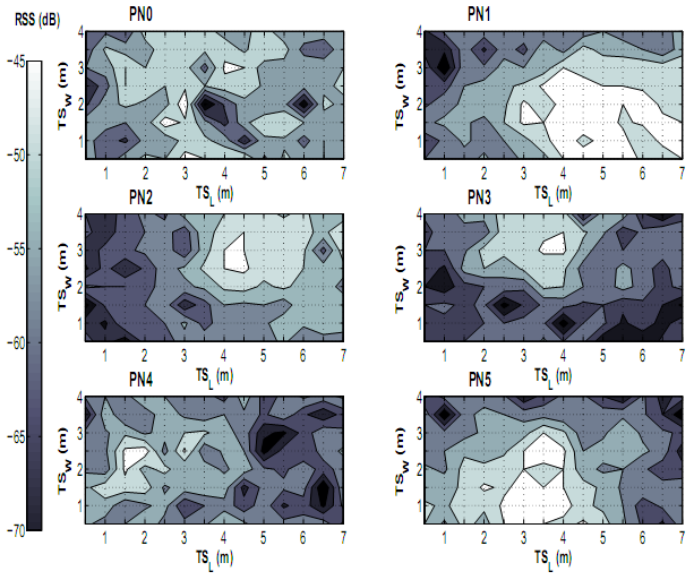

Fig. 5.5 RSS measurements with Hive5 Antenna

PN0 represents the main element (faced down) of the Hive5. This element presents cross-polarization with the MN antenna, making its sectorial identification difficult. In all of the other elements, five clear areas are identified, as seen in Fig. 5.5.

Based on an identical process shown but recurring to WSNs instead of SAs, an average of the RSS mapping for each position was also obtained. For these mappings all four RNs were considered with linear polarized patch antennas. The achieved RSS collection is presented in Fig. 5.6.

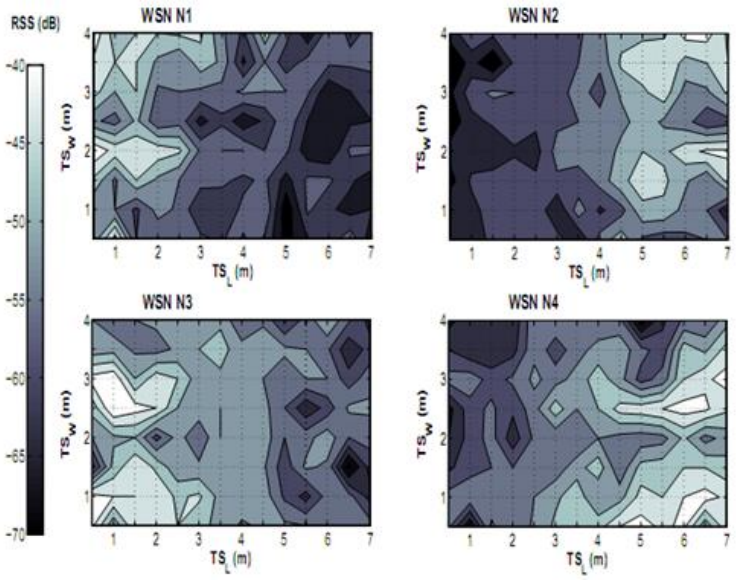

Fig. 5.6 RSS measurements with WSN of four RNs

The calibration of the ANN was performed with the RSS collection acquired.

This specific test considered a supervised learning ANN with a group of training sets (pairs of inputs and known outputs, targets). After the network's training period (made during an offline phase), the system became ready to respond to diverse input collections (online phase).

The inputs for this system were a collection of RSSs, six for the Hive5 and four for the WSN, defining the ANN input layer dimension as six and four neurons respectively. Even of considering a larger input layer for the Hive5, only three to four RSS measurements provide effective information to the ANN. For this reason, this test is considered a fair comparison with an ANN applied to the WSN of four nodes. This RSS input vector is described as:

$$RSS_i = (a_{i1}, a_{i2}, \dots, a_{in}) \tag{5.1}$$

Where a_{ij} corresponds to the RSS collection from point i, and RN identifier j. Like this, the complete RF fingerprinting matrix (M) of m elements is given by combining spatial information with the respective collected RSS vector given as:

$$M = x_i, y_i, RSS_i, i = 1,2, \dots, m \tag{5.2}$$

The outputs of the systems were collected from the position of the tested MN, being represented as X and Y coordinates. In this way, the ANN output layer was defined by two outputs. The number of hidden layers was defined as one because the increase of layers did not demonstrate relevant improvements in this test.

To train the ANN, the odd columns were considered for calibration whereas the even columns were considered for testing, as shown in Fig. 5.4.

To test the performance of the ANN, its dependency to two of the most influential parameters was analyzed, namely the training algorithm and the number of neurons of the hidden layer. One single layer was considered because relevant improvements, consequent from the increase of hidden layers, were not clearly presented in this test.

Although nine training algorithms were analyzed, in this analysis only the three which achieved the best results are presented, namely the gradient descent with adaptive learning-rate back-propagation (GD_ALR_BP), gradient descent with momentum back-propagation (GD_M_BP) and Levenberg-Marquardt back-propagation (LM_BP).

The other parameter considered, which highly influenced the ANN performance, was the number of neurons per hidden layer. In order to avoid over fitting the ANN, an analysis of the optimum number of neurons was performed. As shown in Fig. 5.7, the best compromise between calibration and testing error for the Hive5 was achieved with seven neurons, which being the best performance achieved with the GD_ALR_BP algorithm.

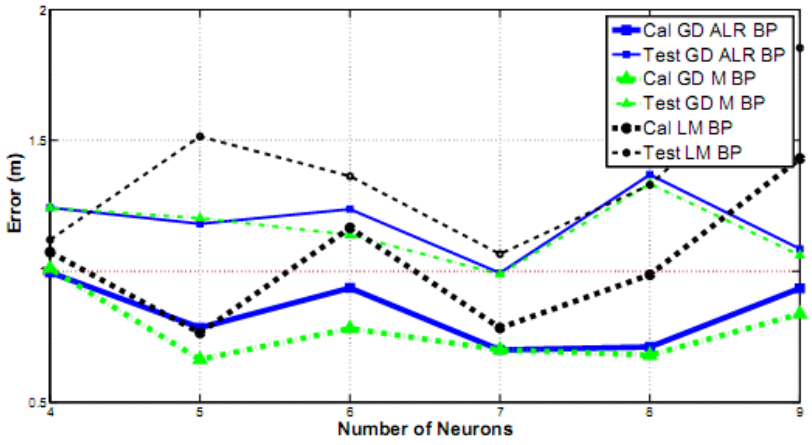

Fig. 5.7 Hive5 ANN Error dependency with number of neurons

For standard gradient descent algorithms the learning rate is held constant throughout training. The performance of the algorithm is very sensitive to the setting of the learning

rate being not practical to determine the optimal learning rate setting before the training. GD_ALR_BP algorithm overpasses this problem because it updates the neurons weight and bias values according to the adaptive learning rate. A detailed description of measured errors is shown in Table 5.1 and presented in Fig. 5.8.

Calibration Error				***Testing Error***			
Mean	**Std**	**Min**	**Max**	**Mean**	**Std**	**Min**	**Max**
0.699	0.50	0.11	2.02	0.99	0.55	0.09	2.61

Table 5.1 Hive5 ANN error with GD_ALR_BP and 7 neurons

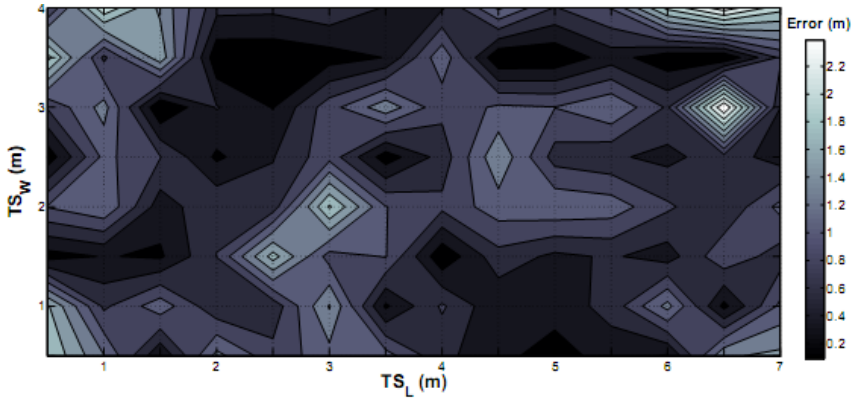

Fig. 5.8 Hive5 ANN Error for GD_ALR_BP, 7 Neurons

In the implementation of the WSN with four nodes the best compromise achieved was with five neurons that also achieved the best performance with GD_ALR_BP algorithm as shown in Fig. 5.9. A detailed description of measured errors for this case is shown in Table 5.2 and presented in Fig. 5.10.

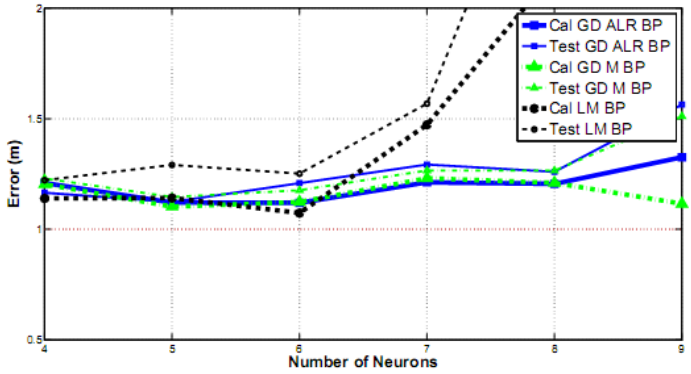

Fig. 5.9 WSN Error dependency with number of neurons

Calibration Error				*Testing Error*			
Mean	**Std**	**Min**	**Max**	**Mean**	**Std**	**Min**	**Max**
1.121	0.47	0.44	2.58	1.12	0.55	0.03	2.54

Table 5.2 WSN ANN error with GD_ALR_BP,5 neurons

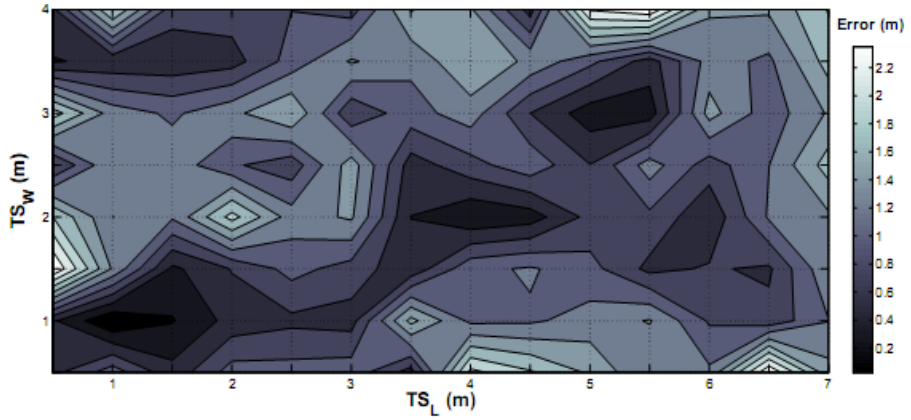

Fig. 5.10 WSN ANN Error for GD_ALR_BP, 5 neurons

As demonstrated by previous results, the ANN performance using the Hive5 Antenna presented better results when compared to a WSN of four nodes under the same localization scenario. The best performance was achieved with seven neurons for the Hive5 and with five neurons for the WSN of four nodes, both with the GD_ALR_BP algorithm. The Hive5 also showed performance advantages, specifically the number of needed nodes, which are significantly reduced with the need of one single node.

One other test was performed considering other sets of calibration and testing points. In this case, two crossing groups of alternate points were considered, instead of alternate columns. Nonetheless, better results were achieved by using the first approach.

5.2 LS NaPis

One of the localization system developed in IT with cooperation with the national navy was the Navy Positioning and Identification Systems (Napis), a full management localization system integrated with several technologies which can support the action forces leaders to perform optimized decisions due to entire system positioning information. The first version of this work was presented in [C2] and the final version in [C4].

One of these scenes is emergency scenarios or military actions. On emergency scenes or military actions, the location and description of events is typically performed by radio and visual contact. According with different scenarios, visual contact and radio communication can become a difficult problem to deal with, or in some cases totally unavailable. We could for instance refer to smoke or foggy scenarios, which can obstruct the visual contact; or civil panic and environmental disturbs which can lead to noisy scenarios, interfering with radio communications and proper description of the running events.

In order to compensate the previous described problems an emergency support system was developed. This system provides location and events description capabilities, integrated with a management system locally accessed or by intermediate of a web service.

The final support system architecture is presented in Fig. 5.12 and can be briefly described into four main blocks, ZigBee location network integrated with panic alerts; Mobile Unite (MU) integrated with a GPS module, ZigBee coordinator, event detection keypad and UHF module; Data Server; and a user interface which provides a web service to location and events management. These four blocks will be detailed described in the next sections.

5.2.1 The system architecture

The first working version of this LS is presented in Fig. 5.11. This system presents an indoor/outdoor localization system divided into 4 main blocks:

- ZigBee location system, responsible for ZigBee modules positioning estimation;
- GPS location system, where GPS modules or typical mobile phones integrated with GPS send their position to the Data Server over TCP/IP or Global Packet Radio Service (GPRS);
- The Data Server is responsible for collecting all position information and sending it to the user interface;
- The User Interface & Service provides a user friendly management application with web service. Like this, management of the system can be processed with a simple remote control since we are connected into the web network.

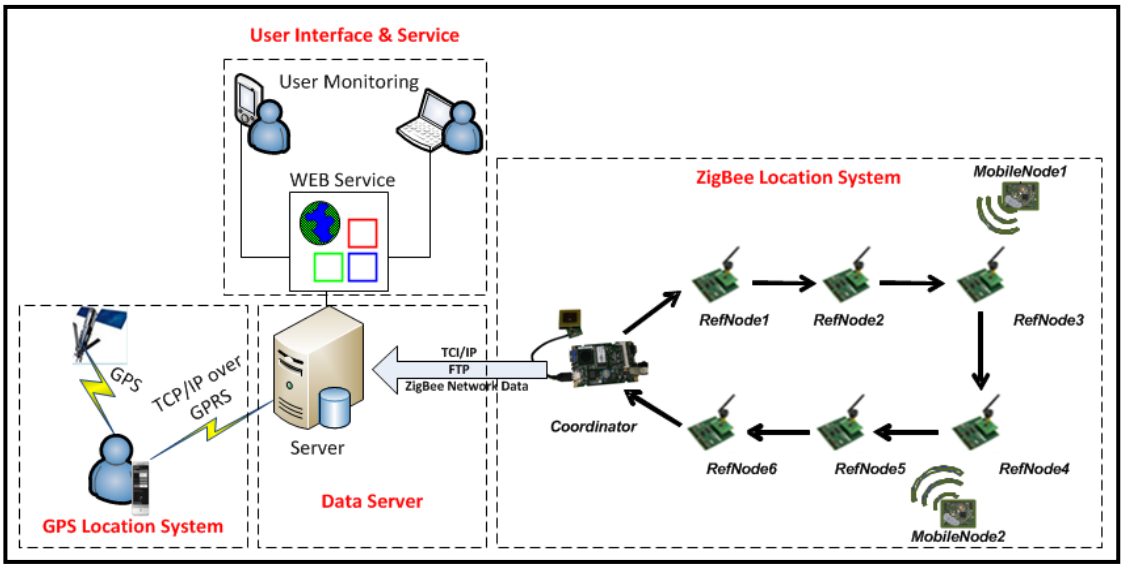

Fig. 5.11 Emergency support system architecture (version 1)

This first version, however, was proven to be unsuitable for emergency scenarios because it is dependent of cellular network for GPRS communication and of internet access which in a catastrophe scenario can be not available. Due to these reasons two new requirements were added to the system: system independent of cellular network and local accessibility.

In order to compensate the previous described problems an emergency support system was developed. This system provides location and events description capabilities, integrated with a management system locally accessed or by intermediate of a web service.

This led to the development of the support system architecture presented in Fig. 5.12 and can be briefly described into four main blocks:

- ZigBee location network integrated with panic alerts;
- Mobile Unite (MU) integrated with a GPS module, ZigBee coordinator, event detection keypad and UHF module;
- Data Server for data management;
- User interface which provides a web service to location and events management. These four blocks will be detailed described in the next sections.

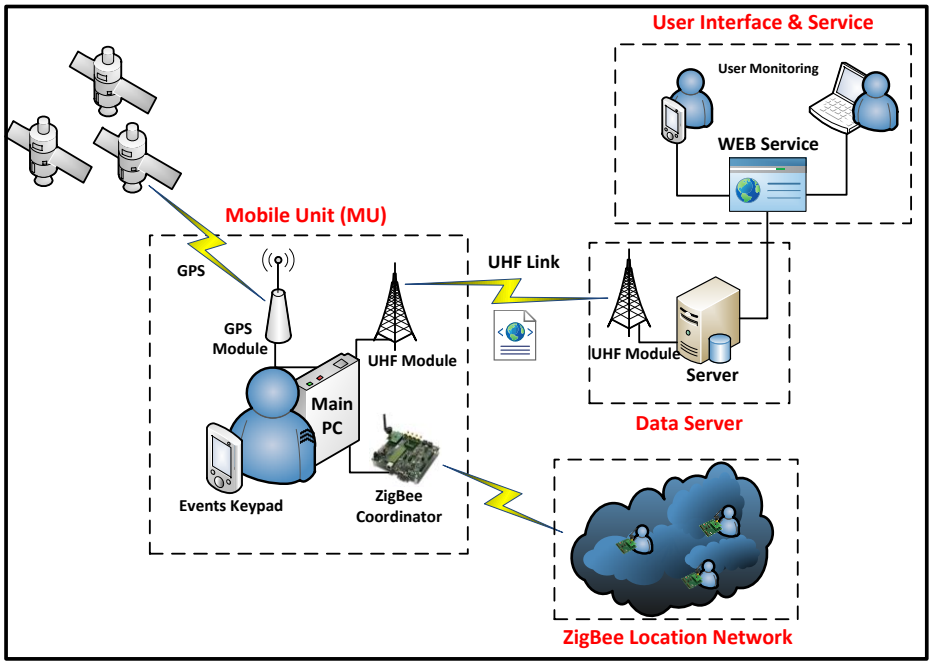

Fig. 5.12 Emergency support system architecture (version 2)

5.2.2 Mobile Unit (MU)

The Mobile Unit represents the main element of the support system, being carried by each intervention group leader. This mobile unit is constituted by a small Personal Computer (PC) integrated with a GPS module providing its absolute position; a ZigBee coordinator to detect panic alerts and relative positioning of ZigBee mobile nodes; a keypad to discriminate events without radio communication needs; and a UHF module for range distance data transfer with the server.

The mobile unit, presented in Fig. 5.13, runs a java application on startup which automatically activates all the system. Like this, the user just needs to turn on the PC to initiate all the correspondent localization process.

Starting the localization process and in case of satellites coverage, the GPS module cyclically sends the absolute location to the main PC by a serial port.

The information of the ZigBee network is converged on the network coordinator and resent to the main PC by a pre-defined serial port. The running java application collects all the data and sends it to the location module which estimates the relative position of the nodes according with a specific algorithm. In this case, the location is based on a Received Signal Strength Indication (RSSI) propagation model. The system will then calculate each GPS position, for each person based on the GPS value of the main PC and the distance to

each ZigBee sensor, this way even if the person that contains the ZigBee node has not a clear view to receive GPS values, it can be located using this method.

Fig. 5.13 Mobile Unit (MU)

For a global integration, these relative positions of end devices are converted into absolute coordinates with the association of GPS module received data.

As previous shown, referring to a correct management intervention action groups and a correct description of the events is of crucial importance. To reduce the chance of information mislead events, discrimination is not performed by voice description but instead, by the use of an event keypad. The group leader can select different events simply pressing the correspondent button with a need of confirmation to avoid mistaken selections. The referred event keypad is presented on Fig. 5.14.

Fig. 5.14 System Events Keypad

All GPS, ZigBee network and event keypad data is converged into the mobile unit running application which cyclically merge all the received data into a XML file as presented in Fig. 5.15.

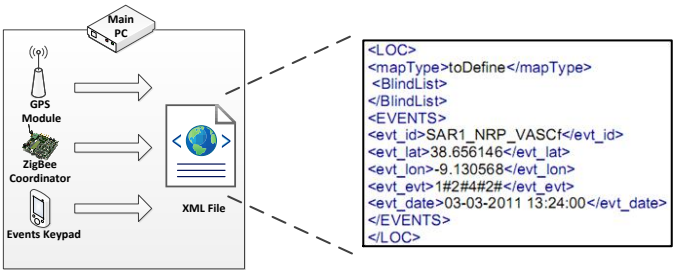

Fig. 5.15 System XML file example

Finally, the created file is sent to the data server by a UHF link. UHF links provide high coverage suitable for emergency scenarios, although, they provide low bandwidth and consequently low data rates. For our system this is not dramatic because only a small size XML file is sent periodically.

5.2.3 ZigBee Localization System

The WSN localization system is based on ZigBee providing like this, low power consumption and a cost effective hardware solution. On this system, the network infrastructure is constituted by a single coordinator for each action group being the WSN managed by a star network topology.

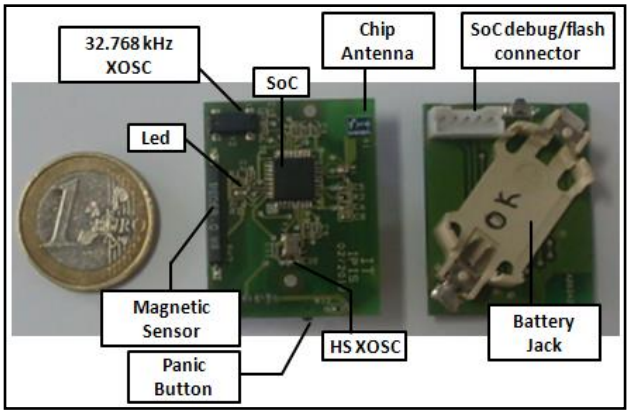

Fig. 5.16 ZigBee module prototype

The mobile node, presented in Fig. 5.17, periodically send blasts to the coordinator, providing the support for localization based in RSSI. The nodes provide alert functionalities with the integration of a panic button and a magnetic sensor.

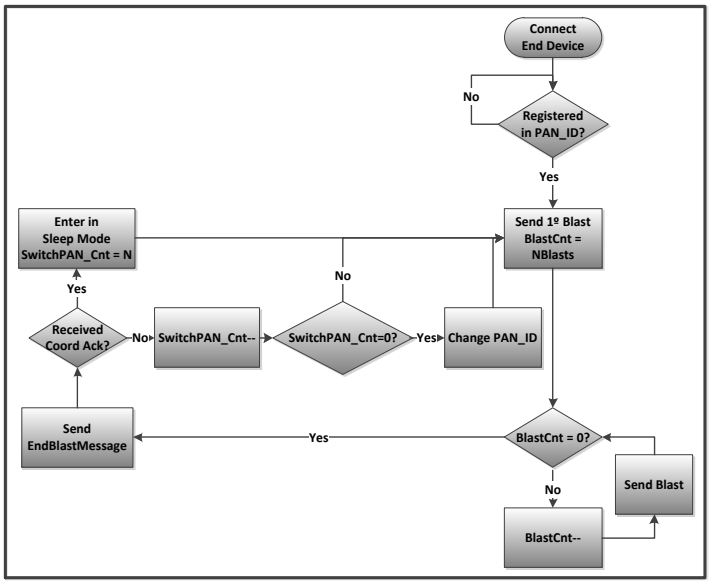

Fig. 5.17 Mobile Node flowchart

5.2.4 Data Server

The Data Server receives the XML sent by the UHF link. The server is composed by a Web access and a MySQL database where geo referenced position of different located devices and events are stored.

This server runs an application which listens to a pre-defined TCP/IP port. It is also responsible for establishing a TCP connection with the UHF module, working as a TCP/UHF gateway, providing the link between the mobile unit and the Data Server.

On the special case of ZigBee modules location, each PC associated to each ZigBee coordinator creates and sends an XML file to a FTP server. With this process accomplished, a message is sent by TCP/IP to data base server referring the uploaded file name. The reception of this message implies the data base server to read referred XML files and corresponding geo-referenced location information.

5.2.5 User interface & Service

The location of different modules can be performed on pre-defined maps or above Google Maps. Its access can be performed locally or by a web page, for this purpose a friendly user website as shown in Fig. 5.18 was developed. After authentication, a multi-user platform for devices management is also provided.

Fig. 5.18 Localization System Interface

By this interface the user can monitor the location of his action group devices as well as events location.

Maps for the different location must be prepared in advance. Maps are geo-referenced images in KML format; this file is loaded and used as the map. This way, the user has the capability to create maps that offers the level of detail he needs for a certain indoor or outdoor location. This feature can be seen in the previous figure, where a map image was integrated on the application, so it is easier to identify modules and events geo-referred.

This interface was integrated with some more options, turning this application very easy to use. These options are presented in Fig. 5.19 and can be described as:

- Set refresh rate (rate of database access);
- Real Time Data (Location data in “real time”);
- See Data Historic (Show location between two dates);
- Define Alerts (Alert the user when a device enter or leaves a defined area);
- Add new Device (Add new device to defined group);
- Edit Existing Device (Edit icon and device permissions).

Fig. 5.19 Web Server Options

5.3 SB-6Log-Periodic System

The Log-Periodic antennas were integrated into a switch-beam structure of six elements as presented in Fig. 5.20.

The switched beam antenna approach provides a simpler and cheaper solution when comparing with an antenna array, making it more suitable for low cost communication systems. Besides the SB-6Log-Periodic antenna this approach also requires the following components: a module capable of measuring RSS, a SP6T RF switch and low loss RF cables as presented in Fig. 5.21 .

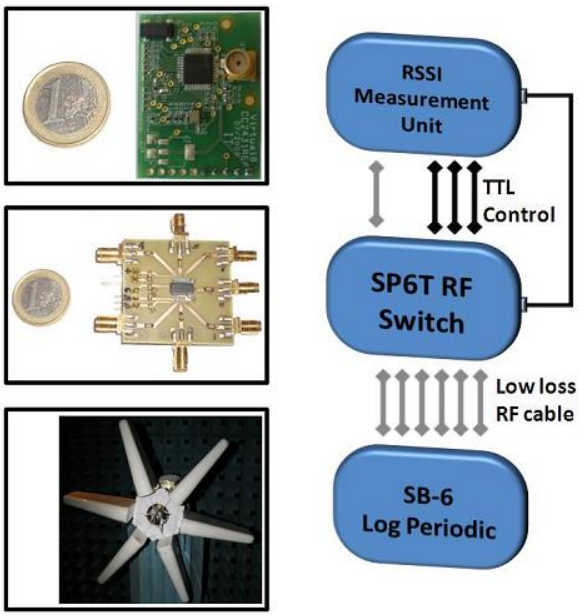

Fig. 5.20 Prototype System architecture

For the presented test a commercial System on Chip (SoC) was considered [144]; a SP6T as the RF Switch [143] and semi-rigid cables of 18 and 23 cm with measured transmission loss below 0.32 dB for considered lengths. These cables are used for antenna array, RF-Switch, and control unit interconnections.

Better figures of the antenna prototype is presented in Fig. 5.21 .

Fig. 5.21 SB-6 Log-Periodic Prototype

5.3.1 Control Application

Here is presented the application to control the antenna.

For the operation of the prototype as a SB-Antenna it is needed to guarantee the correct reception of bursts for each sectorial element. To simulate this purpose it was programmed a device that cyclically sends bursts. The receiver, connected to the SB-Antenna, listen in each sector for 100 ms and changes for the next sector. The received data is sent to the serial port and processed into an application developed in MatLab, Fig. 5.22.

The application shows the received signal strength (RSS) of each antenna defining the angle where the transmitter device is.

As an analogy to the GSM infrastructure that periodically send bursts to all the nodes, the antenna can listen the bursts in all directions, measure the RSS and define the transmitter antenna for the following transmission.

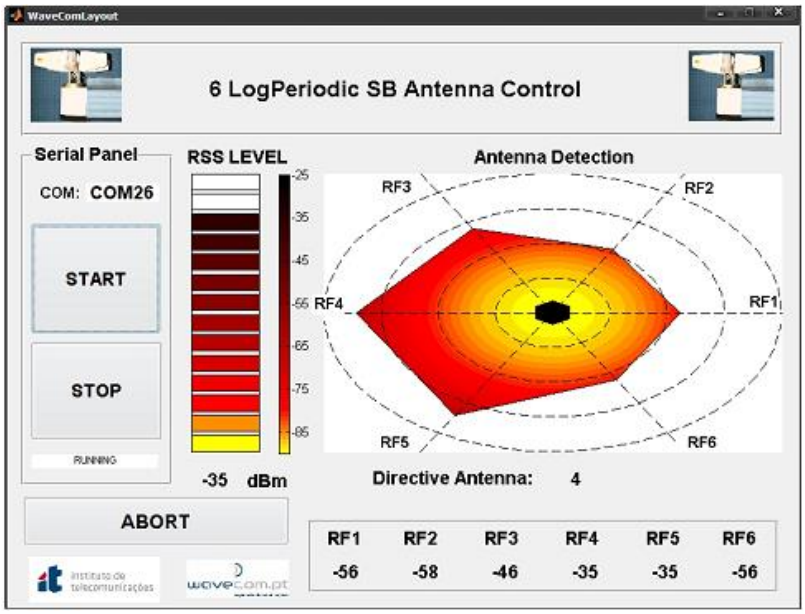

Fig. 5.22 Application Control

5.4 Concluding Remarks

In this chapter it was compared the performance of the Hive5 with a WSN of four nodes under the same fingerprinting algorithm, an ANN. As shown by RSS measurements, the Hive5 provides a better solution when compared to the WSN concerning the resolution and number of required RNs, which can provide a cheaper localization solution. It was verified that a gradient descendent with adaptive learning-rate back-propagation GD_ALR_BP algorithm provided the best localization performance for both approaches, under the considered conditions. Based on these RSS measurements analysis, GD_ALR_BP can be identified and considered as a proper ANN learning algorithm for LSs in indoor environments.

NaPis is a management and location system integrated with several technologies which can support the actions groups' activity under emergency scenarios. This system presents a plug and play solution, crucial for emergency situations. A system integrated with a ZigBee, GPS, keyboard for events description, UHF (Ultra High Frequency) communication link which can be locally managed or with web access if available.

Lastly a SB system based on logarithmic antennas was developed, the SB-6Log-Periodic system.

5.5 Summary of this Chapter

This chapter presents the developed systems during this PhD work.

After the development of several antennas three complete systems were implemented. One based with the Hive5 antenna and based in neural networks. Another, the NaPis, presented a management and LS integrated with several technologies which can support the actions groups' activity under emergency scenarios. And lastly, the SB-6Log-Periodic system, which can be later used for maritime communications.

This work led to the publication of several articles,[J3],[C2] and [C4].

Chapter 6 – Proposed protocol for SA

Communication protocols applied to wireless location systems (WLS) are of crucial importance providing the base for several features namely related to: power consumption[C1], privacy [145], scalability [146] and temporal optimization [147], although they are generally not compliant with each other. Another usual characteristic of WLS protocols is that they do not consider individually the WLS nodes, but instead, as a network where all nodes are assumed to have the same configurations.

Moreover, different antenna approaches (i.e. omnidirectional, antenna arrays, switch beam (SB) antennas), start to be widely implemented in reference nodes (RF, also commonly called anchors) of WLS. These systems have been analyzed as independent networks, with different communication protocols that are not compliant.

Several protocols have been developed for directive antennas operation, hence: different proposals for ready to send (RTS) and clear to send (CTS) transmission [148]; addition of new fields to RTS/CTS [149]; implementation of directional RTS/CTS (DRTS/DCTS) schemes [150]; addition of messages to inform neighbouring nodes about outgoing communications [151]; directional virtual carrier sensing (DVCS) approach [152]; directional MAC protocols (DMAC) - [153]; synchronized MAC protocols based on time division multiple access (TDMA) [154] [155]; and even dealing with multihop techniques [156].

Nevertheless, these systems and protocols have been analyzed as independent networks, with their own communication protocols that are not compliant with each other. Having identified this problem we focused our research on the developed of a generic centralized WLS protocol compliant with RNs integrated with different antenna approaches, namely, omnidirectional, antenna arrays and SB antennas. Another capability of this protocol is that it provides the possibility of individual configuration of mobile nodes (MN, also commonly called tag units) and simultaneous operation of different modes divided as: power consumption, user privacy and precision. The proposed protocol is suitable for low cost WLS mainly based on received signal strength (RSS) and angle of arrival (AoA).

6.1 Proposed Protocol

Different antennas led to different location approaches, implying different communication protocols and consequently protocol incompatibilities. To solve this problem a communication protocol compatible with different type of antennas was proposed. Besides the compatibility there are also available several communication options according to the user main requirements related to power consumption, privacy and precision. This work is deeply analyzed in [J5].

For this proposal the WLS is constituted by three node types: coordinator (the sink of the network) RN (node with fix position) and MN (the element to be located).

The proposed protocol is based on a cyclic configurable beacon transmitted by the coordinator to the entire network. The beacon interval is divided into three main intervals: the beacon transmission, reporting the network configuration parameters; the active period where the network messages are exchanged and an inactive period where devices are mainly in sleeping mode, joining or performing offline configurations. This mode is similar to the beacon-enable mode applied in ZigBee [157].

The beacon description is presented in Fig. 6.1. The beacon informs the network of the time interval until the next beacon transmission, and location configurations.

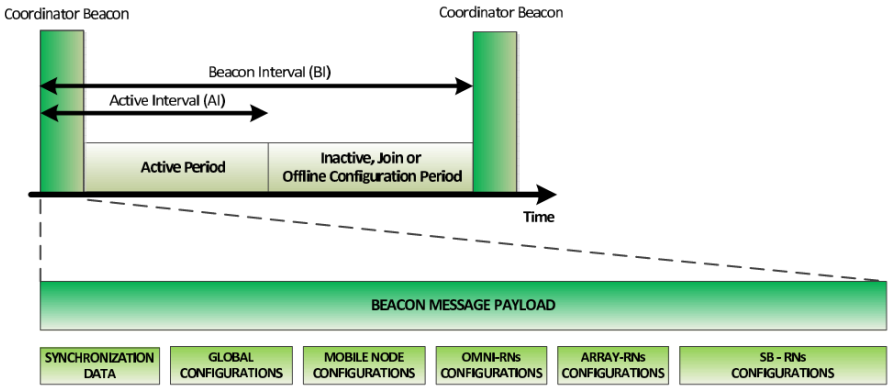

Fig. 6.1 Beacon interval description

Its first field, synchronization data, with the fix size of two bytes informs the network when will be sent the next beacon and the duration of the active interval. The two bytes are

divided in a set of two bits defining the temporal scale and two groups of seven bits defining the beacon and active intervals as seen in Fig. 6.2.

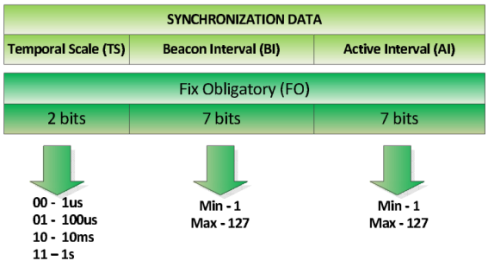

Fig. 6.2 Synchronization Beacon Field Details

The temporal scale was defined as micro, hundred micro, ten milliseconds and one second, although, according with the system requirements other temporal scales can be defined. For an easier interpretation of field's size, figures are described with three different size types: fix obligatory (FO), fix dependent (FD) and variable dependent (VD).

The next beacon field is the global configurations presented in Fig. 6.3 which configures a set of devices to operate on the desired location mode. This field informs the group of nodes to configure the communication mode, the number and interval between blasts and the size of configuration masks according with active flags as shown in Fig. 6.3.

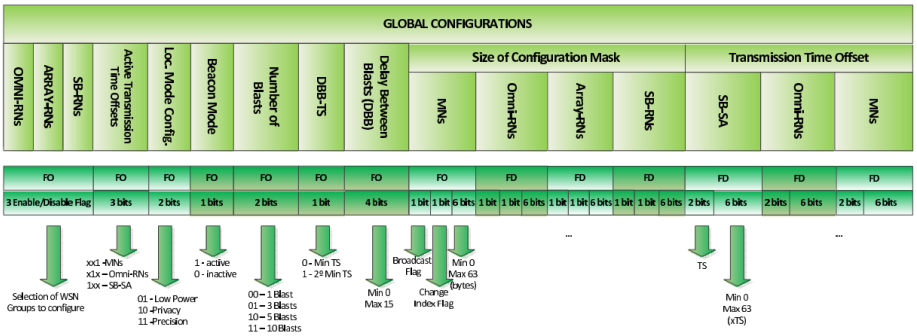

Fig. 6.3 Global Configurations Beacon Field Details

The configuration flags are divided as OMNI-RNs, ARRAY-RNs, SB-RNs and controlled by three bits. Bit one enables the group configurations and bit zero disables it.

There are available three bits to define the availability of time offsets, essential for simultaneous modes of operation.

The next two bits are used to define the configuration mode of this beacon.

Several characteristics are desired according with the application such as low power mode (LPM), client privacy mode (CPM) and precision mode (PM).

All these characteristics have the possibility to operate simultaneously with this protocol, by defining the location protocol mode as shown in Fig. 6.4.

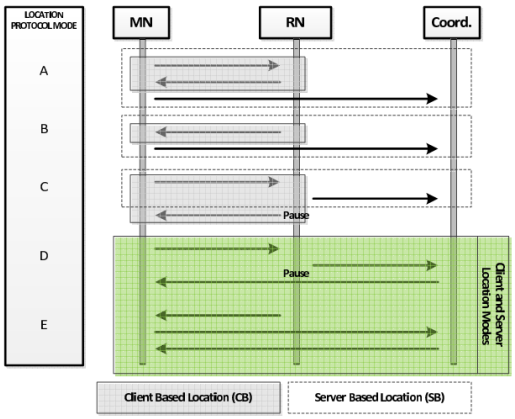

Fig. 6.4 Location Modes

The location mode characteristics are described in detail in Fig. 6.5

LOCATION MODES	CHARACTERISTICS
A (CB)	Do not demand synchronization, No communication with the Coord. Possibility of MN to estimate position
B (CB)	**Demand synchronization, Complete client privacy mode (CPM)**
C (CB)	Do not demand synchronization, Allow location of nearby mobile nodes
A (SB)	Do not demand synchronization (Location Engine Mode)
B (SB)	Demand synchronization (suitable when more MNs than RNs)
C (SB)	**Do not demand synchronization less messages exchanged, Lowest power mode (LPM)**
D	**Do not demand synchronization (Client and Server location) More precise location mode (PM) estimated on server**
E	Demand synchronization (Client and Server location) More precise location estimated on server

Fig. 6.5 Localization Modes description

Then there is available a flag for beacon enable mode, which configures the MNs to work in a non-beacon enable mode in order to avoid the need to listen to all coordinator beacons. The next global configuration fields are the number of blasts and delay between

them. These fields allow the four possible numbers of message transmissions (which can be configurable) and a maximum delay of fifteen times the defined temporal scale.

After, there is provided a byte to define the size of MN configuration mask, Omni-RNs, Array-RNs and SB-RNs according with the previous active configuration flags. For optimization purposes this byte is divided into three parts: broadcast flag (one bit) used to avoid a large MN bit Mask field in case we want to configure the entire network, then there is available a changed index flag (one bit), defines the existence or not of a new MN index for configuration, which can be very useful when only last registered MNs are desired to be configured; and lately, six bits to define the size of the mask, measured in bytes. According to the active transmission time offset flags state, a new field will be added, namely the transmission time offset. This field will give information about the transmission duration of which group of devices is needed for simultaneous operation modes. MN configurations come next with the format shown in Fig. 6.6.

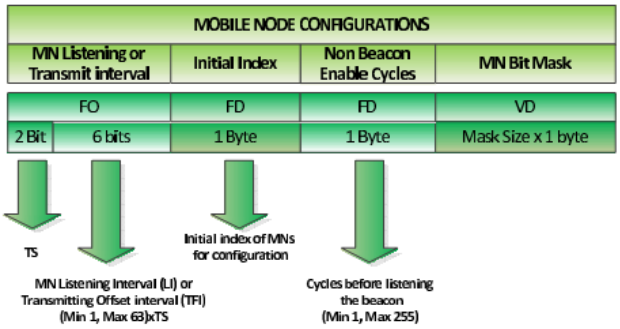

Fig. 6.6 MN configuration details

The first field refers to the interval in which the MN will be listening for messages or start transmitting according to the selected location mode.

Then it is provided a FD field which informs the initial index of the bit mask in case the Changed Index Flag is enabled. Another FD field is available, the non-beacon enable cycles, enabled only when Non Beacon enable flag is active. It informs about the number of transmission cycles without listening to the beacon. The last field refers to the MN Bit Mask defining the list of MN to be configured, previously defined in Size of Configuration Mask field. The next two fields are the Omni-RNs and the Array-RNs configurations. These fields are identical being referenced as a single figure as shown in Fig. 6.7.

Some fields are equal to the ones presented in MN configurations, namely initial index and bit masks. The pause interval is related to location modes where the RNs waits a pause interval before sending the received signal strength (RSS) data collection packet, reducing the number of packets transmitted.

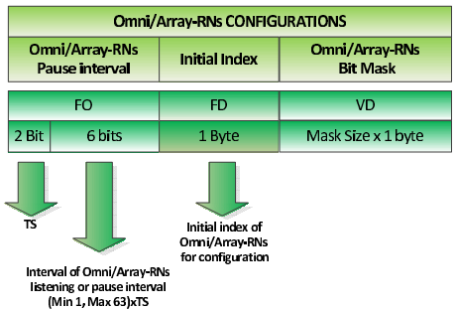

Fig. 6.7 Reference nodes for WSN or antenna arrays integration

The last field of the beacon is the switch-beam (SB-RNs) configurations where the number, interval and bit mask of each different sweep is defined, as shown in Fig. 6.8.

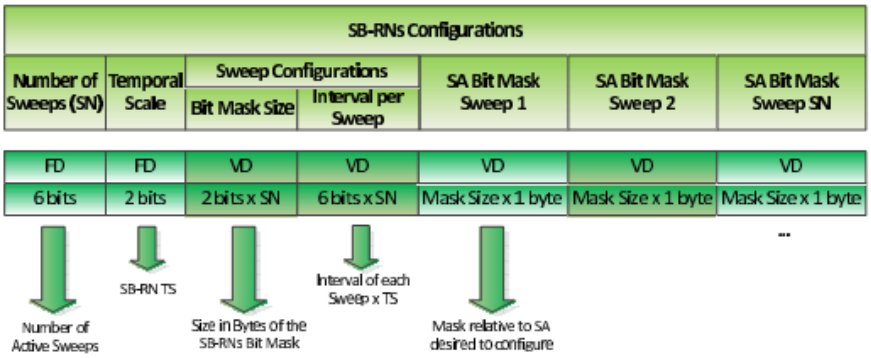

Fig. 6.8 RN Data Details

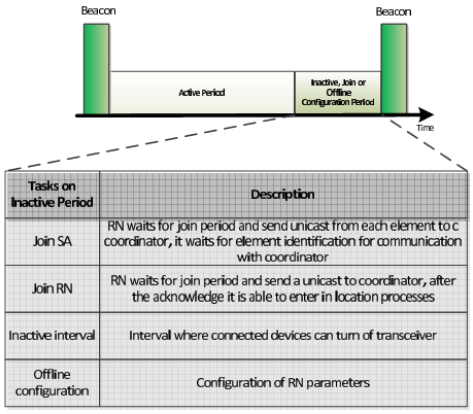

Fig. 6.9 Inactive Period

All described operation modes are performed in active period although several other operations can be performed in non-active period, as shown Fig. 6.9 . This period, identified as Inactive, join or configuration period allows several network operations modes to reduce the impact on the active period. In this interval, the node joining is performed also as offline configurations.

6.2 Localization Processes (LP)

In this section are described the main localization modes available for WLS according to the integrated antennas on RNs. It presents the localization processes for Omni-RNs, Arrays-RNs, SB-RNs, all simultaneous modes and non-beacon enable mode.

6.2.1 LP with Omni-RNs

Typical WLS RNs are integrated with omnidirectional antennas being the nodes position estimated mainly by lateration and fingerprinting techniques.

This protocol allows the operation of three main modes depending on the system requirements and can be divided as low power mode (LPM), client privacy mode (CPM) and precision mode (PM).

The LPM on beacon mode relies on a cyclic transmission of the MNs to the WSN without exchanging messages with it. The MNs listen to the beacon and transmit in their reserved time slot to the RNs according to the index in the Omni-RN bit mask. After this step they enter into a sleep mode. The RNs after a defined pause interval and respective mask index delay, send the RSS data collections to the coordinator.

The second main mode, CPM, relies on a cyclic transmission of the RNs, where the MNs listen to the messages and estimate their own position without exchanging information with the networking, not interfering this way with its privacy.

The last mode, PM relies on the estimation of the MN position in relation to the coordinator, which can implement more complex positioning algorithms, and resend after its position to the corresponding MN. These modes are presented in Fig. 6.10.

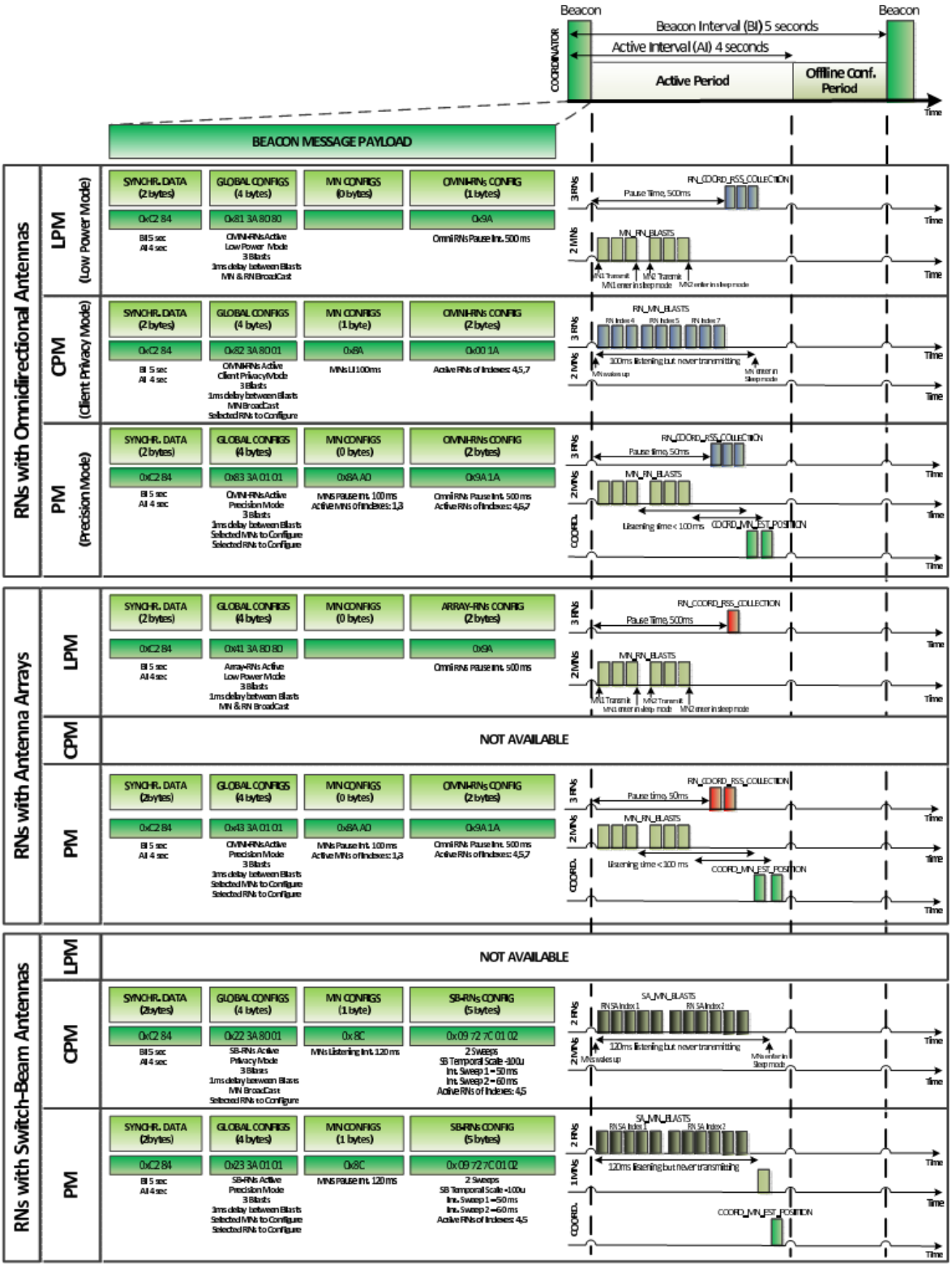

Fig. 6.10 LM available with RNs integrated with Omni, Array and SB antennas

6.2.2 LP with Array-RNs

Another used antennas implementation for WLS is based on antenna arrays. These systems rely mainly on the processing of signal phase and RSS differences on several elements of an antenna array. The communication protocol related to the LPM and PM is similar to the one previously presented for Omni-RN modes, although, it is does not allow CPM since the reception is always performed in the RNs side. A better representation of this process is present in Fig. 6.10.

6.2.3 LP with SB-RNs

This protocol also allows the use of SAs on RNs, more specifically, switch-beam (SB) antennas. The use of SB antennas implies the consecutive sending of bursts in order to measure the RSS on the different beam directions. This burst transmissions can be performed by the MN or by the RN side. Not knowing a priori the number of beams per antenna, the burst transmission is more efficient on the RNs side. This way, the MN has to listen for messages for a pre-defined time interval in which the SB will consecutively transmit bursts per each antenna element. For this reason, this mode is not very suitable for the case in which low power consumption is desired, therefor not available on this type of antennas.

Having RNs with the SB antennas and knowing their direction, they can belong to the same or different synchronized groups in order to reduce transmission intervals that start at the same time and avoid packets collision. This process is shown in Fig. 6.10.

6.2.4 Complete LP

Having described individually the use of the three location processes it is possible to operate with any combination of the three antenna types and any combination of the three main localization modes. In this subsection is described the integration of the three antenna types. The integration of SB on RNs demands the synchronism of the network for listening the SB-RN bursts.

This way, the LPM implies a consequent increase in power consumption. The operation of WSN and array modes for CPM, LPM and PM are identical to the previously described

modes with the difference in the initial listening interval for SB-RNs. These modes are described in Fig. 6.11. In the same figure it is described the LS operation with all antenna types having simultaneous operation of the three referred modes.

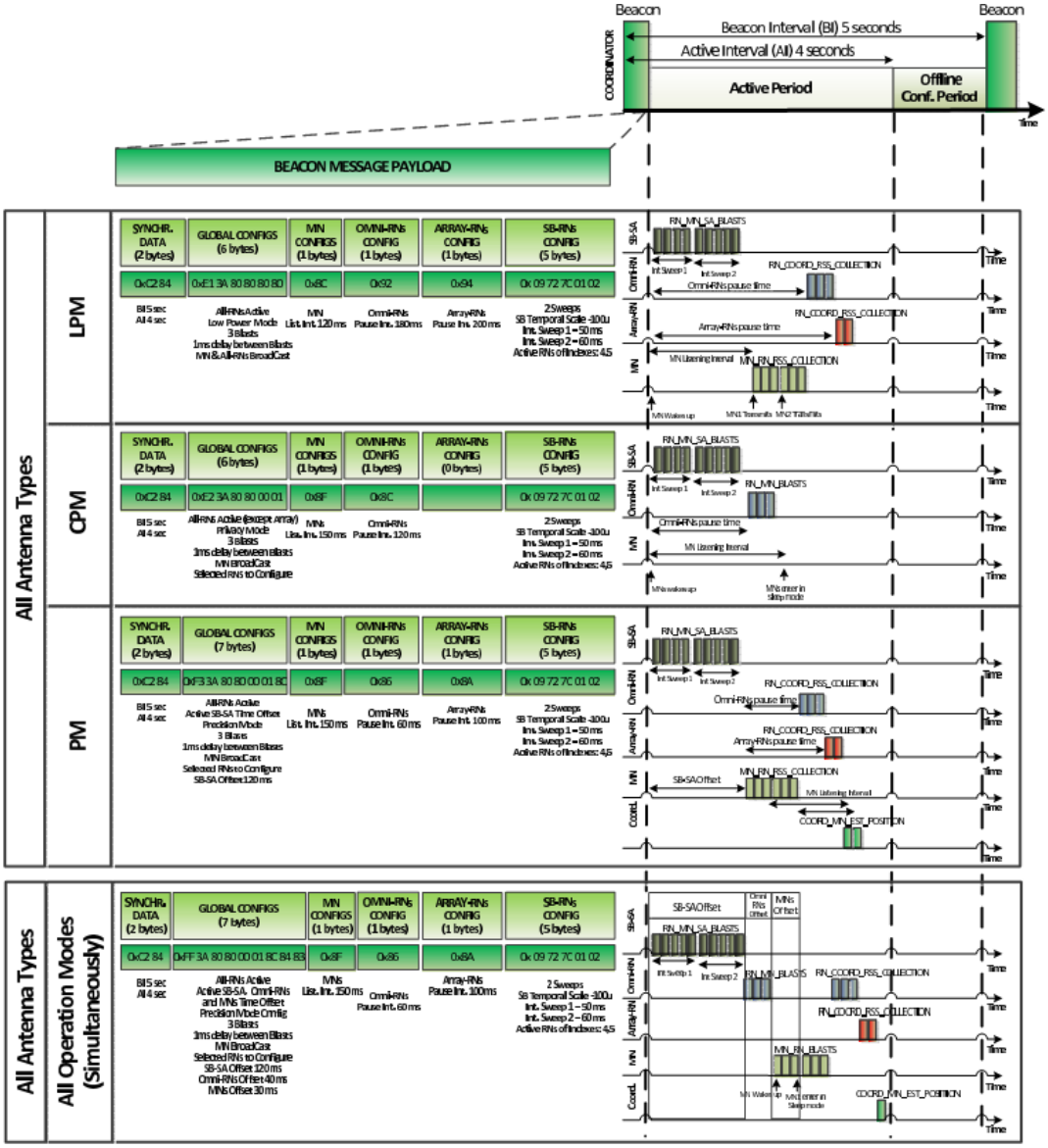

Fig. 6.11 Localization available with RNs integrated with all antenna types modes

6.2.5 LP for Non-Beacon Mode

When long periods without mobile nodes configuration are expected, non-beacon mode can provide lower power consumption than when the beacon enables LPM. This mode allows the MN to transmit without listening for the beacon for long periods. This mode is

typically defined for transmission in inactive periods to avoid packet collisions. In Fig. 6.12 it is described a MN that stays into a non-beacon mode for ten cycles of five seconds.

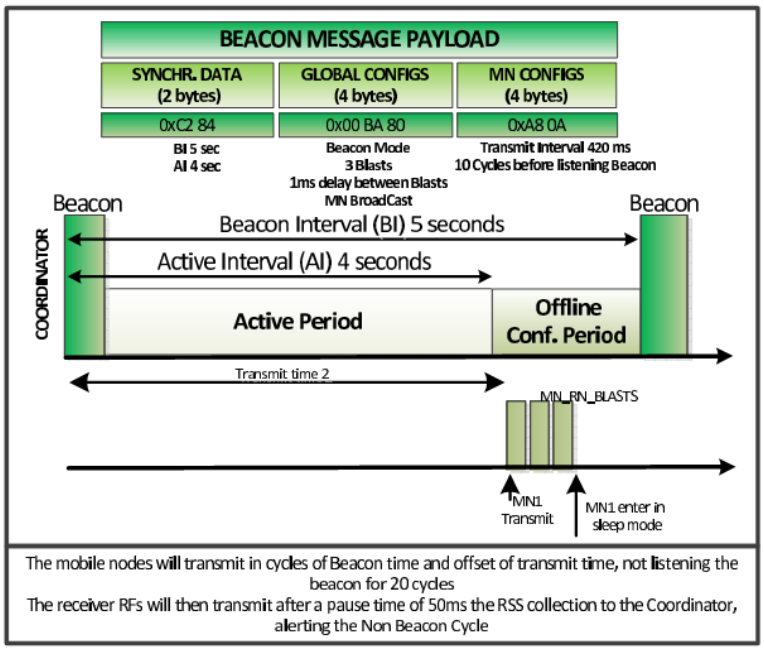

Fig. 6.12 Non Beacon Mode

6.3 Summary of this Chapter

This chapter describes a configurable and compliant communication protocol suitable for WLSs integrated with omnidirectional, arrays and SB antennas. This protocol deals with three essential characteristics for WLS which can operate simultaneously divided as: power consumption, user privacy and precision.

The proposed protocol is suitable for low cost WLS mainly based on received signal strength (RSS) and angle of arrival (AoA).

The work developed in this chapter let to the submission of a paper, mentioned as [J5].

Chapter 7 – Conclusions and Future Work

In this thesis several systems, antennas designs and ideas have been proposed to solve current open issues in the localization system for WSN.

Localization techniques and the most suitable antennas for each system are initially introduced. This study is presented and discussed in [J1]. Based on this study the sectorial antennas proven to be cost effective solutions for WSN where we can easily reduce the number of required RNs. This cost effectiveness is even more evident when switch beam approach is present.

Regarding this study it was proposed a switch-beam antenna for WSN operating at 2.45 GHz. This antenna, named Hive5 was initially presented in [C3] and detailed analyzed in [J2]. The integration of this antenna into an indoor localization system was presented in [J3]. This paper proved good accuracy of the system with the use of a single sectorial antenna and presented similar results comparing with a typical WSN of four nodes. It was also identified that the training algorithm highly influences the accuracy of LS.

Several other localization systems have been presented for several application which have been presented in [C2] and [C4].

Verifying the performance of the two developed systems and the advantages of the use of sectorial antennas it was proposed a communication protocol to integrate different type of antennas and system requirements. For this is was idealized and proposed a configurable and compliant communication protocol suitable for WLSs integrated with omnidirectional, arrays and SB antennas. This protocol deals with three essential characteristics divided as: power consumption, user privacy and precision. This work is presented in [J5].

Based on the same principle of the work presented in [C3] it was developed a switch-beam antenna based on commercial log-periodic antennas for maritime communications.

Other systems were also addressed on this work, which passed by antennas for vehicular communications. This study led to the development of two interesting antennas for 5 GHz, an omnidirectional printed loop antenna for Taxi communications where the in phase and uniform current over the loop allows omnidirectional radiation pattern (even with loop dimensions comparable to the operating wavelength) presented in [C8].

Another antenna was presented, a new printed planar microstrip antenna with elliptical elements. The operating bandwidth of the antenna with usable radiation pattern is about 20%. A new way to match PEM with CP is proposed by the insertion of an inner counter-elliptical slot. This technique provides wide band in polarization for single feed monopoles and can be easily integrated into arrays presented in [J4].

The continuation of the work developed during this PhD is seen by the author in four areas of research: antenna, system, protocol and algorithm.

In the point of view of the antenna, sectorial multi band approaches with polarization diversity could be an interesting area of research. The multi band could allow a wider range of applications and the polarization diversity more information which could be translated in better LS performance.

With the antenna implemented a proper front end would be required in order to guarantee the multi band and polarization diversity discrimination.

The LS could also have a wide range for improvement. The first step should be performed testing the proposed protocol verifying its versatility with different antennas and systems requirements. Analyzed this step an optimized protocol could be required for multi band compatibility.

The last proposed area of research passes by the used algorithm. With new system data achieved new algorithm need to be developed. Considering the multi band, the polarization versatility and the reception of several signals with the use of a SA the correlation of all this information could be used for new algorithms for localization estimation or for data communication.

References

[1] Buratti, C., Conti, A., Dardari, D., Verdone, R.; "An Overview on Wireless Sensor Networks Technology and Evolution", *Sensors Journal*, vol. 9, nº 9, August 2009.

[2] "21 ideas for the 21st century", Business Week, pp. 78-167, 30 August 1999.

[3] Hui Liu, Darabi H., Banerjee P., Jing Liu; "Survey of wireless indoor positioning techniques and systems," *IEEE Transactions on Systems, Man, and Cybernetics, Part C: Applications and Reviews*, vol. 37, nº 6, 2007, pp.1067-1080.

[4] Hightower, J., Want, R., and Borrielo, G.; "SpotON: An Indoor 3D Location Sensing Technology Based on RF Signal Strength", *UW CSE Technical Repport*, University of Washington, Seattle, 2000.

[5] Reichenbach, F., Timmermann, D.; "Indoor Localization with Low Complexity in Wireless Sensor Networks", *2006 IEEE International Conference on*, Aug. 2006, pp. 1018-1023.

[6] Motter, P., Allgayer, R.S., Muller, I., Pereira, C.E., Pignaton de Freitas, E.; "Practical issues in Wireless Sensor Network localization systems using received signal strength indication", *Sensors Applications Symposium (SAS), 2011 IEEE*, Feb. 2011, pp. 227-232.

[7] John L. Volakis, Antennas Engineering Handbook, 4th ed., McGraw-Hill, 2007, Chapter 25, pp. 2-25.

[8] Brás, L.; "Desenvolvimento de sistema de localização indoor de baixo consumo", *Master Thesys*, Universidade de Aveiro, Portugal, July 2009.

[9] IEEE, "IEEE Standard Definitions of Terms for Antennas" Published by The Institute of Electrical and Electronics Engineers, Inc. 345 East 47th Street, New York, NY 10017, USA, June 22, 1983.

[10] Constantine A. Balanis; "Antenna theory, analysis and design" Third edition John Wiley & Sons, Inc. ISBN 0-471-60639-1, Chapter 2, pp. 28.

[11] Constantine A. Balanis; "Antenna theory, analysis and design" Third edition, John Wiley & Sons, Inc. ISBN 0-471-60639-1, Chapter 2, pp. 70-75.

[12] Ansys Corporation, HFSS 3D Full-wave Electromagnetic Field Simulation, online available at http://www.ansys.com/.

[13] G. Strang and G. J. Fix; "An Analysis of the Finite Element Method", Prentice-Hall, Englewood Cliffs, 1973.

[14] Yi Huang and Kevin Boyle; "Antennas from theory to practice", John Wiley & Sons, Inc. ISBN 978-0-470-51028, Chapter 6. pp. 228.

[15] Ansoft Corporation, User's guide – High Frequency Structure Simulator V10, pp. 17. June 2005.

[16] Yi Huang and Kevin Boyle; "Antennas from theory to practice", John Wiley & Sons, Inc. ISBN 978-0-470-51028, Chapter 4, pp. 112.

[17] Agilent technologies; “Agilent Network Analyzer Basics”, accessed online in May 2013 http://cp.literature.agilent.com/litweb/pdf/5965-7917E.pdf.

[18] Constantine A. Balanis; “Antenna theory, analysis and design” Third edition, John Wiley & Sons, Inc. ISBN 0-471-60639-1, Chapter 16, pp. 840-850.

[19] Orbit FR, a microwave vision company, accessed online in October 2011, http://www.orbitfr.com/.

[20] M. C. Thompson, D. M. Waters; “Characteristics of a Tapered Anechoic Chamber”, *IEEE Trans. On Antennas and Propagation*, May 1967.

[21] W.H. Emerson; “Electromagnetic Wave Absorbers and Anechoic Chambers through the Years” *IEEE Trans. On Antennas and Propag*, pp. 484-490, July 1973.

[22] Chistopher L. Holloway, Ronald R. DeLyser, Robert F. German, Paul McKenna, Motohisa Kanda; “Comparison of Electromagnetic Absorber Used in Anechoic and Semi-Anechoic Chambers for Emissions and Immunity Testing of Digital Devices”, *IEEE Trans. On Electromagnetic Compatibility*, vol. 39, nº 1, February 1997.

[23] C.F. Yang, W.D. Burnside, and R.C. Rudduck; “A doubly periodic moment method solution for the analysis and design of an absorber covered wall”, *IEEE Trans. Antennas Propagation*, vol. 41, pp. 600-609, May 1993.

[24] Kefeng Liu; “Conformity EMC Products and Equipment”, Chambers, accessed online in June 2010 http://www.conformity.com/artman/publish/printer_173.shtml.

[25] ETS Lingren, accessed online in June 2010 http://www.ets-lindgren.com/.

[26] Andrew Woods; “Development and Characterization of an Anechoic Chamber”, Bachelor thesys, University of Southern Queensland, June 2006.

[27] Department of Defense United States of America and GPS Navstar, “Global Positioning System Standard Positioning Service Performance Standards”, 4th Edition, USA, 2008.

[28] Russian Institute of Space Device Engineering, “Global Navigation Satellite System GLONASS-Interface Control Document”, Edition 5.1, Moscow, Russia, 2008.

[29] “GALILEO Programme, “The Galileo Project – GALILEO Design consolidation”, European Commission, UK, 2003.

[30] Eric D. Manley, Huzaifa Al Nahas and Jitender S. Deogun; “Localization and tracking in sensor systems,” *IEEE International Conference on Sensor Networks, Ubiquitous, and Trustworthy Computing*, Japan, 2006, pp. 237-242.

[31] R. Want, A. Hopper, V. Falcão and J. Gibbons; “The active badge location system,” *ACM Transactions on Information Systems*, vol. 10, nº. 1, 1992, pp. 91–102.

[32] C. Lee, Y. Chang, G. Park, J. Ryu, S.-G. Jeong, S. Park, J. W. Park, H. C. Lee, K.-s. Hong, and M. H. Lee; “Indoor positioning system based on incident angles of infrared emitters,” *30th Annual Conference of IEEE Industrial Electronics Society*, vol. 3, 2004, pp. 2218–2222.

[33] M. Rodriguez, J. Pece, and C. Escudero; “In-building location using Bluetooth,” *International Workshop on Wireless Ad-hoc Networks*, 2005.

[34] L. Ni, Y. Liu, Y. C. Lau, and A. Patil; “LANDMARC: indoor location sensing using active RFID,” *1st IEEE International Conference on Pervasive Computing and Communications*, 2003, pp. 407-415.

[35] P. Bahl and V. Padmanabhan; “RADAR: an in-building RF-based user location and tracking system,” *IEEE International Conference on Computer Communications (INFOCOM)*, vol. 2, 2000, pp. 775–784.

[36] T. Roos, P. Myllymaki, H. Tirri, P. Misikangas and J. Sievanen; “A probabilistic approach to WLAN user location estimation,” *International Journal of Wireless Information Networks*, vol. 9, nº. 3, 2002, pp. 155-164.

[37] M. Youssef and A. K. Agrawala; “Handling samples correlation in the Horus system,” *23rd Anuual Joint Conference of the IEEE Computer and Communications Society*, Hong Kong, vol. 2, 2004, pp. 1023-1031.

[38] F. Belloni, V. Ranki, A. Kainulainen and A. Richter; "Angle-based indoor positioning system for open indoor environments", *Proc. 6th Workshop on Positioning, Navigation and Communcation*, 2009 pp. 261-265.

[39] UbiSense Company, accessed online in June 2010 at http://www.ubisense.net

[40] Sivanand Krisshnan, Pankaj Sharma, Zhang Guoping and Ong Hwee Woon; “A UWB localization system for indoor robot navigation,” *IEEE International Conference oUltra-Wideband (ICUWB)*, 2007, pp.77-82.

[41] Neyer S. Correal, Spyros Kyperountas, Qicai Shi and Matt Welborn; “An UWB relative location system,” *IEEE Conference on Ultra Wideband System and Technologies*, 2003, pp. 394-397.

[42] S. Ingram, D. Harmer, and M. Quinlan, “Ultrawideband indoor positioning systems and their use in emergencies,” *Position Location and Navigation Symposium (PLANS)*, 2004, pp. 706–715.

[43] Y. Zhang, W. Liu, Y. Fang, and D. Wu, “Secure localization and authentication in ultra-wideband sensor networks,” *IEEE Journal on Selected Areas in Communications*, vol. 24, nº. 4, 2006, pp. 829–835.

[44] N. Priyantha; “The Cricket indoor location system,” Ph.D. dissertation, Massachusetts Institute of Technology, 2005.

[45] Active Bat, accessed online in June 2010 at http://www.cl.cam.ac.uk/research/dtg/attarchive/bat/.

[46] M. Hazas, A. Ward; "A novel broadband ultrasonic location system," *Proc. International Conference on Ubquitous Computing*, 2002, pp. 264-280.

[47] Y. Fukuju, M. Minami, M. Morikawa and T. Aoyama, “DOLPHIN: an autonumous indoor positioning system in ubiquitous computing environment,” *Proc. IEEE Workshop on Software Technologies for Future Embedded Systems*, Hakodate, Japan, 2003.

[48] MotionStar, accessed online in June 2010 at http://www.ascension-tech.com.

[49] A. Mandal, C. V. Lopes, T. Givargis, A. Haghighat, R. Jurdak and P. Baldi; “Beep: 3D indoor positioning using audible sound,” *2nd IEEE Consumer Communications and Networking Conference(CCNC)*, 2005 pp. 348-353.

[50] E. Mangas and A. Bilas; "FLASH: fine-grained localization in wireless sensor networks using acoustic sound transmissions and high precision clock synchronization," *Proc. of 29th IEEE international conference on distributed computing systems*, 2009. p. 289–98.

[51] N. Patwari and A. Hero, "Using proximity and quantized RSS for sensor localization in wireless networks", *Proc. of the 2nd ACM international conference on Wireless sensor networks and applications*, San Diego, USA, 2003.

[52] Rong Peng and M. L. Sichitiu, "Angle of Arrival Localization for wireless sensor networks" *3rd Annual IEEE Communications Society on Sensor and Ad Hoc Communications and Networks*, vol. 1, 2006, pp. 374-382.

[53] V. Honkavirta, T. Perala, S. Ali-Loytty and R. Piche, "A comparative survey of WLAN location fingerprinting methods," *6th workshop on Positioning, Navigation and Communications*, 2009, pp. 243-251.

[54] John L. Volakis, Antennas Engineering Handbook, 4th ed., McGraw-Hill, 2007 Chapter 9, pp 2-35.

[55] Jack H. Winters; "Smart antenna techniques and their application to wireless ad hoc networks," *IEEE Wireless Communications*, vol. 13, nº. 4, 2006, pp. 77-83.

[56] N. H. M. Rais, P. J. Soh, F. Malek, S. Ahmad, N. B. M. Hashim and P. S. Hall; "A review of wearable antennas," *Loughborough Antennas and Propagation Conference (LAPC),* 2009, pp.225-228. To put after Jack H. Winters; "

[57] B. Gupta, S. Sankaralingam and S. Dhar; "Development of wearable and implantable antennas in the last decade: a review," *Mediterranean Microwave Symposium (MMS)*, 2010, pp. 251-267. To put after N. H. M. Rais, P. J. Soh, F. Malek, S. Ahmad, N. B. M. Hashim and P. S. Hall;

[58] K. Aamodt, "CC2431 Location Engine, Application Note AN042, Chipcon Products from Texas Instruments".

[59] Mathieu Bourt and Aldri L. dos Santos; "RFID Tags: positioning principles and localization techniques," *1st IFIP Wireless Days*, 2008, pp. 1-5.

[60] S. S. Hossain and N. Karmakar; "An overview on RFID frequency regulations and antennas," *International Conference on Electrical and Computer Engineering*, 2006, pp- 424-427.

[61] R. C. Hua, and T. G. Ma; "A printed dipole antenna for ultra-high frequency (UHF) radio frequency identification (RFID) handheld reader," *IEEE Transactions on Antennas and Propagation*, vol. 55, nº. 12, 2007, pp. 3742-3745.

[62] C. Phongcharoenpanich and R. Suwalak; "Dual-band RFID reader antenna using annular plate with curved and rectangular slots," *International Conference on Electromagnetics in Advance Applications (ICEAA)*, 2010, pp. 633-636.

[63] W. G. Lim, W. I. Son, K. S. Oh, W. K. Kim and J. W. Yu; "Compact integrated antenna with circulator for UHF RFID system," *IEEE Antennas and Wireless Propagation. Letters*, vol. 7, 2008, pp. 673-675.

[64] T. N. Chang, and J. M. Lin; "A novel circularly polarized patch antenna with a serial multi-slot type of loading," *IEEE Transactions on Antennas Propagation*, vol. 55, nº. 11, 2007, pp. 3345-3348.

[65] D. Z. Kim and et al; “Helical reflector antenna with a wideband CP for RFID reader,” *Asia Pacific Microwave Conference (APMC 2009),* 2009, pp. 1032-1035.

[66] Wang-Ik, W. G. Lim, M. Q. Lee, S. B. Min, J. W. Yu; “Design of quadrifilar spiral antenna with integrated module for UHF RFID Reader,” *Asia Pacific Microwave Conference (APMC 2009),* 2009, pp. 1028-1031.

[67] Z. N. Chen, X. Qing, and H. L Chung; “A universal UHF RFID reader antenna,” *IEEE Transactions on Microwave Theory and Techniques*, vol. 57, nº. 5, 2009, pp. 1275-1282.

[68] Pavel V. Nikitin and K. V. S. Rao; “Antennas and propagation in UHF RFID systems,” *IEEE International Conference on RFID,* 2008, pp. 277-288.

[69] Federal Communications Commission, Washington, DC, “FCC report and order on ultra wideband technology”, 2002.

[70] D, Benedetto, T. Kaiser, D. Porcino, A. Molisch and I. Oppermann; “UWB Communication Systems - A comprehensive overview,” Hindawi Publishing Corporation, 2006.

[71] A. F. Molisch, P. Orlik, Z. Sahinogly and J. Zhang; “UWB-based sensor networks and the IEEE 802.15.4a standard - a tutorial,” *1st International Conference on Communications and Networking in China (ChinaCom06),* 2006, pp. 1-6.

[72] E. Karapistoli, F. N. Pavlidou, I. Gragopoulos, and I. Tsetsinas; “An overview of the IEEE 802.15.4a standard,” *IEEE Communications Magazine,* vol. 48, nº. 1, 2010, pp. 47–53.

[73] R. Burda, A. Lewandowski and C. Wietfeld; “A hybrid indoor localization using beacon enabled meshing and ToA in IEEE 802.15.4 Networks,” *IEEE Vehicular Technology Conference,* 2008, pp. 118-122.

[74] Ismail Guvenc and Chia Chin Chong; “A survey on ToA based wireless localization and NLOS mitigation techniques,” *IEEE Communications Surveys & Tutorials*, vol. 11, nº 3, 2009, pp. 107-124.

[75] I. Oppermann, L. Stoica, A. Rabbachin, Z. Shelby, and J. Haapola; "UWB wireless sensor networks: Uwen - a practical example," *IEEE Communications Magazine,* vol. 42, nº. 12, 2004, pp. S27-S32.

[76] K. Y. Yazdandoost and R. Kohno; “Ultra wideband antenna", *IEEE Communication Magazine,* vol. 42, nº. 6, 2004, pp. S29-S32.

[77] M. R. Mahfouz, A. E. Fathy, M. J. Kuhn and Y. Wang; “Recent trends and advances in UWB positioning,” *IEEE MTT-S International Microwave Workshop on Wireless Sensing, Local Positioning, and RFID (IMWS 2009),* China, 2009, pp. 1-4.

[78] Pengcheng Li, Jianxin Liang and Xiaodong Chen; “Study of Printed Elliptical/Circular Slot Antennas for Ultrawideband Applications,” *IEEE Transactions on Antennas and Propagation*, vol. 54, nº. 6, 2006, pp. 1670-1675.

[79] M. A. P. Solis, G. M. G. Tejada, H. J. Aguilar; “State of the art in ultra-wideband antennas,” *2nd International Conference on Electrical and Electronics Engineering (ICEEE) and XI Conference on Electrical Engineering (CIE 2005),* Mexico, 2005.

[80] Raj Kular and P. Bansode; “On the design of ultra wide band antenna based on fractal geometry,” *ITU-T Kaleidoscope: Beyond the Internet? - Innovations for Future Networks and Services*, 2010, pp. 1-5.

[81] Kin-Lu Wong, Chih-Hsien Wu and Saou-Wen Su; “Ultrawide-Band square planar metal-plate monopole antenna with a trident-shaped feeding strip,” *IEEE Transactions on Antenna and Propagation*, vol. 53, nº. 4, 2005, pp. 1262-1269.

[82] Gee Lim, Zhao Wang, Chi-Un Lei, Yuanzhe Wang and K. L. Man; “Ultra Wideband antennas – past and present,” *IAENG International Journal of Computer Science*, vol. 37, nº. 3, 2010.

[83] R. Movahedinia and M. N. Azarmanesh; “Ultra-wideband band-notched printed monopole antenna,” *IET Microwaves, Antennas & Propagation*, vol. 4, nº. 12, 2010, pp. 2179-2186.

[84] Chen Yu, Wei Hong and Zhenqi Kuai; “Multiple stopbands ultra wide band antenna,” *2008 International Conference on Microwave and Millimeter Wave Technology*, vol.4, 2008, pp. 1872-1874.

[85] J. R. Panda,R. S. Kshetrimayum; "A compact CPW-fed ultra-wideband antenna with 5 GHz/6 GHz band-notch function," *India Conference (INDICON), 2009 Annual IEEE*, 2009, pp. 1-4.

[86] Shau-Gang Mao, Jen-Chun Yeh and Shiou-Li Chen; “Ultrawideband circularly polarized spiral antenna using integrated balun with application to time-domain target detection,” *IEEE Transactions on Antennas and Propagation*, vol. 57, nº. 7, 2009, pp. 1914-1920.

[87] Cidronali, A.; Maddio, S.; Giorgetti, G.; Magrini, I.; Gupta, S.K.S.; Manes, G.; “A 2.45 GHz smart antenna for location-aware single-anchor indoor applications,” *Microwave Symposium Digest, 2009. MTT '09. IEEE MTT-S International*, pp.1553-1556, 7-12 June 2009.

[88] Xiaobing Sun, Yugang Ma, Jin Xu, Jian Zhang and Junjun Wang; “A High Accuracy Mono-Station UWB Positioning System,” *IEEE International Conference on Ultra-Wideband (ICUWB2008)*, vol. 1, 2008, pp. 201-204.

[89] X. Qing, Z. N. Chen, T. S. P. See; “Sectored Antenna Array for Indoor Mono-station UWB Positioning Applications,” *3rd European Conference on Antenna and Propagation (EuCAP 2009)*, 2009, pp. 822-825.

[90] A. E. C. Tan, M. Y. W. Chia and K. Rambabu; “Angle accuracy of antenna noise corrupted ultra-wideband monopulse receiver,” *IEEE International Conference on Ultra-Wideband (ICUWB 2007)*, 2007, pp. 586-589.

[91] J. D. Taylor, Introduction to ultra-wideband radar systems. Boca Raton: CRC Press, 1995.

[92] P. Kulakowski, et al; “Angle of Arrival localization based on antenna arrays for wireless sensor networks,” *Computers and Electrical Engineering Journal*, 2010.

[93] Chin-Heng Lim, Y. W., B. P. Ng, C. M. S. See; “A real-time indoor Wi-Fi localization system utilizing smart antennas,” *IEEE Transactions on Consumer Electronics*, vol. 53, nº. 2, 2007, pp. 618-622.

[94] A. Erdogan, V. Coskun, and A. Kavak; "The Sectoral Sweeper Scheme for Wireless Sensor Networks: Adaptive Antenna Array Based Sensor Unit Management and Location Estimation", *Wireless Personal Communications,* vol. 39, nº. 4, 2006, pp. 415-433.

[95] ChulYoung Park, et al; "Localization algorithm design and implementation to utilization RSSI and AOA of Zigbee", *5th International Conference on Future Information Technology*, 2010, pp. 1-4.

[96] D. J. Kim, S. H. Kim, Y. K. Kim, H. Lim and J. H. Jang; "Switched microstrip array antenna for RFID system," *38th European Microwave Conference (EuMC 2008),* 2008, pp 1254-1257.

[97] Hajar El Arja, Bernard Huyart and Xavier Begaud; "Joint ToA/DoA measurements for UWB indoor propagation channel using MUSIC algorithm," *European Wireless Technology Conference (EuWIT 2009),* 2009, pp. 124-127.

[98] Nasimuddin, Z. N. Chen, X. Qing and T.S.P See; "Sectorised antenna array and measurement methodology for indoor ultra-wideband applications," *IET Microwave Antennas & Propagation,* vol 3, nº 4, 2009, pp-621-629.

[99] Arun Raaza, Pallawi, Animesh Rana, Gopal. S. Joshi ans Amit Mehta, "Multiple beams switching double square loop on UWB systems," International Symposium in Information Technology (ITSim), vol. 2, 2010, pp. 575-579.

[100] Yu-Chuan Su, Marek E. Bialkowski, Feng-Chi E. Tsai and Kai-Hong Cheng; "UWB swtiched beam array antenna employing UWB butler matrix," *International Workshop on Antenna Technology: Small Antennas and Novel Metamaterials (iWAT 2008),* 2008, pp. 199-202.

[101] S. Fasseta, A. Chelouah, A. Sibille and C. Roblin; "Design of dedicated seven-port dividers for sectored circular antenna array feeding," *Annals of Telecommunications*, vol. 54, nº. 1-2, pp. 68-75, 1998.

[102] N. Honma, T. Seki, K. Nishikawa, K. Tsunekawa and K. Sawaya; "Compact six-sector antenna employing three intersecting dual-beam microstrip Yagi-Uda arrays with common director," *IEEE Transactions on Antennas and Propagation*, vol. 54, nº. 11, 2006, pp. 3055-3062.

[103] J. Cheng. M. Hashiguchi, K. Ligusa and T. Ohira; "Electronically steerable parasitic array radiator antenna for omni and sector pattern forming applications to wireless ad hoc networks," *IEEE Proc. on Microwave Antennas and Propagation*, vol. 150, nº. 4, 2003, pp. 203-208.

[104] Monika Sulkowska, Krzysztof Nyka and Lukasz Kulas; "Localization in wireless sensor networks using switched parasitic antennas," *18th International Conference on Microwave Radar and Wireless Communications (MIKON)*, 2010, pp. 1-4.

[105] K. Ligusa, K. Sato and M. Fujise; "A slim electronically steerable parasitic array radiator antenna," *6th International Conference on ITS Telecommunications Proceedings,* 2006, pp. 386-389.

[106] Stelios A. Mitilineos and Christos N. Capsalis; "A new, low-cost, switched beam and fully adaptive antenna array for 2.4 GHz ISM applications," *IEEE Transactions on Antennas and Propagation*, vol. 55, nº. 9, 2007, pp. 2502-2508.

[107] Y. Okamoto and A. Hirose; "Wideband adaptive antenna using selective feeding and stagger tuning," *Electronic* Letters, vol. 44, nº 19, 2008, pp. 1116-1117.

[108] D. Kornek, C. Orlob and I. Rolfes; "A sierpinski shaped patch antenna for beam switching," *IEEE Antennas and Propagation Society International Symposium (APSURSI'09)*, 2009, pp. 1-4.

[109] Hui Li and Z. H. Feng; "Switched planar hexagonal array of equilateral triangle patches for HIPERLAN terminals," *4th International Conference on Microwave and Millimeter Wave Technology (ICMMT)*, 2004, pp. 204-206.

[110] R. Siragusa, P. Lemaitre-Auger and S. Tedjini; "Tunable near-field focused circular phase-array antenna for 5.8 GHz RFID applications," *IEEE Antennas and Wireless Propagation Letters*, vol. 10, 2011, pp. 33-36.

[111] Fasseta and A. Sibille; "Switched angular diversity BSSA array antenna for WLAN," *Electronics Letters*, vol. 36, nº 8, 2000, pp. 702-703.

[112] A. Kalis, T. Antonakapoulos and V. Makios; "A printed circuit switched array antenna for indoor communications," *IEEE Transactions on Consumer Electronics*, vol 46, nº 3, 2000, pp. 531-538.

[113] R. J. Weber and Y. Huang; "A wideband circular array for frequency and 2D direction estimation and tracking," *IEEE Aerospace Conference*, 2010, pp. 1-8.

[114] A. Y. J. Chan and J. Litva; "MUSIC and maximum likelihood techniques on two-dimensional DOA estimation with uniform circular array," *IEEE Proc. - Radar, Sonar and Navigation*, vol. 142, nº. 3, 1995 pp. 105–114.

[115] M. Kanaan and K. Pahlavan; "A comparison of wireless geolocation algorithms in the indoor environment," *IEEE Wireless Communications and Networking Conference*, vol. 1, 2004 pp. 177-182.

[116] C. P. Mathews and M. D. Zoltowski; "Eigenstructure techniques for 2-D angle estimation with uniform circular arrays," *IEEE Trans. On Signal Processing*, vol. 42, nº. 9, 1994, pp. 2395–2407.

[117] Winston K. G. Seah, and Alvin T. S. Chan; "Challenges in Protocol Design for Wireless Sensor Netwoks Powered by Ambient Energy Harvesting", *Technical Report Series*, ECSTR11, 2011.

[118] ChulYoung Park; DaeHeon Park; JangWoo Park; YangSun Lee; Youngeun An; "Localization Algorithm Design and Implementation to Utilization RSSI and AOA of Zigbee," *Future Information Technology (FutureTech), 5th International Conference on*, pp.1-4, 21-23 May 2010.

[119] Matthews, J.C.G.; Pettit, G.; "Development of flexible, wearable antennas," *Antennas and Propagation EuCAP 2009. 3rd European Conference on*, pp.273-277, 23-27 March 2009.

[120] Kajiwara, A.; "Line-of-sight indoor radio communication using circular polarized waves," *Vehicular Technology, IEEE Transactions on*, vol. 44, nº. 3, pp.487-493, Aug 1995.

[121] Methfessel, Sebastian; Schmidt, Lorenz-Peter; "Design of a balanced-fed patch-excited horn antenna at millimeter-wave frequencies," *Antennas and Propagation (EuCAP), 2010 Proceedings of the Fourth European Conference on*, pp.1-4, 12-16 April 2010.

[122] L-Com Global Connectivity Products; "HyperLink Wireless 800-2500MHz BroadBand 11 dBi Radome Enclosed Log Periodic Antenna", online accessed in Kune 2013 at http://www.ispsupplies.com/categories/Dual-Band-Antennas/L-com-HG824-11LP-NF.html.

[123] Fu-Ren Hsiao and Kin-Lu Wong.; "Omnidirectional planar folded dipole antenna", *Antennas and Propagation, IEEE Transactions on*, vol. 7, nº 52, pp. 1898 – 1902, July 2004.

[124] E.A. Soliman, M.S. Ibrahim, and A.K. Abdelmageed.; "Dual-polarized omnidirectional planar slot antenna for wlan applications", *Antennas and Propagation, IEEE Transactions on*, vol. 9, nº 53, pp. 3093 – 3097, Sep. 2005.

[125] R. Bancroft and B. Bateman.; "An omnidirectional planar microstrip antenna", *Antennas and Propagation, IEEE Transactions on*, vol. 11, nº. 52, pp. 3151 – 3154, Nov. 2004.

[126] Jiusheng Li; "An omnidirectional microstrip antenna for wimax applications", *Antennas and Wireless Propagation Letters, IEEE*, nº. 10, pp. 167 –169, 2011.

[127] Xing Chen, Kama Huang, and Xiao-Bang Xu.; "A novel planar slot array antenna with omnidirectional pattern", *Antennas and Propagation, IEEE Transactions on*, vol. 12, nº 59, pp. 4853 –4857, Dec. 2011.

[128] B. Gallagher, H. Akatsuka, and H. Suzuki., "Wireless communications for vehicle safety: Radio link performance and wireless connectivity methods", *Vehicular Technology Magazine, IEEE*, vol. 4, nº. 1, pp. 4 –24, December. 2006.

[129] Meireles, M. Boban, P. Steenkiste, O. Tonguz, and J. Barros., "Experimental study on the impact of vehicular obstructions in vanets", *Vehicular Networking Conference (VNC), 2010 IEEE*, pages 338 –345, December 2010

[130] Toh, B. Y., Cahill, R. and Fusco, V. F.; "Understanding and measuring circular polarization," *Education, IEEE Transaction on*, vol. 46, nº. 3, pp. 313-318, August 2003.

[131] Rao, P.N.; Sarma, N.; "Fractal boundary circularly polarised single feed microstrip antenna," *Electronics Letters*, vol. 44, nº. 12, pp.713-714, June 2008.

[132] Jia-Yi Sze; Hsu, C. -I G; Min-Hua Ho; Yu-He Ou; Ming-Ting Wu; "Design of Circularly Polarized Annular-Ring Slot Antennas Fed by a Double-Bent Microstripline," *Antennas and Propagation, IEEE Transactions on*, vol. 55, nº. 11, pp.3134,3139, Nov. 2007.

[133] Nasimuddin; Chen, Z. N.; "Aperture-coupled asymmetrical c-shaped slot microstrip antenna for circular polarisation," *Microwaves, Antennas and Propagation, IET*, vol.3, nº.3, pp.372-378, April 2009.

[134] Yang, S. S., Lee, K. F., Kishk, A. A., and Luk, K. M.; "Design and study of wideband single feed circularly polarized microstrip antennas," *Progress In Electromagnetics Research*, vol. 80, pp. 45-61, 2008.

[135] Rezaeieh, S. A. and Kartal, M.; "A new triple band circularly polarized square slot antenna design with crooked T and F-shape and strips for wireless applications," *Progress In Electromagnetics Research*, vol. 121, pp. 1-18, 2011.

[136] Kasabegoudar, V. G. and Vinoy, K. J.; "A broadband suspended microstrip antenna for circular polarization," *Progress in Electromagnetics Research*, vol. 90, pp. 353-368, 2009.

[137] Lee, W.-S, Oh, K.-S, Yu, J.-W.; "A wideband planar monopole antenna array with circular polarized and band-notched characteristics," *Progress in Electromagnetics Research*, vol. 128, pp. 381-398, 2012.

[138] Ghobadi, A.; Dehmollaian, M., "A Printed Circularly Polarized Y-Shaped Monopole Antenna," *Antennas and Wireless Propagation Letters, IEEE*, vol.11, pp.22,25, 2012.

[139] Varum, T.; Matos, J. N.; Pinho, P.; Oliveira, A.O.; "Printed Antenna for DSRC Systems with Omnidirectional Circular Polarization", *Proc IEEE Conf. on Intelligent Transportation Systems*, Anchorage, United States, vol. 1, pp. 1 - 4, September, 2012.

[140] Yang, S.-S.; Chair, R.; KISHK, A.A.; Lee, K-F; Luk, Kwai-Man; "Study on Sequential Feeding Networks for Subarrays of Circularly Polarized Elliptical Dielectric Resonator Antenna," *Antennas and Propagation, IEEE Transactions on*, vol.55, nº.2, pp.321,333, Feb. 2007.

[141] Sun, Y. Y.; Cheung, S. W.; Yuk, T. I.; "Studies of Planar Antennas with Different Radiator Shapes for Ultra-wideband Body-centric Wireless Communications", *Progress In Electromagnetics Research Symposium (PIERS)*, Suzhou, China, September 2011.

[142] Chipcon Products from Texas Instruments, "A true System-on-Chip solution for 2,4GHZ IEEE 802.15.4/ZigBee", CC2430 Data Sheet (rev 2.1) SWRS036F, 2010.

[143] Hittite Microwave Corporation, "HMC252QS24/252QS24E, GaAs MMIC SP6T Non-Reflective Switch, DC - 3Ghz", v05.0505.

[144] CC1001 Datasheet, Chipcon Products from Texas Instruments, accessed online in July 2012 in " http://www.ti.com/product/cc1110f32.

[145] Wang Wei-ping; Chen Liang; Wang Jian-xin; "A Source-Location Privacy Protocol in WSN Based on Locational Angle," *Communications, 2008. ICC '08. IEEE International Conference on*, pp.1630-1634, 19-23 May 2008.

[146] Alazzawi L.; Elkateeb, A.; "Performance Evaluation of the WSN Routing Protocols Scalability," *J. Comp. Sys., Netw. and Comm.*, pp. 1-9, 2008.

[147] Fonseca J.A., Bartolomeu P.; "A MAC Protocol to Manage Communications in Localization Systems based in IEEE802.15.4," *IECON 2008, the 34th Annual Conference of the IEEE Industrial Electronics Society*, Orlando, USA, November 10-13, 2008.

[148] Nasipuri, A.; Ye, S.; You, J.; Hiromoto, R.E.; "A MAC protocol for mobile ad hoc networks using directional antennas," *Wireless Communications and Networking Confernce, 2000. WCNC. 2000 IEEE*, vol. 3, pp.1214-1219, 2000.

[149] ElBatt, T.; Anderson, T.; Ryu, B.; "Performance evaluation of multiple access protocols for ad hoc networks using directional antennas," *Wireless Communications and Networking, WCNC 2003. IEEE*, vol. 2, pp. 982-987, 20-20 March 2003.

[150] Yu Wang; Garcia-Luna-Aceves, J.J.; "Spatial reuse and collision avoidance in ad hoc networks with directional antennas," *Global Telecommunications Conference, GLOBECOM '02. IEEE*, vol. 1, pp. 112- 116, 17-21 Nov. 2002.

[151] S. Bandyopadhyay, K. Hausike, S. Horisawa, S. Tawara; "An adaptive MAC and Directional Routing Protocol for ad hoc wireless networks using ESPAR antenna," *Proceedings of the ACM MOBIHOC*, October 2001.

[152] M. Takai, J. Martin, A. Ren, and R. Bagrodia; "Directional virtual carrier sensing for directional antennas in mobile ad hoc networks," *ACM MOBIHOC*, Lausanne, Switzerland, June 2002.

[153] R. Choudhury, X. Yang, R. Ramanathan, and N. Vaidya; "Using Directional Antennas for Medium Access Control in Ad Hoc Networks," *Proceedings of the 8th annual int. conf. on Mobile computing and networking*, pp. 59-70, Sept. 2002.

[154] L. Bao, J J Garcia-Luna-Aceves; "Transmission Scheduling in Ad Hoc Networks with Directional Antennas," *Proceedings of the 8th annual international conference on Mobile computing and networking*, pp. 48-49, Sept. 2002.

[155] Wang, J.; Fang, Y.; Wu, D.; "SYN-DMAC: a directional MAC protocol for ad hoc networks with synchronization," *Military Communications Conference, MILCOM 2005. IEEE*, vol. 4, pp.2258-2263 17-20 Oct. 2005.

[156] Bazan, O.; Jaseemuddin, M.; "On the Design of Opportunistic MAC Protocols for Multihop Wireless Networks with Beamforming Antennas," *Mobile Computing, IEEE Transactions on*, vol. 10, nº. 3, pp.305-319, March 2011.

[157] Khan, S.A.; Aziz, H.; Maqsood, S.; Faisal, S.; "Clustered home area network: A beacon enabled IEEE 802.15.4 approach," *Emerging Technologies, 2008. ICET 2008. 4th International Conference on*, pp.193-198, 18-19 Oct. 2008.